

CITATION REPORT

List of articles citing

Shell-isolated nanoparticle-enhanced Raman spectroscopy

DOI: 10.1038/nature08907
Nature, 2010, 464, 392-5.

Source: <https://exaly.com/paper-pdf/48503205/citation-report.pdf>

Version: 2024-04-10

This report has been generated based on the citations recorded by exaly.com for the above article. For the latest version of this publication list, visit the link given above.

The third column is the impact factor (IF) of the journal, and the fourth column is the number of citations of the article.

#	Paper	IF	Citations
2328	MOF-Based Separator in an LiO ₂ Battery: An Effective Strategy to Restrain the Shuttling of Dual Redox Mediators.		
2327	In Situ Shell-Isolated Nanoparticle-Enhanced Raman Spectroscopy to Unravel Sequential Hydrogenation of Phenylacetylene over Platinum Nanoparticles.		
2326	.		
2325	The polymorphism linked to the human insulin gene: its lack of association with either IDDM or NIDDM in Japanese. 1986 , 113, 268-71		12
2324	Quantum plasmonics with quantum dot-metal nanoparticle molecules: influence of the Fano effect on photon statistics. 2010 , 105, 263601		229
2323	FDTD for plasmonics: Applications in enhanced Raman spectroscopy. 2010 , 55, 2635-2642		48
2322	The electrode/ionic liquid interface: electric double layer and metal electrodeposition. 2010 , 11, 2764-78		119
2321	Multifunctional Au-Coated TiO ₂ Nanotube Arrays as Recyclable SERS Substrates for Multifold Organic Pollutants Detection. 2010 , 20, 2815-2824		434
2320	Die nächste Generation moderner Spektroskopie: oberflächenverstärkte Raman-Streuung durch Metallnanopartikel. 2010 , 122, 9513-9515		3
2319	The next generation of advanced spectroscopy: surface enhanced Raman scattering from metal nanoparticles. 2010 , 49, 9325-7		67
2318	Preparation of metal@silica core-shell particle films by interfacial self-assembly. 2010 , 350, 58-62		22
2317	NMR and FT Raman characterisation of regioselectively sulfated chitosan regarding the distribution of sulfate groups and the degree of substitution. 2010 , 51, 4698-4705		43
2316	Deposition of Ag nanostructures on TiO ₂ thin films by RF magnetron sputtering. 2010 , 256, 7096-7101		34
2315	Spectroscopy: expanding versatility. <i>Nature</i> , 2010 , 464, 357	50.4	39
2314	News in brief. 2010 , 7, 345-345		
2313	Optimally designed nanolayered metal-dielectric particles as probes for massively multiplexed and ultrasensitive molecular assays. 2010 , 107, 13620-5		28
2312	. 2010 ,		2

2311	Theoretical and Experimental Analysis of the Sensitivity of Guided Mode Resonance Sensors. 2010 , 114, 21150-21157	36
2310	Free-standing optical gold bowtie nanoantenna with variable gap size for enhanced Raman spectroscopy. 2010 , 10, 4952-5	410
2309	Bridging the gap between electrochemical and organometallic activation: benzyl chloride reduction at silver cathodes. 2010 , 132, 17199-210	83
2308	Gold mesostructures with tailored surface topography and their self-assembly arrays for surface-enhanced Raman spectroscopy. 2010 , 10, 5006-13	278
2307	Plasmon-modulated light scattering from gold nanocrystal-decorated hollow mesoporous silica microspheres. 2010 , 4, 6565-72	31
2306	Hypersonic vibrations of Ag@SiO ₂ (cubic core)-shell nanospheres. 2010 , 4, 7692-8	26
2305	Portable surface-enhanced Raman scattering sensor for rapid detection of aniline and phenol derivatives by on-site electrostatic preconcentration. 2010 , 82, 9299-305	97
2304	Fabrication of the funnel-shaped three-dimensional plasmonic tip arrays by directional photofluidization lithography. 2010 , 4, 7175-84	51
2303	High-order nonlinearity of silica-gold nanoshells in chloroform at 1560 nm. 2010 , 18, 21636-44	27
2302	Characterization of hotspots in a highly enhancing SERS substrate. 2011 , 136, 4472-9	55
2301	Deep ultraviolet tip-enhanced Raman scattering. 2011 , 47, 9131-3	37
2300	New insights on the Au(core)/Pt(shell) nanoparticle structure in the sub-monolayer range: SERS as a surface analyzing tool. 2011 , 47, 3174-6	22
2299	Spectroscopy of molecular junctions. 2011 , 40, 2293-305	49
2298	Gold nanorod ensembles as artificial molecules for applications in sensors. 2011 , 21, 16759	57
2297	Plasmonically active micron-sized beads for integrated solid-phase synthesis and label-free SERS analysis. 2011 , 47, 12762-4	9
2296	Preparation and characterization of an ultrathin carbon shell coating a silver core for shell-isolated nanoparticle-enhanced Raman spectroscopy. 2011 , 47, 5873-5	32
2295	Decorating gold nano-spheres, -rods and -cubes with gold nanodots. 2011 ,	
2294	Dressing plasmons in particle-in-cavity architectures. 2011 , 11, 1221-6	87

2293	Mixed DNA-functionalized nanoparticle probes for surface-enhanced Raman scattering-based multiplex DNA detection. 2011 , 47, 7407-9	66
2292	Sombrero-shaped plasmonic nanoparticles with molecular-level sensitivity and multifunctionality. 2011 , 5, 6449-57	30
2291	Understanding the Behavior of New Plasmonic Probes with Sub-Nanometric Resolution in Field Enhanced Scanning Optical Microscopy. 2011 , 115, 10455-10461	4
2290	Effect of Aromatic AmineMetal Interaction on Surface Vibrational Raman Spectroscopy of Adsorbed Molecules Investigated by Density Functional Theory. 2011 , 115, 4174-4183	49
2289	Effect of the dielectric properties of substrates on the scattering patterns of gold nanorods. 2011 , 5, 4865-77	80
2288	Overlayer surface-enhanced Raman spectroscopy for studying the electrodeposition and interfacial chemistry of ultrathin ge on a nanostructured support. 2011 , 5, 1818-30	11
2287	In situ gap-mode Raman spectroscopy on single-crystal Au(100) electrodes: tuning the torsion angle of 4,4'-biphenyldithiols by an electrochemical gate field. 2011 , 133, 7332-5	74
2286	Wrinkled nanoporous gold films with ultrahigh surface-enhanced Raman scattering enhancement. 2011 , 5, 4407-13	209
2285	Intramolecular Ligand Dynamics in d15-(PPh3)-Capped Gold Nanoparticles Investigated by 2H NMR. 2011 , 115, 3297-3303	20
2284	Metallic membranes with subwavelength complementary patterns: distinct substrates for surface-enhanced Raman scattering. 2011 , 5, 5472-7	13
2283	Redox-switching in a viologen-type adlayer: an electrochemical shell-isolated nanoparticle enhanced Raman spectroscopy study on Au(111)-(111) single crystal electrodes. 2011 , 5, 5662-72	74
2282	Tunable Silver Nanocap Superlattice Arrays for Surface-Enhanced Raman Scattering. 2011 , 115, 24328-24333	25
2281	Crystal face dependent chemical effects in surface-enhanced Raman scattering at atomically defined gold facets. 2011 , 11, 1716-22	86
2280	Multidentate-protected colloidal gold nanocrystals: pH control of cooperative precipitation and surface layer shedding. 2011 , 133, 7268-71	31
2279	Experimental and theoretical investigations on the negative influence of an applied magnetic field on SERS of Ag nanoparticles. 2011 , 47, 11237-9	21
2278	Plasmon-enhanced resonance Raman scattering and fluorescence in Langmuir-Blodgett monolayers. 2011 , 83, 284-8	29
2277	Surface chemistry: a non-negligible parameter in determining optical properties of small colloidal metal nanoparticles. 2011 , 13, 11814-26	37
2276	Electromagnetic Theory of Tunable SERS Manipulated with Spherical Anisotropy in Coated Nanoparticles. 2011 , 115, 8893-8899	19

2275	Single molecule detection from a large-scale SERS-active AuAg substrate. 2011 , 1, 112	172
2274	Fabrication of a Au nanoporous film by self-organization of networked ultrathin nanowires and its application as a surface-enhanced Raman scattering substrate for single-molecule detection. 2011 , 83, 9131-7	51
2273	Magnesium nanocrystal-polymer composites: A new platform for designer hydrogen storage materials. 2011 , 4, 4882	89
2272	Metallo-dielectric photonic crystals for surface-enhanced Raman scattering. 2011 , 5, 3027-33	46
2271	A scheme for detecting every single target molecule with surface-enhanced Raman spectroscopy. 2011 , 11, 5013-9	155
2270	Reversible assembly and disassembly of gold nanorods induced by EDTA and its application in SERS tuning. 2011 , 27, 3381-90	73
2269	Synthetically directed self-assembly and enhanced surface-enhanced Raman scattering property of twinned crystalline Ag/Ag homojunction nanoparticles. 2011 , 27, 2204-10	51
2268	Plasmon-Enhanced Fluorescence and Spectral Modification in SHINEF. 2011 , 115, 20419-20424	45
2267	Excitation and reemission of molecules near realistic plasmonic nanostructures. 2011 , 11, 482-7	105
2266	A two-step temperature-raising process to gold nanoplates with optical and surface enhanced Raman spectrum properties. 2011 , 13, 2281	25
2265	Surface-enhanced Raman scattering-active nanostructures and strategies for bioassays. 2011 , 6, 1463-80	108
2264	Functionalizing metal nanostructured film with graphene oxide for ultrasensitive detection of aromatic molecules by surface-enhanced Raman spectroscopy. 2011 , 3, 2944-52	144
2263	Tuning chemical enhancement of SERS by controlling the chemical reduction of graphene oxide nanosheets. 2011 , 5, 952-8	275
2262	Sensitive and versatile detection of the fouling process and fouling propensity of proteins on polyvinylidene fluoride membranes via surface-enhanced Raman spectroscopy. 2011 , 83, 1709-16	44
2261	Infrared and Raman spectroscopic studies of the antimicrobial effects of garlic concentrates and diallyl constituents on foodborne pathogens. 2011 , 83, 4137-46	42
2260	Effect of graphene Fermi level on the Raman scattering intensity of molecules on graphene. 2011 , 5, 5338-44	151
2259	Recent progress in SERS biosensing. 2011 , 13, 11551-67	488
2258	Plasmonic nanoantennas: fundamentals and their use in controlling the radiative properties of nanoemitters. 2011 , 111, 3888-912	1015

- 2257 Approaching the electromagnetic mechanism of surface-enhanced Raman scattering: from self-assembled arrays to individual gold nanoparticles. **2011**, 40, 1296-304 159
- 2256 Mapping Hot-Spots in Hexagonal Arrays of Metallic Nanotriangles with Azobenzene Polymer Thin Films. **2011**, 115, 15318-15323 41
- 2255 Highly spectral dependent enhancement of upconversion emission with sputtered gold island films. **2011**, 47, 979-81 90
- 2254 Shell-isolated nanoparticle-enhanced Raman spectroscopy: expanding the versatility of surface-enhanced Raman scattering. **2011**, 4, 129-50 159
- 2253 Metal/Semiconductor Contacts Induce the Charge-Transfer Mechanism of Surface-Enhanced Raman Scattering. **2011**, 115, 18378-18383 59
- 2252 Protein-based SERS technology monitoring the chemical reactivity on an Eynuclein-mediated two-dimensional array of gold nanoparticles. **2011**, 27, 12782-7 16
- 2251 Magnetic separation and immunoassay of multi-antigen based on surface enhanced Raman spectroscopy. **2011**, 47, 4225-7 54
- 2250 Shell-Isolated Nanoparticle-Enhanced Raman Spectroscopy (SHINERS) Based on Gold-Core Silica-Shell Nanorods. **2011**, 225, 775-784 19
- 2249 Sum-Frequency Generation Vibrational Spectroscopy of an Extramolecular Chemical Bond. **2011**, 2, 2770-2773 12
- 2248 Core-shell nanoparticle based SERS from hydrogen adsorbed on a rhodium(111) electrode. **2011**, 47, 2023-5 51
- 2247 Plasmonic enhancements of photocatalytic activity of Pt/n-Si/Ag photodiodes using Au/Ag core/shell nanorods. **2011**, 133, 16730-3 114
- 2246 Plasmon Enhanced Spectroscopy of N,N'-Dialkylquinacridones Used as Codopants in OLEDs. **2011**, 115, 16838-16843 7
- 2245 Extraordinary enhancement of Raman scattering from pyridine on single crystal Au and Pt electrodes by shell-isolated Au nanoparticles. **2011**, 133, 15922-5 152
- 2244 NanoBiosensing. **2011**, 26
- 2243 Rapid, large-scale, sonochemical synthesis of 3D nanotextured silver microflowers as highly efficient SERS substrates. **2011**, 21, 18817 61
- 2242 A new route for the synthesis of polyhedral gold mesocages and shape effect in single-particle surface-enhanced Raman spectroscopy. **2011**, 47, 5157-9 51
- 2241 Synthesis and characterization of gold nanoparticles coated with ultrathin and chemically inert dielectric shells for SHINERS applications. **2011**, 65, 620-6 48
- 2240 The rational development of molecularly imprinted polymer-based sensors for protein detection. **2011**, 40, 1547-71 570

2239	Seeded Growth Synthesis of Uniform Gold Nanoparticles with Diameters of 1500 nm. 2011 , 115, 4502-4506	294
2238	Structure of plasmonic aerogel and the breakdown of the effective medium approximation. 2011 , 36, 358-60	4
2237	Functionalized arrays of Raman-enhancing nanoparticles for capture and culture-free analysis of bacteria in human blood. 2011 , 2, 538	201
2236	Self-assembled plasmonic core-shell clusters with an isotropic magnetic dipole response in the visible range. 2011 , 5, 6586-92	96
2235	Rapid Determination of Metabolites in Bio-fluid Samples by Raman Spectroscopy and Optimum Combinations of Chemometric Methods. 2011 , 29, 2525-2532	8
2234	Tuning gold nanorod-nanoparticle hybrids into plasmonic Fano resonance for dramatically enhanced light emission and transmission. 2011 , 11, 49-55	94
2233	Crystal engineering and SERS properties of Ag@Fe ₃ O ₄ nanohybrids: from heterodimer to core-shell nanostructures. 2011 , 21, 17930	56
2232	Hierarchical MnMoO ₄ (4)/CoMoO ₄ (4) heterostructured nanowires with enhanced supercapacitor performance. 2011 , 2, 381	897
2231	Electrochemical and optical biosensors based on nanomaterials and nanostructures A Review. 2011 , S3, 1308-1331	1
2230	Electrochemical and optical biosensors based on nanomaterials and nanostructures: a review. 2011 , 3, 1308-31	37
2229	Electrochemistry at Platinum Single Crystal Electrodes. 2011 , 75-170	37
2228	Enhancement of Raman scattering by two orders of magnitude using photonic nanojet of a microsphere. 2011 , 109, 103103	50
2227	Nanoantenna-enhanced gas sensing in a single tailored nanofocus. 2011 , 10, 631-6	753
2226	Applications of Raman-based techniques to on-site and in-vivo analysis. 2011 , 30, 1462-1476	36
2225	Molecular mechanism of kidney injury of mice caused by exposure to titanium dioxide nanoparticles. 2011 , 195, 365-70	134
2224	Investigation of resonant properties of metal core-shell nanoparticles using T-matrix calculations. 2011 , 112, 2733-2740	3
2223	SERS detection of protein biochip fabricated by etching polystyrene template. 2011 , 82, 456-60	6
2222	Raman spectroscopy: Recent advancements, techniques and applications. 2011 , 57, 163-176	328

2221	Silver-platinum core-shell nanoparticles for surface-enhanced Raman spectroscopy. 2011 , 57, 261-269	9
2220	Shell-isolated nanoparticle-enhanced Raman spectroscopy of pyridine on smooth silver electrodes. 2011 , 56, 10652-10657	23
2219	Protein-ligand binding investigated by a single nanoparticle TERS approach. 2011 , 47, 2065-7	36
2218	A highly sensitive protocol (FRET/SIMNSEF) for the determination of mercury ions: a unity of fluorescence quenching of graphene and enhancement of nanogold. 2011 , 47, 10389-91	29
2217	Templated techniques for the synthesis and assembly of plasmonic nanostructures. 2011 , 111, 3736-827	981
2216	Surface enhanced optical spectroscopies for bioanalysis. 2011 , 136, 3831-53	104
2215	The Dinitrogen-Ligated Triaurum Cation, Aurodiazanylium, Auronitrenium, Auroammonia, and Auroammonium. 2011 , 123, 2214-2218	1
2214	Silver-embedded zeolite crystals as substrates for surface-enhanced Raman scattering. 2011 , 46, 3162-3168	11
2213	Gas-phase preparation and size control of Fe nanoparticles. 2011 , 103, 1015-1020	7
2212	Effect of non-specificity in shape, size, and dielectric properties on electromagnetic extinction and optical field enhancement from spherical nanolayered metal-dielectric particles. 2011 , 130, 991-1000	4
2211	FT Raman investigation of novel chitosan sulfates exhibiting osteogenic capacity. 2011 , 83, 60-65	30
2210	Three powerful research tools from single cells into single molecules: AFM, laser tweezers, and Raman spectroscopy. 2011 , 165, 485-96	4
2209	Convective assembly of linear gold nanoparticle arrays at the micron scale for surface enhanced Raman scattering. 2011 , 4, 1117-1128	33
2208	Remote Excitation Polarization-Dependent Surface Photochemical Reaction by Plasmonic Waveguide. 2011 , 6, 681-687	43
2207	Shaped gold and silver nanoparticles. 2011 , 5, 1-24	24
2206	Soft X-ray induced oxidation on acrylic acid grafted luminescent silicon quantum dots in ultrahigh vacuum. 2011 , 208, 2424-2429	11
2205	Au ₂₅ @SiO ₂ : quantum clusters of gold embedded in silica. 2011 , 7, 204-8	57
2204	Carbon nanotube-tipped endoscope for in situ intracellular surface-enhanced Raman spectroscopy. 2011 , 7, 540-5	49

2203	Label-free indirect immunoassay using an avidin-induced surface-enhanced Raman scattering substrate. 2011 , 7, 316-20	32
2202	Raman-active two-tiered Ag nanoparticles with a concentric cavity. 2011 , 7, 3276-80	10
2201	In-situ partial sintering of gold-nanoparticle sheets for SERS applications. 2011 , 7, 3487-92	15
2200	3D self-assembled plasmonic superstructures of gold nanospheres: synthesis and characterization at the single-particle level. 2011 , 7, 3445-51	68
2199	SERS detection of proteins on micropatterned protein-mediated sandwich substrates. 2011 , 42, 1492-1496	14
2198	Study of Raman spectrum of uranium using a surface-enhanced Raman scattering technique. 2011 , 42, 885-887	8
2197	A Novel Nanoparticle-Based Disposable Electrochemical Immunosensor for Diagnosis of Exposure to Toxic Organophosphorus Agents. 2011 , 21, 4371-4378	71
2196	A SERS-active microfluidic device with tunable surface plasmon resonances. 2011 , 32, 3378-84	50
2195	Surface-enhanced fluorescence from fluorophore-assembled monolayers by using Ag@SiO ₂ nanoparticles. 2011 , 12, 992-8	16
2194	Design and synthesis of Raman reporter molecules for tissue imaging by immuno-SERS microscopy. 2011 , 4, 453-63	29
2193	Surface-Enhanced Fluorescence with Shell-Isolated Nanoparticles (SHINEF). 2011 , 123, 691-694	5
2192	Surface-enhanced fluorescence with shell-isolated nanoparticles (SHINEF). 2011 , 50, 665-8	124
2191	The dinitrogen-ligated triaurum cation, aurodiazenylium, auronitrenium, auroammonia, and auroammonium. 2011 , 50, 2166-70	5
2190	Peptide mesocrystals as templates to create an Au surface with stronger surface-enhanced Raman spectroscopic properties. 2011 , 17, 3370-5	56
2189	Synthesis of concave palladium nanocubes with high-index surfaces and high electrocatalytic activities. 2011 , 17, 9915-9	89
2188	Controlled synthesis of Ag/Ag/C hybrid nanostructures and their surface-enhanced Raman scattering properties. 2011 , 17, 13386-90	8
2187	A review on the fabrication of substrates for surface enhanced Raman spectroscopy and their applications in analytical chemistry. 2011 , 693, 7-25	786
2186	Highly sensitive detection of clenbuterol using competitive surface-enhanced Raman scattering immunoassay. 2011 , 697, 61-6	85

2185	Polyhedral silver mesocages for single particle surface-enhanced Raman scattering-based biosensor. 2011 , 32, 4877-84	67
2184	Adsorption of 4-mercaptopyridine onto laser-ablated gold, silver and copper oxide films: A comparative surface-enhanced Raman scattering investigation. 2011 , 991, 103-107	41
2183	Surface-enhanced Raman scattering at well-defined single crystalline faces of platinum-group metals induced by gap-mode plasmon excitation. 2011 , 221, 175-180	28
2182	Experimental demonstration of the electromagnetic mechanism underlying surface enhanced Raman scattering using single nanoparticle spectroscopy. 2011 , 219, 167-179	8
2181	Surface enhanced Raman scattering spectroscopy of Ag nanoparticle aggregates directly photo-reduced on pathogenic bacterium (<i>Helicobacter pylori</i>). 2011 , 221, 181-186	10
2180	Silicon nanowires-based highly-efficient SERS-active platform for ultrasensitive DNA detection. 2011 , 6, 122-130	224
2179	Photoinduced interaction of colloidal TiO ₂ nanoparticles with lysozyme: Evidences from spectroscopic studies. 2011 , 131, 1975-1981	39
2178	A Colloidal Route to Detection of Organic Molecules Based on Surface-Enhanced Raman Spectroscopy Using Nanostructured Substrate Derived from Aerosols. 2011 , 50, 06GG10	
2177	Tunable SERS from aluminium nanohole arrays in the ultraviolet region. 2011 , 47, 3909-11	55
2176	Metastable state nanoparticle-enhanced Raman spectroscopy for highly sensitive detection. 2011 , 47, 3583-5	63
2175	Green synthesis of rosettelike silver nanocrystals with textured surface topography and highly efficient SERS performances. 2011 , 13, 5709	22
2174	Evaporative self-assembly of gold nanorings via a surface acoustic wave atomization. 2011 ,	2
2173	Modulation of surface-enhanced Raman spectra by depth selective excitation of embedded indium tin oxide nanoisland arrays. 2011 , 44, 215305	5
2172	Biofunctionalization of Nanomaterials. 2011 , 1-38	3
2171	Metallic nanocone array photonic substrate for high-uniformity surface deposition and optical detection of small molecules. 2011 , 22, 245710	12
2170	Plasmonic nano-architectures for surface enhanced Raman scattering: a review. 2012 , 6, 064503	84
2169	Controlled growth and multi-photon luminescence of hexagonal arrays of Au nanoparticles on anodic aluminum oxide templates. 2012 , 111, 123110	6
2168	Nanotechnology-based approaches for rapid detection of chemical and biological contaminants in foods. 2012 , 317-334	1

2167	Surface enhanced Raman scattering and localized surface plasmon resonance of nanoscale ultrathin films prepared by atomic layer deposition. 2012 , 101, 023112	12
2166	Large-scale homogeneously distributed Ag-NPs with sub-10 nm gaps assembled on a two-layered honeycomb-like TiO ₂ film as sensitive and reproducible SERS substrates. 2012 , 23, 385705	30
2165	Surface enhanced raman scattering excited by dielectric-loaded surface plasmon polariton waveguides. 2012 ,	
2164	Surface-enhanced Raman scattering of SnO ₂ bulk material and colloidal solutions. 2012 , 85,	34
2163	Gold Nanoparticles. 2012 , 1	
2162	In situ real-time diffuse reflection infrared Fourier transform spectroscopy (DRIFTS) study of hydrogen adsorption and desorption on Ir/SiO ₂ catalyst. 2012 , 66, 600-5	5
2161	Voltage controlled nanoparticle plasmon resonance tuning through anodization. 2012 ,	
2160	2.In-situ?????????????????. 2012 , 80, 654-659	0
2159	Bifunctional Au-nanorod@Fe ₃ O ₄ nanocomposites: synthesis, characterization, and their use as bioprobes. 2012 , 14, 1	12
2158	Trimethylsilyl-terminated oligo(phenylene ethynylene)s: an approach to single-molecule junctions with covalent Au-C bonds. 2012 , 134, 19425-31	133
2157	Improved Photocatalytic Activity of Shell-Isolated Plasmonic Photocatalyst /TiO ₂ by Promoted LSPR. 2012 , 116, 26535-26542	87
2156	Biological Applications of SERS Using Functional Nanoparticles. 2012 , 181-234	6
2155	Ag@SiO ₂ Core-Shell Nanostructures: Distance-Dependent Plasmon Coupling and SERS Investigation. 2012 , 3, 1459-64	147
2154	Molecularly-mediated assemblies of plasmonic nanoparticles for Surface-Enhanced Raman Spectroscopy applications. 2012 , 41, 7085-107	319
2153	A silver nanoparticle based surface enhanced resonance Raman scattering (SERRS) probe for the ultrasensitive and selective detection of formaldehyde. 2012 , 4, 7358-61	27
2152	Dispersible gold nanorod dimers with sub-5 nm gaps as local amplifiers for surface-enhanced Raman scattering. 2012 , 12, 3828-32	120
2151	Multiphonon Resonant Raman Scattering and Photoinduced Charge-Transfer Effects at ZnO/Molecule Interfaces. 2012 , 116, 26908-26918	33
2150	Polymer nanofibers embedded with aligned gold nanorods: a new platform for plasmonic studies and optical sensing. 2012 , 12, 3145-50	149

2149	Face-Dependent Shell-Isolated Nanoparticle Enhanced Raman Spectroscopy of 2,2'-Bipyridine on Au(100) and Au(111). 2012 , 116, 5128-5140	60
2148	Tailored silica coated Ag nanoparticles for non-invasive surface enhanced Raman spectroscopy of biomolecular targets. 2012 , 2, 805-808	18
2147	Silicon-based reproducible and active surface-enhanced Raman scattering substrates for sensitive, specific, and multiplex DNA detection. 2012 , 100, 203104	63
2146	Gold nanoparticles for diagnostic sensing and therapy. 2012 , 393, 142-153	70
2145	Solid-state spectroscopic characterization of β -chitins deacetylated in homogeneous solutions. 2012 , 116, 4584-92	20
2144	Characterization of chemical speciation in ultrathin uranium oxide layered films. 2012 , 84, 10380-7	14
2143	Surface-Enhanced Fluorescence: Mapping Individual Hot Spots in Silica-Protected 2D Gold Nanotriangle Arrays. 2012 , 116, 11665-11670	38
2142	Highly reproducible and sensitive surface-enhanced Raman scattering from colloidal plasmonic nanoparticle via stabilization of hot spots in graphene oxide liquid crystal. 2012 , 4, 6649-57	45
2141	Ultrahigh-density array of silver nanoclusters for SERS substrate with high sensitivity and excellent reproducibility. 2012 , 6, 249-55	241
2140	Multiple depositions of Ag nanoparticles on chemically modified agarose films for surface-enhanced Raman spectroscopy. 2012 , 4, 137-42	70
2139	A facile and general preparation of high-performance noble-metal-based free-standing nanomembranes by a reagentless interfacial self-assembly strategy. 2012 , 4, 6974-80	9
2138	Application of surface enhanced Raman spectroscopy to the study of SOFC electrode surfaces. 2012 , 14, 5919-23	27
2137	Porous gold nanodisks with multiple internal hot spots. 2012 , 14, 9131-6	41
2136	Polymer-single-crystal@nanoparticle nanosandwich for surface enhanced Raman spectroscopy. 2012 , 22, 15526	35
2135	Synergism of interparticle electrostatic repulsion modulation and heat-induced fusion: a generalized one-step approach to porous network-like noble metals and their alloy nanostructures. 2012 , 22, 349-354	24
2134	Hydrothermal synthesis of mesoporous silica spheres: effect of the cooling process. 2012 , 4, 7114-20	26
2133	Functionalized shell-isolated nanoparticle-enhanced Raman spectroscopy for selective detection of trinitrotoluene. 2012 , 137, 4644-6	55
2132	Batch fabrication of disposable screen printed SERS arrays. 2012 , 12, 876-81	172

2131	Probing the Conformational Transition of 2,2'-Bipyridyl under External Field by Surface-Enhanced Raman Spectroscopy. 2012 , 116, 2884-2890	13
2130	Surface-Enhanced Raman Scattering of 4-Aminobenzenethiol on Ag and Au: pH Dependence of b2-Type Bands. 2012 , 116, 4774-4779	77
2129	Magnetic dipolar interactions in solid gold nanosphere dimers. 2012 , 134, 4477-80	28
2128	[email'protected] CoreShell Colloidal Nanoparticles Prepared by the Hydrothermal Route and the Low Temperature HeatingStirring Method and Their Application in Surface Enhanced Raman Scattering. 2012 , 116, 12283-12294	44
2127	Interface synthesis of gold mesocrystals with highly roughened surfaces for surface-enhanced Raman spectroscopy. 2012 , 22, 1998-2006	75
2126	Photosynthetic Bacterial Light-Harvesting Antenna Complexes Adsorbed on Silica Nanoparticles Revealed by Silica Shell-Isolated Au Nanoparticle-Enhanced Raman Spectroscopy. 2012 , 116, 6993-6999	10
2125	Surface-enhanced Raman scattering-active Au/SiO ₂ nanocomposites prepared using sonoelectrochemical pulse deposition methods. 2012 , 4, 4700-7	33
2124	Plasmon Resonance of Isolated Gold Hollow Nanoparticles and Nanoparticle Pairs: Insights from Electronic Structure Calculations. 2012 , 116, 1755-1763	9
2123	Fabrication of Large-Area, High-Enhancement SERS Substrates with Tunable Interparticle Spacing and Application in Identifying Microorganisms at the Single Cell Level. 2012 , 116, 3320-3328	28
2122	SERS on (111) Surface Nanofacets at Pt Nanoparticles: The Case of Acetaldehyde Oxime Reduction. 2012 , 116, 10781-10789	11
2121	Surface-Enhanced Raman Scattering on Hierarchical Porous Cuprous Oxide Nanostructures in Nanoshell and Thin-Film Geometries. 2012 , 3, 651-7	54
2120	Shell thickness-dependent Raman enhancement for rapid identification and detection of pesticide residues at fruit peels. 2012 , 84, 255-61	341
2119	Induced surface enhancement in coral Pt island films attached to nanostructured Ag electrodes. 2012 , 28, 5819-25	10
2118	Label-free detection in biological applications of surface-enhanced Raman scattering. 2012 , 38, 67-78	78
2117	Gold Nanorods Performing as Dual-Modal Nanoprobes via Metal-Enhanced Fluorescence (MEF) and Surface-Enhanced Raman Scattering (SERS). 2012 , 116, 12240-12249	107
2116	Gold mesoflower arrays with sub-10 nm intraparticle gaps for highly sensitive and repeatable surface enhanced Raman spectroscopy. 2012 , 23, 165604	26
2115	Tip-enhanced Raman detection of antibody conjugated nanoparticles on cellular membranes. 2012 , 84, 7408-14	40
2114	Nanomaterials for sensing and destroying pesticides. 2012 , 112, 5317-38	389

2113	Molecule-dependent plasmonic enhancement of fluorescence and Raman scattering near realistic nanostructures. 2012 , 6, 9828-36	45
2112	A SERS study of thiocyanate adsorption on Au-core Pd-shell nanoparticle film electrodes. 2012 , 665, 70-75	18
2111	Diagnostic applications of Raman spectroscopy. 2012 , 8, 545-58	143
2110	Theoretical study of medium-sized clusters of (Al ₂ O ₃) _n [From single cage to core-shell cage. 2012 , 981, 86-89	3
2109	Bottom-Up Tailoring of Plasmonic Nanopeapods Making Use of the Periodical Topography of Carbon Nanocoil Templates. 2012 , 22, 5157-5165	13
2108	Dispersible surface-enhanced Raman scattering nanosheets. 2012 , 24, 6065-70	62
2107	Selective Visual Detection of TNT at the Sub-Zeptomole Level. 2012 , 124, 9734-9738	6
2106	Selective visual detection of TNT at the sub-zeptomole level. 2012 , 51, 9596-600	97
2105	Facile fabrication of SERS arrays through galvanic replacement of silver onto electrochemically deposited copper micropatterns. 2012 , 13, 3786-9	14
2104	Surface-enhanced Raman spectroscopy spectra of Mexican dyestuffs. 2012 , 43, 1551-1559	28
2103	Enormous surface-enhanced Raman scattering from dimers of flower-like silver mesoparticles. 2012 , 8, 3400-5	27
2102	Metal oxide nanoparticle mediated enhanced Raman scattering and its use in direct monitoring of interfacial chemical reactions. 2012 , 12, 4242-6	95
2101	Melamine sensing in milk products by using surface enhanced Raman scattering. 2012 , 84, 9303-9	150
2100	Generation of Pronounced Resonance Profile of Charge-Transfer Contributions to Surface-Enhanced Raman Scattering. 2012 , 116, 2515-2520	29
2099	Silver-coated magnetite-carbon core-shell microspheres as substrate-enhanced SERS probes for detection of trace persistent organic pollutants. 2012 , 4, 5210-6	117
2098	Au/TiO ₂ /Au as a Plasmonic Coupling Photocatalyst. 2012 , 116, 6490-6494	189
2097	Engineering natural materials as surface-enhanced Raman spectroscopy substrates for in situ molecular sensing. 2012 , 4, 6599-608	23
2096	Au@SiO ₂ core-shell nanoparticles for laser desorption/ionization time of flight mass spectrometry. 2012 , 137, 2454-8	21

2095	Fine-tuning longitudinal plasmon resonances of nanorods by thermal reshaping in aqueous media. 2012 , 23, 105602	46
2094	Metal Nanoparticles in Biomedical Applications. 2012 , 477-519	3
2093	Real-time molecular imaging throughout the entire cell cycle by targeted plasmonic-enhanced Rayleigh/Raman spectroscopy. 2012 , 12, 5369-75	85
2092	Controlled Architectures in LbL Films for Sensing and Biosensing. 2012 , 951-983	5
2091	High quality gold nanorods and nanospheres for surface-enhanced Raman scattering detection of 2,4-dichlorophenoxyacetic acid. 2012 , 23, 495710	13
2090	Regiospecific plasmonic assemblies for in situ Raman spectroscopy in live cells. 2012 , 134, 1699-709	240
2089	Gold nanoparticle functionalized artificial nacre: facile in situ growth of nanoparticles on montmorillonite nanosheets, self-assembly, and their multiple properties. 2012 , 6, 8250-60	70
2088	Taking Plasmonic CoreShell Nanoparticles Toward Laser Threshold. 2012 , 116, 7546-7551	16
2087	Silica-Covered Silver and Gold Nanoresonators for Raman Analysis of Surfaces of Various Materials. 2012 , 116, 16167-16174	26
2086	Purification implications on SERS activity of silica coated gold nanospheres. 2012 , 84, 7906-11	26
2085	Controllable synthesis and catalysis application of hierarchical PS/Au core-shell nanocomposites. 2012 , 387, 47-55	19
2084	Synthesis of SERS active Ag ₂ S nanocrystals using oleylamine as solvent, reducing agent and stabilizer. 2012 , 47, 2579-2583	27
2083	Study on the synthesis of Ag/AgCl nanoparticles and their photocatalytic properties. 2012 , 47, 3452-3458	33
2082	Synthesis of gold@carbon dots composite nanoparticles for surface enhanced Raman scattering. 2012 , 14, 7360-6	132
2081	Highly sensitive, reproducible, and stable SERS sensors based on well-controlled silver nanoparticle-decorated silicon nanowire building blocks. 2012 , 22, 14127	46
2080	Graphene oxide sheath on Ag nanoparticle/graphene hybrid films as an antioxidative coating and enhancer of surface-enhanced Raman scattering. 2012 , 4, 6545-51	86
2079	Hydrophobic Teflon films as concentrators for single-molecule SERS detection. 2012 , 22, 20986	69
2078	Ordered array of gold semishells on TiO ₂ spheres: an ultrasensitive and recyclable SERS substrate. 2012 , 4, 2180-5	169

2077	Cellular-Like Gold Nanofeet: Synthesis, Functionalization, and Surface Enhanced Fluorescence Detection for Mercury Contaminations. 2012 , 7, 487-494	18
2076	Multiple Surface Plasmon Resonances in Compound Structure with Metallic Nanoparticle and Nanohole Arrays. 2012 , 7, 659-663	17
2075	BmNPV resistance of silkworm larvae resulting from the ingestion of TiO ₂ nanoparticles. 2012 , 150, 221-8	17
2074	Synthesis of spatially uniform metal alloys nanocrystals via a diffusion controlled growth strategy: The case of Au-Pd alloy trisoctahedral nanocrystals with tunable composition. 2012 , 5, 618-629	31
2073	Raman Spectroscopy for Nanomaterials Characterization. 2012 ,	73
2072	Raman Spectroscopy of Biomolecules at Electrode Surfaces. 2012 , 269-334	0
2071	Standing Ag nanoplate-built hollow microsphere arrays: Controllable structural parameters and strong SERS performances. 2012 , 22, 3177	44
2070	Fabricating a reversible and regenerable Raman-active substrate with a biomolecule-controlled DNA nanomachine. 2012 , 134, 19957-60	99
2069	Tuning the interparticle distance in nanoparticle assemblies in suspension via DNA-triplex formation: correlation between plasmonic and surface-enhanced Raman scattering responses. 2012 , 3, 2262	50
2068	Surface-enhanced Raman spectroscopic study of p-aminothiophenol. 2012 , 14, 8485-97	223
2067	Vibrational spectroscopy as a probe of molecule-based devices. 2012 , 41, 1929-46	31
2066	Surface Enhanced Raman Scattering. 2012 , 33, 216-222	
2065	Surface-Enhanced Raman Scattering as an Emerging Characterization and Detection Technique. 2012 , 2012, 1-15	16
2064	Synthesis, characterization and surface enhanced Raman scattering of hollow gold@silica double shell nanostructures. 2012 , 1, 275-291	4
2063	Highly ordered arrays of particle-in-bowl plasmonic nanostructures for surface-enhanced raman scattering. 2012 , 8, 2548-54	75
2062	Experimental confirmation of local field enhancement determining far-field measurements with shell-isolated silver nanoparticles. 2012 , 8, 2964-7	34
2061	Synthesis, characterization, and 3D-FDTD simulation of Ag@SiO ₂ nanoparticles for shell-isolated nanoparticle-enhanced Raman spectroscopy. 2012 , 28, 9140-6	101
2060	Signal amplification using functional nanomaterials for biosensing. 2012 , 41, 2122-34	438

2059	Plasmon-Controlled Fluorescence: Beyond the Intensity Enhancement. 2012 , 3, 191-202	339
2058	Surface-enhanced Raman spectroscopy (SERS): progress and trends. 2012 , 403, 27-54	593
2057	Single molecule directivity enhanced Raman scattering using nanoantennas. 2012 , 12, 2625-30	107
2056	Controlled fabrication of silver nanoneedles array for SERS and their application in rapid detection of narcotics. 2012 , 4, 2663-9	105
2055	Synthesis and application of surface enhanced Raman scattering (SERS) tags of Ag@SiO ₂ core/shell nanoparticles in protein detection. 2012 , 22, 7767	80
2054	Modification of two-level-atom resonance fluorescence near a plasmonic nanostructure. 2012 , 85,	40
2053	Gold-modified silver nanorod arrays: growth dynamics and improved SERS properties. 2012 , 22, 1150-1159	41
2052	Gold nanoparticle-enabled biological and chemical detection and analysis. 2012 , 41, 2849-66	557
2051	Three-tiered Au nano-disk array for broadband interaction with light. 2012 , 4, 2847-50	3
2050	Fluorophore-doped core-multishell spherical plasmonic nanocavities: resonant energy transfer toward a loss compensation. 2012 , 6, 6250-9	70
2049	Plasmonic percolation: plasmon-manifested dielectric-to-metal transition. 2012 , 6, 7162-71	76
2048	Surface enhanced Raman spectroscopy on a flat graphene surface. 2012 , 109, 9281-6	442
2047	Four degree of freedom liquid dispenser for direct write capillary self-assembly with sub-nanoliter precision. 2012 , 83, 015104	1
2046	Portable smart films for ultrasensitive detection and chemical analysis using SERS and SERRS. 2012 , 43, 474-477	25
2045	Clean and reproducible SERS substrates for high sensitive detection by solid phase synthesis and fabrication of Ag-coated Fe ₃ O ₄ microspheres. 2012 , 43, 848-856	58
2044	Adsorption and reduction reactions of anthraquinone derivatives on gold electrodes studied with electrochemical surface-enhanced Raman spectroscopy. 2012 , 43, 1367-1373	11
2043	High performance Au/Ag core/shell bipyramids for determination of thiram based on surface-enhanced Raman scattering. 2012 , 43, 1374-1380	59
2042	Ultra sensitive surface-enhanced Raman scattering detection based on monolithic column as a new type substrate. 2012 , 43, 1392-1396	27

2041	Effects of the agglomeration state on the Raman properties of Co ₃ O ₄ nanoparticles. 2012 , 43, 1443-1448	83
2040	Effects of trap density on the surface-enhanced Raman scattering of molecules adsorbed on TiO ₂ (Degussa P25). 2012 , 43, 1920-1923	7
2039	Multifunctional TiO ₂ -Coated Ag Nanowire Arrays as Recyclable SERS Substrates for the Detection of Organic Pollutants. 2012 , 2012, 3176-3182	64
2038	Dynamic nanoparticle assemblies. 2012 , 45, 1916-26	198
2037	Engineering plasmonic gold nanostructures and metamaterials for biosensing and nanomedicine. 2012 , 24, 5153-65	113
2036	Nanomaterials-based sensors for applications in environmental monitoring. 2012 , 22, 18101	160
2035	Inhibition assay of yeast cell walls by plasmon resonance Rayleigh scattering and surface-enhanced Raman scattering imaging. 2012 , 28, 8952-8	18
2034	Optimization of the Field Enhancement and Spectral Bandwidth of Single and Coupled Bimetal CoreShell Nanoparticles for Few-Cycle Laser Applications. 2012 , 7, 99-106	10
2033	Increased chemical enhancement of Raman spectra for molecules adsorbed on fluorinated reduced graphene oxide. 2012 , 50, 4512-4517	41
2032	Multifunctional ZnO/Ag nanorod array as highly sensitive substrate for surface enhanced Raman detection. 2012 , 94, 157-62	43
2031	Detection of DNA hybridization using electrochemical impedance spectroscopy and surface enhanced Raman scattering. 2012 , 19, 59-62	16
2030	SERS: Materials, applications, and the future. 2012 , 15, 16-25	1469
2029	Brillouin study of confined eigenvibrations of silver nanocubes. 2012 , 152, 501-503	2
2028	Comparison investigation of near- and far-field properties for plasmon resonance of silver nanosphere dimers. 2012 , 10, 16-24	7
2027	Optical antenna for photofunctional molecular systems. 2012 , 18, 1564-70	6
2026	Surface-enhanced Raman scattering of molecules adsorbed on Co-doped ZnO nanoparticles. 2012 , 43, 61-64	33
2025	Shell-isolated nanoparticle enhanced Raman spectroscopy (SHINERS) investigation of benzotriazole film formation on Cu(100), Cu(111), and Cu(poly). 2012 , 43, 46-50	64
2024	Synthesis of ultrathin and compact Au@MnO ₂ nanoparticles for shell-isolated nanoparticle-enhanced Raman spectroscopy (SHINERS). 2012 , 43, 40-45	87

2023	Large area fabrication of leaning silicon nanopillars for surface enhanced Raman spectroscopy. 2012 , 24, OP11-8	255
2022	Speckled SiO ₂ @Au Core-shell Particles as Surface Enhanced Raman Scattering Probes. 2013 , 8, 185-191	31
2021	Intragastric exposure to titanium dioxide nanoparticles induced nephrotoxicity in mice, assessed by physiological and gene expression modifications. 2013 , 10, 4	44
2020	Enhancement of antidandruff activity of shampoo by biosynthesized silver nanoparticles from <i>Solanum trilobatum</i> plant leaf. 2013 , 3, 431-439	22
2019	Refractive-Index-Enhanced Raman Spectroscopy and Absorptiometry of Ultrathin Film Overlaid on an Optical Waveguide. 2013 , 117, 16175-16181	14
2018	Semi-hydrogenation of alkynes at single crystal, nanoparticle and biogenic nanoparticle surfaces: the role of defects in Lindlar-type catalysts and the origin of their selectivity. 2013 , 162, 57-75	40
2017	Large-scale fabrication of nanodimple arrays for surface-enhanced Raman scattering. 2013 , 15, 12680-7	12
2016	Nanoscience, nanotechnology and spectrometry. 2013 , 86, 3-13	68
2015	In vivo characterization of protein uptake by yeast cell envelope: single cell AFM imaging and Tip-enhanced Raman scattering study. 2013 , 138, 5371-83	22
2014	Identification of molecular recognition of Langmuir-Blodgett monolayers using surface-enhanced Raman scattering spectroscopy. 2013 , 49, 8680-2	5
2013	Design of an anti-aggregated SERS sensing platform for metal ion detection based on bovine serum albumin-mediated metal nanoparticles. 2013 , 49, 7334-6	21
2012	Bi-functional ZnO-RGO-Au substrate: photocatalysts for degrading pollutants and SERS substrates for real-time monitoring. 2013 , 49, 3049-51	68
2011	Hierarchical Photonic Synthesis of Hybrid Nanoparticle Assemblies. 2013 , 4, 2630-2636	19
2010	A simple method to prepare the magnetic Ni@Au core-shell nanostructure for the cycle surface enhanced Raman scattering substrates. 2013 , 44, 987-993	19
2009	Facile fabrication of leafy spikes-like silver dendrite crystals for SERS substrate. 2013 , 48, 4125-4133	6
2008	Remote-Excitation Time-Dependent Surface Catalysis Reaction Using Plasmonic Waveguide on Sites of Single-Crystalline Crossed Nanowires. 2013 , 8, 249-254	17
2007	Electron Energy Loss and One- and Two-Photon Excited SERS Probing of Hot Plasmonic Silver Nanoaggregates. 2013 , 8, 763-767	15
2006	Surface-enhanced Raman imaging of red blood cell membrane with highly uniform active substrates obtained using block copolymers self-assembly. 2013 ,	0

2005	Gold mesoparticles with precisely controlled surface topographies for single-particle surface-enhanced Raman spectroscopy. 2013 , 1, 5567	48
2004	Silica-coated Au/Ag nanorods with tunable surface plasmon bands for nanoplasmonics with single particles. 2013 , 291, 585-594	13
2003	Exploiting the nanoparticle plasmon effect: observing drug delivery dynamics in single cells via Raman/fluorescence imaging spectroscopy. 2013 , 7, 7420-7	142
2002	Kinetics of thiocyanate orientation conversion on Pt surface studied by in situ step-scan time-resolved microscope FTIR spectroscopy. 2013 , 58, 622-626	
2001	Raman spectroscopic investigation on TiO ₂ -N719 dye interfaces using Ag@TiO ₂ nanoparticles and potential correlation strategies. 2013 , 14, 2217-24	31
2000	Direct analysis of trichloropyridinol in human saliva using an Au nanoparticles-based immunochromatographic test strip for biomonitoring of exposure to chlorpyrifos. 2013 , 114, 261-7	28
1999	DNA-mediated wirelike clusters of silver nanoparticles: an ultrasensitive SERS substrate. 2013 , 5, 7798-807	85
1998	Nanoreactors for simultaneous remote thermal activation and optical monitoring of chemical reactions. 2013 , 135, 13616-9	57
1997	Near-Infrared SERS Nanoprobes with Plasmonic Au/Ag Hollow-Shell Assemblies for In Vivo Multiplex Detection. 2013 , 23, 3719-3727	106
1996	Rapid determination of melamine in milk and milk powder by surface-enhanced Raman spectroscopy and using cyclodextrin-decorated silver nanoparticles. 2013 , 180, 1173-1180	78
1995	Facile synthesis of core-shell-satellite Ag/C/Ag nanocomposites using carbon nanodots as reductant and their SERS properties. 2013 , 15, 6305	20
1994	Metal nanoparticles for nano-imaging and nano-analysis. 2013 , 15, 13713-22	43
1993	Multifunctional nanoparticle@MOF core-shell nanostructures. 2013 , 25, 5819-25	253
1992	Immune recognition construct plasmonic dimer for SERS-based bioassay. 2013 , 44, 1253-1258	5
1991	Hydrogen treatment-improved uniform deposition of Ag nanoparticles on ZnO nanorod arrays and their visible-light photocatalytic and surface-enhanced Raman scattering properties. 2013 , 8, 325	12
1990	Gold nanoarray deposited using alternating current for emission rate-manipulating nanoantenna. 2013 , 8, 295	5
1989	Bioinspired patterning with extreme wettability contrast on TiO ₂ nanotube array surface: a versatile platform for biomedical applications. 2013 , 9, 2945-53	144
1988	Surface molecular imprinting onto silver microspheres for surface enhanced Raman scattering applications. 2013 , 50, 106-10	45

1987	Enhancement of SERS background through charge transfer resonances on single crystal gold surfaces of various orientations. 2013 , 135, 17387-92	56
1986	Combined optical and electrochemical methods for studying electrochemistry at the single molecule and single particle level: recent progress and perspectives. 2013 , 15, 20797-807	53
1985	Rapid synthesis of gold nanostructures with cyclic and linear ketones. 2013 , 3, 21919	13
1984	Si seed layer thickness effect on the structure of ultrathin tetrahedral amorphous carbon films. 2013 , 235, 117-120	3
1983	Excitation of Surface Plasmon Resonance in Composite Structures Based on Single-Layer Superaligned Carbon Nanotube Films. 2013 , 117, 23190-23197	12
1982	Label-free surface-enhanced Raman spectroscopy for sensitive DNA detection by DNA-mediated silver nanoparticle growth. 2013 , 85, 11788-93	98
1981	Perfect narrow-band absorber based on a monolayer of metallodielectric microspheres. 2013 , 103, 211105	13
1980	Fabrication and magnetic-induced aggregation of Fe ₃ O ₄ /Au noble metal composites for superior SERS performances. 2013 , 15, 1	13
1979	Self-assembled Ag nanoparticles for surface enhanced Raman scattering. 2013 , 20, 361-366	22
1978	Silver nano islands enhanced Raman scattering on large area grating substrates fabricated by two beam laser interference. 2013 , 29, 1006-1010	7
1977	Fabrication of nanowire network AAO and its application in SERS. 2013 , 8, 495	5
1976	Recent Advances in DNA Microarray Technology: an Overview on Production Strategies and Detection Methods. 2013 , 3, 428-450	21
1975	Large-area high-performance SERS substrates with deep controllable sub-10-nm gap structure fabricated by depositing Au film on the cicada wing. 2013 , 8, 437	38
1974	Optical nanoantennas. 2013 , 56, 539-564	146
1973	Giant photoluminescence emission in crystalline faceted Si grains. 2013 , 3, 2674	7
1972	Arrays of Nanoscale Gold Dishes Containing Engineered Substructures. 2013 , 1, 814-818	8
1971	Ultra-sensitive graphene-plasmonic hybrid platform for label-free detection. 2013 , 25, 4918-24	173
1970	Diazotization-coupling reaction-based selective determination of nitrite in complex samples using shell-isolated nanoparticle-enhanced Raman spectroscopy. 2013 , 116, 712-8	52

1969	Silver nanocrystals of various morphologies deposited on silicon wafer and their applications in ultrasensitive surface-enhanced Raman scattering. 2013 , 85, 48-56	14
1968	Separation, identification and fast determination of organophosphate pesticide methidathion in tea leaves by thin layer chromatography-surface-enhanced Raman scattering. 2013 , 5, 5560	35
1967	Phase-segregation induced growth of core-shell Fe ₂ O ₃ /SnO ₂ heterostructures for lithium-ion battery. 2013 , 15, 6715	26
1966	Generation of scalable quasi-3D metallo-dielectric SERS substrates through orthogonal reactive ion etching. 2013 , 1, 3110	10
1965	Nanogaps in 2D Ag-nanocap arrays for surface-enhanced Raman scattering. 2013 , 44, 1666-1670	14
1964	Tandem assays of protein and glucose with functionalized core/shell particles based on magnetic separation and surface-enhanced Raman scattering. 2013 , 9, 3259-64	9
1963	Humic acids-based one-step fabrication of SERS substrates for detection of polycyclic aromatic hydrocarbons. 2013 , 138, 1523-8	43
1962	Volume shrinkage induced formation of porous Ag sub-microcubes via solid-liquid reaction for SERS. 2013 , 15, 2588	14
1961	Ultrasensitive and recyclable SERS substrate based on Au-decorated Si nanowire arrays. 2013 , 42, 14324-30	45
1960	Highly controlled bifunctional Ag@rubrene core-shell nanostructures: surface-enhanced fluorescence and Raman scattering. 2013 , 1, 4146	11
1959	Synthesis of size-controlled silver nanodecahedrons and their application for core-shell surface enhanced Raman scattering (SERS) tags. 2013 , 3, 966-974	8
1958	Phase formation, magnetic and optical properties of epitaxially grown icosahedral Au@Ni nanoparticles with ultrathin shells. 2013 , 15, 2527	24
1957	Construction of core-shell Fe ₂ O ₃ @SnO ₂ nanohybrids for gas sensors by a simple flame-assisted spray process. 2013 , 3, 22373	20
1956	A new-type dynamic SERS method for ultrasensitive detection. 2013 , 44, 21-28	50
1955	Conjugated polymer mediated synthesis of nanoparticle clusters and core/shell nanoparticles. 2013 , 54, 485-489	6
1954	Surface analysis using shell-isolated nanoparticle-enhanced Raman spectroscopy. 2013 , 8, 52-65	304
1953	Controllable and reproducible construction of a SERS substrate and its sensing applications. 2013 , 5, 523-6	15
1952	Graphene-veiled gold substrate for surface-enhanced Raman spectroscopy. 2013 , 25, 928-33	189

1951	Surface enhanced fluorescence and Raman scattering by gold nanoparticle dimers and trimers. 2013 , 113, 033102	62
1950	Multifunctional Fe ₃ O ₄ @Ag/SiO ₂ /Au core-shell microspheres as a novel SERS-activity label via long-range plasmon coupling. 2013 , 29, 690-5	86
1949	Fabrication of Ag/Au core-shell nanowire as a SERS substrate. 2013 , 35, 690-692	23
1948	An optimal substrate design for SERS: dual-scale diamond-shaped gold nano-structures fabricated via interference lithography. 2013 , 5, 1836-42	50
1947	Core-shell noble-metal@metal-organic-framework nanoparticles with highly selective sensing property. 2013 , 52, 3741-5	475
1946	Gold Nanoparticle Capping Layers: Structure, Dynamics, and Surface Enhancement Measured Using 2D-IR Spectroscopy. 2013 , 125, 662-666	14
1945	Gold nanoparticle capping layers: structure, dynamics, and surface enhancement measured using 2D-IR spectroscopy. 2013 , 52, 634-8	49
1944	Gold cluster coatings enhancing Raman scattering from surfaces: Ink analysis and document identification. 2013 , 423, 73-78	17
1943	Facile preparation of silver nanoparticle films as an efficient surface-enhanced Raman scattering substrate. 2013 , 283, 52-57	19
1942	Polymer shell as a protective layer for the sandwiched gold nanoparticles and their recyclable catalytic property. 2013 , 395, 91-8	13
1941	Tuning the electromagnetic field coupling between nanoporous silver and silver nanoparticles connected by hybridized oligonucleotide. 2013 , 555, 178-181	4
1940	4-Mercaptopyridine adsorbed on pure palladium island films: A combined SERS and DFT investigation. 2013 , 1035, 231-235	12
1939	In situ SERS probing of nano-silver coated individual yeast cells. 2013 , 49, 536-41	45
1938	Rapid and large-scale synthesis of pitaya-like silver nanostructures as highly efficient surface-enhanced Raman scattering substrates. 2013 , 105, 117-23	10
1937	A microfluidic device integrating plasmonic nanodevices for Raman spectroscopy analysis on trapped single living cells. 2013 , 111, 314-319	27
1936	SERS tags: novel optical nanoprobe for bioanalysis. 2013 , 113, 1391-428	1003
1935	Capping-agent-free synthesis of substrate-supported porous icosahedral gold nanoparticles. 2013 , 5, 2983-9	7
1934	Regenerative silver nanoparticles for SERRS investigation of metmyoglobin with conserved heme pocket. 2013 , 3, 6839	7

1933	Shell-isolated nanoparticle-enhanced Raman spectroscopy: Nanoparticle synthesis, characterization and applications in electrochemistry. 2013 , 688, 5-11	35
1932	The chemical origin of enhanced signals from tip-enhanced Raman detection of functionalized nanoparticles. 2013 , 138, 3150-7	25
1931	Surface-enhanced Raman scattering (SERS) from Au:Ag bimetallic nanoparticles: the effect of the molecular probe. 2013 , 4, 509-515	147
1930	Spontaneous emission in the presence of a spherical plasmonic metamaterial. 2013 , 87,	22
1929	Surface enhanced Raman spectroscopy by titanium nitride non-continuous thin films. 2013 , 531, 144-146	19
1928	Nanoparticle assemblies: dimensional transformation of nanomaterials and scalability. 2013 , 42, 3114-26	188
1927	Plasmon enhanced spectroscopy. 2013 , 15, 5355-63	97
1926	Electro-oxidation of Au(111) in contact with aqueous electrolytes: New insight from in situ vibration spectroscopy. 2013 , 112, 853-863	47
1925	Off-resonance surface-enhanced Raman spectroscopy from gold nanorod suspensions as a function of aspect ratio: not what we thought. 2013 , 7, 2099-105	114
1924	Fabrication of graphene oxide/Ag hybrids and their surface-enhanced Raman scattering characteristics. 2013 , 397, 103-7	29
1923	Bifunctional quantum dot-decorated Ag@SiO ₂ nanostructures for simultaneous immunoassays of surface-enhanced Raman scattering (SERS) and surface-enhanced fluorescence (SEF). 2013 , 1, 2198-2204	29
1922	MONODISPERSED SILICA NANOSPHERES ENCAPSULATING Fe ₃ O ₄ AND LaF ₃ :Eu ³⁺ NANOPARTICLES FOR MRI CONTRAST AGENT AND LUMINESCENT IMAGING. 2013 , 06, 1250052	2
1921	Graphene: a platform for surface-enhanced Raman spectroscopy. 2013 , 9, 1206-24	390
1920	Plasmonic smart dust for probing local chemical reactions. 2013 , 13, 1816-21	93
1919	Optical response of individual Au-Ag@SiO ₂ heterodimers. 2013 , 7, 2522-31	77
1918	The Structure, Energy, Confinement, and Enhancement of Hot Spots between Two Nanoparticles. 2013 , 117, 7744-7750	7
1917	Core-shell plasmonic nanostructures to fine-tune long "Au nanoparticle-fluorophore" distance and radiative dynamics. 2013 , 421, 101-108	22
1916	Field-enhanced Raman scattering by silver nanoparticle with graded SiO ₂ coating. 2013 , 102, 153105	4

1915	Electromagnetic field redistribution in hybridized plasmonic particle-film system. 2013 , 102, 153108	45
1914	Correlated imaging--a grand challenge in chemical analysis. 2013 , 138, 1924-39	46
1913	Plasmon-enhanced chemical reactions. 2013 , 1, 5790	230
1912	Magnetic silver hybrid nanoparticles for surface-enhanced resonance Raman spectroscopic detection and decontamination of small toxic molecules. 2013 , 7, 3212-20	65
1911	Biomarker discovery and applications for foods and beverages: proteomics to nanoproteomics. 2013 , 93, 74-92	36
1910	Surface-imprinted core-shell Au nanoparticles for selective detection of bisphenol A based on surface-enhanced Raman scattering. 2013 , 777, 57-62	115
1909	Ag@zinc-tetraphenylporphyrin core-shell nanostructures with unusual thickness-tunable fluorescence. 2013 , 49, 3513-5	9
1908	Surface-enhanced Raman scattering in cancer detection and imaging. 2013 , 31, 249-57	320
1907	Facile synthesis of gelatin-protected silver nanoparticles for SERS applications. 2013 , 44, 823-826	17
1906	Layer-by-layer assembly of Ag nanowires into 3D woodpile-like structures to achieve high density "hot spots" for surface-enhanced Raman scattering. 2013 , 29, 7061-9	106
1905	Highly effective and reproducible surface-enhanced Raman scattering substrates based on Ag pyramidal arrays. 2013 , 6, 159-166	63
1904	Revealing the secondary structural changes of amyloid β peptide by probing the spectral fingerprint characters. 2013 , 44, 670-674	26
1903	Trace detection of cyanide based on SERS effect of Ag nanoplate-built hollow microsphere arrays. 2013 , 248-249, 435-41	46
1902	Durable plasmonic cap arrays on flexible substrate with real-time optical tunability for high-fidelity SERS devices. 2013 , 5, 4569-74	64
1901	Optical properties of single coupled plasmonic nanoparticles. 2013 , 15, 4100-9	26
1900	Exploring graphene nanocolloids as potential substrates for the enhancement of Raman scattering. 2013 , 5, 5085-90	18
1899	Chemical Mechanism and Tunability of Surface-Enhanced Raman Scattering of Pyridine on Heteronuclear Coinage Metal Diatomic Clusters: A Density Functional Study. 2013 , 117, 12544-12551	15
1898	Strongly coupled nanorod vertical arrays for plasmonic sensing. 2013 , 25, 3863-8	35

1897	Nanoparticle surface electromagnetic fields studied by single-particle nonlinear optical spectroscopy. 2013 , 15, 4177-82	14
1896	Surface-enhanced Raman scattering-based sensing in vitro: facile and label-free detection of apoptotic cells at the single-cell level. 2013 , 85, 2809-16	77
1895	Experimental investigations on the weakening effect of magnetic fields on surface-enhanced Raman scattering. 2013 , 44, 525-530	7
1894	Surface optimization of optical antennas for plasmonic enhancement of photoelectrochemical reactions. 2013 , 112, 864-868	5
1893	Hierarchical Mo-decorated Co ₃ O ₄ nanowire arrays on Ni foam substrates for advanced electrochemical capacitors. 2013 , 1, 8593	79
1892	Rapid synthesis and characterization of ultra-thin shell Au@SiO ₂ nanorods with tunable SPR for shell-isolated nanoparticle-enhanced Raman spectroscopy (SHINERS). 2013 , 44, 1120-1125	21
1891	Picomolar detection of mercuric ions by means of gold-silver core-shell nanorods. 2013 , 5, 6731-5	38
1890	Vertically aligned gold nanorod monolayer on arbitrary substrates: self-assembly and femtomolar detection of food contaminants. 2013 , 7, 5993-6000	197
1889	Optical Properties of Silver and Gold Tetrahedral Nanopyramid Arrays Prepared by Nanosphere Lithography. 2013 , 117, 14778-14786	76
1888	Electrochemical Seed-Mediated Growth of Surface-Enhanced Raman Scattering Active Au(111)-Like Nanoparticles on Indium Tin Oxide Electrodes. 2013 , 117, 15817-15828	23
1887	Bilayered Raman-intense gold nanostructures with hidden tags (BRIGHTs) for high-resolution bioimaging. 2013 , 25, 1022-7	126
1886	Mass-Based Photothermal Comparison Among Gold Nanocrystals, PbS Nanocrystals, Organic Dyes, and Carbon Black. 2013 , 117, 8909-8915	73
1885	Controllable two-stage droplet evaporation method and its nanoparticle self-assembly mechanism. 2013 , 29, 6232-41	68
1884	Creating, characterizing, and controlling chemistry with SERS hot spots. 2013 , 15, 21-36	531
1883	Hydrogen Adsorption and Oxidation on Pt Film: An in Situ Real-Time Attenuated Total Reflection Infrared (ATR-IR) Spectroscopic Study. 2013 , 117, 12537-12543	11
1882	Solution-dispersible Au nanocube dimers with greatly enhanced two-photon luminescence and SERS. 2013 , 5, 5368-74	48
1881	Signal Amplification Using Nanomaterials for Biosensing. 2013 , 17-41	1
1880	Investigating the effect of aging on transpassive behavior of Ni-based alloys in sulfuric acid with shell-isolated nanoparticle enhanced Raman spectroscopy (SHINERS). 2013 , 67, 67-74	22

1879	In situ SERS monitoring of photochemistry within a nanojunction reactor. 2013 , 13, 5985-90	70
1878	Rapid atto-molar level detection of surface-enhanced Raman spectroscopy technique based on glycidyl methacrylate-ethylene dimethacrylate (GMA-EDMA) porous material. 2013 , 44, 1004-1009	8
1877	Ultrafast Third-Order Optical Nonlinearity in Au Triangular Nanoprism with Strong Dipole and Quadrupole Plasmon Resonance. 2013 , 117, 20127-20132	46
1876	Scalable preparation of ultrathin silica-coated Ag nanoparticles for SERS application. 2013 , 5, 10643-9	35
1875	Label-free SERS monitoring of chemical reactions catalyzed by small gold nanoparticles using 3D plasmonic superstructures. 2013 , 135, 1657-60	35 ¹
1874	Fabrication of Large-area 3-D Ordered Silver-coated Colloidal Crystals and Macroporous Silver Films Using Polystyrene Templates. 2013 , 5, 182-190	11
1873	Photoreduction of 4,4'-dimercaptoazobenzene on ag revealed by Raman scattering spectroscopy. 2013 , 29, 183-90	33
1872	Au@SiO ₂ core/shell nanoparticle assemblage used for highly sensitive SERS-based determination of glucose and uric acid. 2013 , 44, 1671-1677	42
1871	Chapter 9:Nanoelectrochemistry in the people's republic of China. 275-335	1
1870	Monodisperse SnO ₂ -coated gold nanoparticles are markedly more stable than analogous SiO ₂ -coated gold nanoparticles. 2013 , 5, 2479-84	30
1869	New progress of plasmonics in complex metal nanostructures. 2013 , 56, 2327-2336	8
1868	Sculpting the analytical volume in and around nanoparticle sensors using a multilayer geometry. 2013 , 85, 3842-8	
1867	Silver nanoparticle-embedded microbubble as a dual-mode ultrasound and optical imaging probe. 2013 , 5, 9217-23	24
1866	Facile approach to prepare Pd nanoarray catalysts within porous alumina templates on macroscopic scales. 2013 , 5, 12695-700	21
1865	Controlled Surface Enhanced Resonance Raman Scattering (SERRS) in Biological Environment. 2013 , 146, 88-98	3
1864	In situ SHINERS at electrochemical single-crystal electrode/electrolyte interfaces: tuning preparation strategies and selected applications. 2013 , 7, 8940-52	52
1863	A novel bio-detecting chip based on the opened fiber surface plasmon enhancement mechanism. 2013 ,	
1862	Tuning of optical properties by atomic layer deposition. 2013 ,	

1861	Surface enhanced Raman scattering on non-SERS active substrates and in situ electrochemical study based on a single gold microshell. 2013 , 25, 2056-61	20
1860	Facile Synthesis of Mono-Dispersed Polystyrene (PS)/Ag Composite Microspheres via Modified Chemical Reduction. 2013 , 6, 5625-5638	25
1859	CuO and Co ₃ O ₄ Nanoparticles: Synthesis, Characterizations, and Raman Spectroscopy. 2013 , 2013, 1-6	155
1858	Engineering Metal Nanostructure for SERS Application. 2013 , 2013, 1-12	20
1857	Portable Measurement System Based on Raman Spectroscopy. 2013 , 321-324, 688-691	1
1856	Detection of atomic spin labels in a lipid bilayer using a single-spin nanodiamond probe. 2013 , 110, 10894-8	89
1855	Silver-decorated ZnO hexagonal nanoplate arrays as SERS-active substrates: An experimental and simulation study. 2013 , 28, 3374-3383	8
1854	Hazards of nanotechnology. 2013 , 36, 389-399	0
1853	SHINERS and plasmonic properties of Au Core SiO ₂ shell nanoparticles with optimal core size and shell thickness. 2013 , 44, 994-998	68
1852	Surface-enhanced Raman scattering from graphene covered gold nanocap arrays. 2013 , 114, 183520	17
1851	Microstructured polymer-based substrates with broadband absorption for surface-enhanced Raman scattering. 2013 , 44, 1678-1681	4
1850	Fabrication of Self-Standing Silver Nanoplate Arrays by Seed-Decorated Electrochemical Route and Their Structure-Induced Properties. 2013 , 2013, 1-7	9
1849	Quantum dynamical simulations of local field enhancement in metal nanoparticles. 2013 , 25, 125304	18
1848	Noble Metal Nanoparticles. 2013 , 303-388	24
1847	High-harmonic and single attosecond pulse generation using plasmonic field enhancement in ordered arrays of gold nanoparticles with chirped laser pulses. 2013 , 21, 2195-205	49
1846	Synthesis of Porous Gold Based on Gold-Thiol Coordination Polymer and Its Application in SERS Detection with High Activity and High Reproducibility. 2013 , 42, 407-409	
1845	Core-Shell Noble-Metal@Metal-Organic-Framework Nanoparticles with Highly Selective Sensing Property. 2013 , 125, 3829-3833	80
1844	Grand challenges in analytical chemistry: towards more bright eyes for scientific research, social events and human health. 2013 , 1, 5	12

1843	Synthesis and characterization of surface-enhanced Raman-scattered gold nanoparticles. 2013 , 8, 4327-38	19
1842	Immunomagnetic nanoparticle-based assays for detection of biomarkers. 2013 , 8, 4543-52	23
1841	Guided-Mode Resonance Grating with Self-Assembled Silver Nanoparticles for Surface-Enhanced Raman Scattering Spectroscopy. 2014 , 1, 380-389	13
1840	. 2014 ,	15
1839	. 2014 ,	1
1838	. 2014 ,	8
1837	Synthesis of silver nanowires as a SERS substrate for the detection of pesticide thiram. 2014 , 133, 411-6	55
1836	Deep-ultraviolet surface plasmon resonance of Al and Al core /Al ₂ O ₃ shell nanosphere dimers for surface-enhanced spectroscopy. 2014 , 23, 097303	4
1835	Generalized green synthesis of diverse LnF ₃ /Ag hybrid architectures and their shape-dependent SERS performances. 2014 , 4, 9205-9212	11
1834	Raman Scattering Surface Signal Enhancement: Induced by Au@SiO ₂ core-shell nanoclusters and nanorods.. 2014 , 8, 29-36	
1833	Ordered nanocap array composed of SiO ₂ -isolated Ag islands as SERS platform. 2014 , 30, 15285-91	35
1832	Study on the application of Raman spectroscopy on detecting water hardness. 2014 , 86, 417-20	1
1831	Silica-covered Au nanoresonators for fluorescence modulating of a graphene quantum dot. 2014 , 23, 097803	2
1830	Au/Ag nanoalloy shells as near-infrared SERS nanoprobe for the detection of protein. 2014 , 1, 045408	6
1829	An effective surface-enhanced Raman scattering template based on gold nanoparticle/silicon nanowire arrays. 2014 , 23, 067802	3
1828	Plasmon management in index engineered 2.5D hybrid nanostructures for surface-enhanced Raman scattering. 2014 , 6, e123-e123	6
1827	Oberflächenverstärkte Raman-Spektroskopie: Konzepte und chemische Anwendungen. 2014 , 126, 4852-4894	74
1826	Surface-Enhanced Raman Spectroscopy (SERS): General Introduction. 2014 , 1-34	9

1825	Note: Raman microspectroscopy integrated with fluorescence and dark field imaging. 2014 , 85, 056109	22
1824	Surface Enhanced Raman Scattering Based on Dielectric-Loaded Surface Plasmon Polariton Waveguides. 2014 , 901, 25-28	
1823	Electrochemical setup--a unique chance to simultaneously control orbital energies and vibrational properties of single-molecule junctions with unprecedented efficiency. 2014 , 16, 25942-9	12
1822	Conversion of AgCl nanocubes to Ag/AgCl nanohybrids via solid-liquid reaction for surface-enhanced Raman scattering detection. 2014 , 9, 297-301	4
1821	Feasibility study of localized plasmon based Raman signal enhancements using silver nanoislands. 2014 ,	
1820	Residual pesticide detection on food with particle-enhanced Raman scattering. 2014 ,	
1819	Nanowire-supported plasmonic waveguide for remote excitation of surface-enhanced Raman scattering. 2014 , 3, e199-e199	167
1818	ZnGa ₂ O ₄ nanorod arrays decorated with Ag nanoparticles as surface-enhanced Raman-scattering substrates for melamine detection. 2014 , 15, 1624-31	14
1817	Plasmonic hydrogen sensing with nanostructured metal hydrides. 2014 , 8, 11925-40	155
1816	Silver nanoparticle aggregates by room temperature electron reduction: preparation and characterization. 2014 , 4, 63079-63084	13
1815	The simplest plasmonic molecules: Metal nanoparticle dimers and trimers. 2014 , 21, 26-39	62
1814	Simple and sensitive detection of cyanide using pinhole shell-isolated nanoparticle-enhanced Raman spectroscopy. 2014 , 45, 619-626	27
1813	A Boronate Affinity Sandwich Assay: An Appealing Alternative to Immunoassays for the Determination of Glycoproteins. 2014 , 126, 10554-10557	11
1812	Mapping nanoscale light fields. 2014 , 8, 919-926	139
1811	High performance surface-enhanced Raman scattering via dummy molecular imprinting onto silver microspheres. 2014 , 50, 14331-3	22
1810	Identification and characterization of colorectal cancer using Raman spectroscopy and feature selection techniques. 2014 , 22, 25895-908	50
1809	Fabrication of uniform substrate based on silver nanoparticles decorated glycidyl methacrylate-ethylene dimethacrylate porous material for ultrasensitive surface-enhanced Raman scattering detection. 2014 , 45, 47-53	11
1808	Plasmonic Core/Satellite Heterostructure with Hierarchical Nanogaps for Raman Spectroscopy Enhanced by Shell-Isolated Nanoparticles. 2014 , 2, 788-793	6

- ¹⁸⁰⁷ Chemical Sciences: Contributions to Building a Sustainable Society and Sharing of International Responsibilities. **2014**, 101-139
- ¹⁸⁰⁶ Gold crescent nanodisk array for nanoantenna-enhanced sensing in subwavelength areas. **2014**, 53, 7236-40 11
- ¹⁸⁰⁵ DFT study on the influence of electric field on surface-enhanced Raman scattering from pyridine-thetal complex. **2014**, 45, 62-67 19
- ¹⁸⁰⁴ Au dotted magnetic network nanostructure and its application for on-site monitoring femtomolar level pesticide. **2014**, 10, 1325-31 40
- ¹⁸⁰³ Porous Anodic Aluminum Oxide Decorated with Gold Nanoparticles for Surface-Enhanced Raman Scattering. **2014**, 898, 15-18
- ¹⁸⁰² Enhanced fluorescence from dye molecules by Au nanoparticles on asymmetric double-stranded DNA and mechanism. **2014**, 104, 141910 5
- ¹⁸⁰¹ Surface-enhanced Raman spectroscopy based on self-assembly structure of silver nanoparticles. **2014**,
- ¹⁸⁰⁰ Nanoplasmonic hydrogen sensing. **2014**, 1
- ¹⁷⁹⁹ Stamping surface-enhanced Raman spectroscopy for label-free, multiplexed, molecular sensing and imaging. **2014**, 19, 050501 34
- ¹⁷⁹⁸ Morphology Controllable Preparation of Gold Nanoplates through an Eco-Friendly Wet-Chemical Route. **2014**, 887-888, 108-111
- ¹⁷⁹⁷ Plasmonic properties of Au/SiO₂ nanoparticles: effect of gold size and silica dielectric layer thickness. **2014**, 18, S4-701-S4-705 4
- ¹⁷⁹⁶ Low-cost, high-sensitivity SERS nano-bio-chip for kinase profiling, drug monitoring and environmental detection: a translational platform technology. **2014**, 1
- ¹⁷⁹⁵ Engineering the synthesis of silica-gold nano-urchin particles using continuous synthesis. **2014**, 6, 13228-35 17
- ¹⁷⁹⁴ Microfluidics & nanotechnology: towards fully integrated analytical devices for the detection of cancer biomarkers. **2014**, 4, 55590-55598 25
- ¹⁷⁹³ Surface Plasmon Resonance and Raman Scattering Activity of the Au/Ag x O/Ag Multilayer Film. **2014**, 31, 047302 5
- ¹⁷⁹² AuNPs@mesoSiO₂ composites for SERS detection of DTNB molecule. **2014**, 51, 297-303 28
- ¹⁷⁹¹ Robust SERS substrates with massive nanogaps derived from silver nanocubes self-assembled on massed silver mirror via 1,2-ethanedithiol monolayer as linkage and ultra-thin spacer. **2014**, 143, 1331-1337 9
- ¹⁷⁹⁰ Exploring type II microcalcifications in benign and premalignant breast lesions by shell-isolated nanoparticle-enhanced Raman spectroscopy (SHINERS). **2014**, 132, 397-402 16

1789	Microwave assisted in situ synthesis of Ag@NaCMC films and their reproducible surface-enhanced Raman scattering signals. 2014 , 602, 94-100	20
1788	In situ surface enhanced Raman spectroscopic studies of solid electrolyte interphase formation in lithium ion battery electrodes. 2014 , 256, 324-328	59
1787	Fast enrichment and ultrasensitive in-situ detection of pesticide residues on oranges with surface-enhanced Raman spectroscopy based on Au nanoparticles decorated glycidyl methacrylate-ethylene dimethacrylate material. 2014 , 46, 108-114	26
1786	Self-assembled Au nanoparticle arrays on thiol-functionalized resin beads for sensitive detection of paraquat by surface-enhanced Raman scattering. 2014 , 455, 104-110	11
1785	Hole arrayed metal-insulator-metal structure for surface enhanced Raman scattering by self-assembling polystyrene spheres. 2014 , 9, 64-68	6
1784	Narrowband Light Total Antireflection and Absorption in Metal Film Array Structures by Plasmonic Near-Field Coupling. 2014 , 9, 17-25	9
1783	Fundamental studies on enhancement and blinking mechanism of surface-enhanced Raman scattering (SERS) and basic applications of SERS biological sensing. 2014 , 9, 31-46	55
1782	Optical Properties of Noncontinuous Gold Shell Engineered on Silica Mesosphere. 2014 , 9, 121-127	8
1781	Recent progress in surface enhanced Raman spectroscopy for the detection of environmental pollutants. 2014 , 181, 23-43	187
1780	Surface-enhanced Raman spectroscopy: concepts and chemical applications. 2014 , 53, 4756-95	1533
1779	Vibrational spectroscopy for probing molecular-level interactions in organic films mimicking biointerfaces. 2014 , 207, 199-215	26
1778	Facile fabrication and perfect cycle stability of 3D NiO@CoMoO ₄ nanocomposite on Ni foam for supercapacitors. 2014 , 4, 17884	45
1777	The size-controllable, one-step synthesis and characterization of gold nanoparticles protected by synthetic humic substances. 2014 , 144, 168-178	25
1776	Periodic silver nanodishes as sensitive and reproducible surface-enhanced Raman scattering substrates. 2014 , 4, 3487-3493	33
1775	Varying SiO ₂ thickness of core-shell noble-grains on a gradient sensing plate to enhance field Raman scattering. 2014 , 72, 419-424	
1774	Plasmon-Enhanced Scattering and Fluorescence Used for Ultrasensitive Detection in Langmuir-Blodgett Monolayers. 2014 , 243-256	1
1773	Activation of oxygen on gold and silver nanoparticles assisted by surface plasmon resonances. 2014 , 53, 2353-7	306
1772	In situ Characterization of SiO ₂ Nanoparticle Biointeractions Using BrightSilica. 2014 , 24, 3765-3775	47

1771	Synthesis of silver nanocubes as a SERS substrate for the determination of pesticide paraoxon and thiram. 2014 , 121, 63-9	70
1770	Shell-Isolated Nanoparticle-Enhanced Raman Spectroscopy (SHINERS). 2014 , 163-192	7
1769	Direct readout SERS multiplex sensing of pesticides via gold nanoplate-in-shell monolayer substrate. 2014 , 451, 48-55	5
1768	Experimental Demonstration of Electromagnetic Mechanism of SERS and Quantitative Analysis of SERS Fluctuation Based on the Mechanism. 2014 , 59-87	2
1767	Non-resonant SERS Using the Hottest Hot Spots of Plasmonic Nanoaggregates. 2014 , 19-35	3
1766	State of the art Raman techniques for biological applications. 2014 , 68, 338-47	23
1765	A disordered silver nanowires membrane for extraction and surface-enhanced Raman spectroscopy detection. 2014 , 139, 2525-30	39
1764	Spectroscopy of scattered light for the characterization of micro and nanoscale objects in biology and medicine. 2014 , 68, 133-54	16
1763	Determination of iodate in iodized salt and water samples by shell-isolated nanoparticle-enhanced Raman spectroscopy. 2014 , 181, 1301-1308	10
1762	Silver nanoparticles protected by monolayer graphene as a stabilized substrate for surface enhanced Raman spectroscopy. 2014 , 66, 713-719	106
1761	Preparation and properties of noble metal core/shell nanostructures prepared by excimer laser ablation in liquid solutions. 2014 , 26, 022001	11
1760	Evanescence-field-induced Raman scattering for bio-friendly fingerprinting at sub-cellular dimension. 2014 , 128, 414-21	3
1759	Catalytic and SERS Activities of Tryptophan-EDTA Capped Silver Nanoparticles. 2014 , 640, 1095-1101	5
1758	Fabrication of gold nanoparticle-embedded metal-organic framework for highly sensitive surface-enhanced Raman scattering detection. 2014 , 86, 3955-63	160
1757	Surface-Enhanced Raman Spectroscopy for the Chemical Analysis of Food. 2014 , 13, 317-328	230
1756	In-Situ Immobilization of Silver Nanoparticles on Self-Assembled Honeycomb-Patterned Films Enables Surface-Enhanced Raman Scattering (SERS) Substrates. 2014 , 118, 11478-11484	41
1755	Design and synthesis of 3D Co ₃ O ₄ @MMoO ₄ (M=Ni, Co) nanocomposites as high-performance supercapacitor electrodes. 2014 , 130, 660-669	94
1754	Exotic 3D Hierarchical ZnO@Ag Hybrids as Recyclable Surface-Enhanced Raman Scattering Substrates for Multifold Organic Pollutant Detection. 2014 , 2014, 2432-2439	28

1753	Probing the location of hot spots by surface-enhanced Raman spectroscopy: toward uniform substrates. 2014 , 8, 528-36	119
1752	Enhanced single-molecule spectroscopy in highly confined optical fields: from μ 2-Fabry-Pérot resonators to plasmonic nano-antennas. 2014 , 43, 1263-86	31
1751	Silver nanocrystals with special shapes: controlled synthesis and their surface-enhanced Raman scattering properties. 2014 , 4, 98-104	20
1750	Transparent free-standing metamaterials and their applications in surface-enhanced Raman scattering. 2014 , 6, 132-9	37
1749	Particle-Arrayed Silver Mesocubes Synthesized via Reducing Silver Oxide Mesocrystals for Surface-Enhanced Raman Spectroscopy. 2014 , 31, 390-397	21
1748	3D TiO ₂ submicrostructures decorated by silver nanoparticles as SERS substrate for organic pollutants detection and degradation. 2014 , 49, 560-565	22
1747	Controllable metal-enhanced fluorescence in organized films and colloidal system. 2014 , 207, 164-77	77
1746	Direct in situ observation of Li ₂ O evolution on Li-rich high-capacity cathode material, Li[Ni(x)Li((1-2x)/3)Mn((2-x)/3)]O ₂ (0 ≤ x ≤ 0.5). 2014 , 136, 999-1007	339
1745	Brushing, a simple way to fabricate SERS active paper substrates. 2014 , 6, 2066-2071	68
1744	Combining 3-D plasmonic gold nanorod arrays with colloidal nanoparticles as a versatile concept for reliable, sensitive, and selective molecular detection by SERS. 2014 , 16, 5563-70	56
1743	Exploration of the growth process of ultrathin silica shells on the surface of gold nanorods by the localized surface plasmon resonance. 2014 , 25, 045704	9
1742	Self-focusing Au@SiO nanorods with rhodamine 6G as highly sensitive SERS substrate for carcinoembryonic antigen detection. 2014 , 2, 629-636	60
1741	Simple SERS substrates: powerful, portable, and full of potential. 2014 , 16, 2224-39	171
1740	Ultrasensitive Detection of Enrofloxacin in Chicken Muscles by Surface-Enhanced Raman Spectroscopy Using Amino-Modified Glycidyl Methacrylate-Ethylene Dimethacrylate (GMA-EDMA) Powdered Porous Material. 2014 , 7, 1219-1228	23
1739	Chemical mechanical polishing of thin film diamond. 2014 , 68, 473-479	96
1738	Three-dimensional noble-metal nanostructure: A new kind of substrate for sensitive, uniform, and reproducible surface-enhanced Raman scattering. 2014 , 23, 087801	5
1737	Derivatization of Colloidal Gold Nanoparticles Toward Their Application in Life Sciences. 2014 , 66, 153-206	
1736	Plasmonics in composite nanostructures. 2014 , 17, 372-380	52

1735	Interactions between silver nanoparticles and polyvinyl alcohol nanofibers. 2014 , 4, 087111	23
1734	One-nanometer-precision control of Al(2)O(3) nanoshells through a solution-based synthesis route. 2014 , 53, 12776-80	77
1733	Ultrasensitive analyte detection with plasmonic paper dipsticks and swabs integrated with branched nanoantennas. 2014 , 2, 10446-10454	51
1732	Extending the shell-isolated nanoparticle-enhanced Raman spectroscopy approach to interfacial ionic liquids at single crystal electrode surfaces. 2014 , 50, 14740-3	35
1731	One-Nanometer-Precision Control of Al ₂ O ₃ Nanoshells through a Solution-Based Synthesis Route. 2014 , 126, 12990-12994	14
1730	Controlling the Catalytic Efficiency on the Surface of Hollow Gold Nanoparticles by Introducing an Inner Thin Layer of Platinum or Palladium. 2014 , 5, 4088-94	25
1729	A silver nanoparticle embedded hydrogel as a substrate for surface contamination analysis by surface-enhanced Raman scattering. 2014 , 139, 5283-9	31
1728	Sub-5 nm nanobowl gaps electrochemically templated by SiO ₂ -coated Au nanoparticles as surface-enhanced Raman scattering hot spots. 2014 , 50, 3958-61	8
1727	Raman scattering and plasmonic photocatalysis of single particles of NaYF ₄ :Yb,Er@Ag under near-infrared laser excitation. 2014 , 139, 5983-8	12
1726	Plasmon enhanced fluorescence with aggregated shell-isolated nanoparticles. 2014 , 86, 10246-51	35
1725	Hierarchical silver mesoparticles with tunable surface topographies for highly sensitive surface-enhanced Raman spectroscopy. 2014 , 2, 4534-4542	71
1724	SERS performance of graphene oxide decorated silver nanoparticle/titania nanotube array. 2014 , 4, 41734-41743	43
1723	Geometric thermal phase diagrams for studying the thermal dynamic stability of hollow gold nanoballs at different temperatures. 2014 , 16, 6623-9	7
1722	Highly surface-roughened caterpillar-like Au/Ag nanotubes for sensitive and reproducible substrates for surface enhanced Raman spectroscopy. 2014 , 4, 45856-45861	8
1721	In situ loading of Ag nanocontacts onto silica nanospheres: a SERS platform for ultrasensitive detection. 2014 , 4, 2776-2782	31
1720	A femtogram level competitive immunoassay of mercury(II) based on surface-enhanced Raman spectroscopy. 2014 , 50, 9112-4	24
1719	In situ SERS detection of emulsifiers at lipid interfaces using label-free amphiphilic gold nanoparticles. 2014 , 139, 5075-8	3
1718	A metal-dielectric-graphene sandwich for surface enhanced Raman spectroscopy. 2014 , 6, 9925-9	24

1717	Inclusion of guest materials in aqueous coordination network shells spontaneously generated by reacting 2,5-dimercapto-1,3,4-thiadiazole with nanoscale metallic silver. 2014 , 4, 34294	8
1716	Ultrasensitive and reproducible surface-enhanced Raman scattering detection via an optimized adsorption process and filter-based substrate. 2014 , 6, 4130	5
1715	Cu@SiO ₂ nanowires: synthesis, cathodoluminescence and SERS response. 2014 , 4, 31887-31891	1
1714	Multifunctional SERS substrates of Fe ₃ O ₄ @Ag ₂ Se/Ag: construction, properties and application. 2014 , 6, 7083	6
1713	Microfluidic-SERS devices for one shot limit-of-detection. 2014 , 139, 3227-3234	31
1712	Rapid analysis of trace volatile formaldehyde in aquatic products by derivatization reaction-based surface enhanced Raman spectroscopy. 2014 , 139, 3614-21	64
1711	On-line surface enhanced Raman spectroscopic detection in a recyclable Au@SiO ₂ modified glass capillary. 2014 , 45, 736-744	23
1710	Wafer-scale double-layer stacked Au/Al ₂ O ₃ @Au nanosphere structure with tunable nanospacing for surface-enhanced Raman scattering. 2014 , 10, 3933-42	28
1709	Preparation and magnetic properties of Fe ₂ O ₃ @SiO ₂ core shell ellipsoids with different aspect ratios. 2014 , 38, 4351	18
1708	Rapid simultaneous detection of multi-pesticide residues on apple using SERS technique. 2014 , 139, 5148-54	86
1707	Plasmonic-enhanced self-cleaning activity on asymmetric Ag/ZnO surface-enhanced Raman scattering substrates under UV and visible light irradiation. 2014 , 2, 7747-7753	40
1706	Large-area fabrication of highly reproducible surface enhanced Raman substrate via a facile double sided tape-assisted transfer approach using hollow Au-Ag alloy nanourchins. 2014 , 6, 2567-72	46
1705	Tilt boundary induced heteroepitaxy in chemically grown dendritic silver nanostructures on germanium and their optical properties. 2014 , 16, 16730-9	18
1704	An in situ approach for facile fabrication of robust and scalable SERS substrates. 2014 , 6, 7232-6	7
1703	Single point calibration for semi-quantitative screening based on an internal reference in thin layer chromatography-SERS: the case of Rhodamine B in chili oil. 2014 , 6, 7218-7223	23
1702	Superhydrophobic Ag nanostructures on polyaniline membranes with strong SERS enhancement. 2014 , 16, 22867-73	17
1701	Fast fabrication of homogeneous Ag nanostructures on dual-acid doped polyaniline for SERS applications. 2014 , 4, 16121-16126	5
1700	A sensitive SERS assay for detecting proteins and nucleic acids using a triple-helix molecular switch for cascade signal amplification. 2014 , 50, 9409-12	32

1699	Polarization-dependent enhanced photoluminescence and polarization-independent emission rate of quantum dots on gold elliptical nanodisc arrays. 2014 , 6, 7237-42	11
1698	Stable Ag@oxides nanoplates for surface-enhanced Raman spectroscopy of amino acids. 2014 , 6, 8853-8	19
1697	Reactive ion etching-assisted surface-enhanced Raman scattering measurements on the single nanoparticle level. 2014 , 104, 243104	27
1696	Plasmonic properties of silver nanoparticles embedded in diamond like carbon films: Influence of structure and composition. 2014 , 317, 1041-1046	25
1695	Green synthesis of large-scale highly ordered core@shell nanoporous Au@Ag nanorod arrays as sensitive and reproducible 3D SERS substrates. 2014 , 6, 15667-75	101
1694	CoreShell Catalysts of Metal Nanoparticle Core and MetalOrganic Framework Shell. 2014 , 4, 4409-4419	281
1693	Simultaneous SERS and surface-enhanced fluorescence from dye-embedded metal core-shell nanoparticles. 2014 , 16, 8791-4	25
1692	A boronate affinity sandwich assay: an appealing alternative to immunoassays for the determination of glycoproteins. 2014 , 53, 10386-9	199
1691	Active and stable liquid water innovatively prepared using resonantly illuminated gold nanoparticles. 2014 , 8, 2704-13	35
1690	Determination of adsorbed species of hypophosphite electrooxidation on Ni electrode by in situ infrared with shell-isolated nanoparticle-enhanced Raman spectroscopy. 2014 , 48, 5-9	4
1689	Thin layer chromatography coupled with surface-enhanced Raman scattering as a facile method for on-site quantitative monitoring of chemical reactions. 2014 , 86, 7286-92	48
1688	Synergistic effect of surface plasmonic particles in PbS/TiO ₂ heterojunction solar cells. 2014 , 128, 386-393	8
1687	Reconstruction and electrochemical oxidation of Au(110) surface in 0.1 M H ₂ SO ₄ . 2014 , 139, 281-288	17
1686	Label-free aptasensor based on ultrathin-linker-mediated hot-spot assembly to induce strong directional fluorescence. 2014 , 136, 6802-5	46
1685	A new dielectric ta-C film coating of Ag-nanoparticle hybrids to enhance TiO ₂ photocatalysis. 2014 , 25, 125703	6
1684	Enhanced SERS Stability of R6G Molecules with Monolayer Graphene. 2014 , 118, 11827-11832	59
1683	Recent developments in Raman spectroscopy for the detection of food chemical hazards. 2014 , 191-206	1
1682	Explosives detection in a lasing plasmon nanocavity. 2014 , 9, 600-4	153

1681	Electrochemical Surface-Enhanced Raman Spectroscopy (EC-SERS): Early History, Principles, Methods, and Experiments. 2014 , 113-135	1
1680	Applications of Electrochemical Surface-Enhanced Raman Spectroscopy (EC-SERS). 2014 , 137-162	4
1679	Universal surface-enhanced Raman scattering amplification detector for ultrasensitive detection of multiple target analytes. 2014 , 86, 2205-12	95
1678	Improving SERS activity of inositol hexaphosphate capped silver nanoparticles: Fe ³⁺ as a switcher. 2014 , 53, 7227-32	14
1677	Noninvasive prostate cancer screening based on serum surface-enhanced Raman spectroscopy and support vector machine. 2014 , 105, 091104	63
1676	Enhancing the SERS performance of semiconductor nanostructures through a facile surface engineering strategy. 2014 , 320, 591-595	18
1675	Morphology and composition controlled synthesis of flower-like silver nanostructures. 2014 , 9, 302	22
1674	Out-diffused silver island films for surface-enhanced Raman scattering protected with TiO ₂ films using atomic layer deposition. 2014 , 9, 398	26
1673	Responsive Au@polymer hybrid microgels for the simultaneous modulation and monitoring of Au-catalyzed chemical reaction. 2014 , 2, 9514	37
1672	The controlled fabrication of Tip-On-Tip SERS probes. 2014 , 4, 4718-4722	12
1671	Monolithic NPG nanoparticles with large surface area, tunable plasmonics, and high-density internal hot-spots. 2014 , 6, 8199-207	69
1670	Gold-nanoparticle-decorated hybrid mesoflowlers: an efficient surface-enhanced Raman scattering substrate for ultra-trace detection of prostate specific antigen. 2014 , 118, 14085-91	18
1669	Detection of explosives by surface enhanced Raman scattering using substrate with a monolayer of ordered Au nanoparticles. 2014 , 317, 940-945	14
1668	Detection of low-concentration contaminants in solution by exploiting chemical derivatization in surface-enhanced Raman spectroscopy. 2014 , 86, 9006-12	17
1667	Modular plasmonic antennas built of ultrathin silica-shell silver-core nanoparticles. 2014 , 30, 7919-27	21
1666	A rapid green strategy for the synthesis of Au "heatball"-like nanoparticles using green tea for SERS applications. 2014 , 16, 1	6
1665	Synergistic modulation of surface interaction to assemble metal nanoparticles into two-dimensional arrays with tunable plasmonic properties. 2014 , 10, 609-16	42
1664	Surface-enhanced Raman scattering active substrates by liquid flame spray deposited and inkjet printed silver nanoparticles. 2014 , 21, 339-344	5

1663	Interfacial self-assembled functional nanoparticle array: a facile surface-enhanced Raman scattering sensor for specific detection of trace analytes. 2014 , 86, 6660-5	57
1662	MGITC facilitated formation of AuNP multimers. 2014 , 30, 8342-9	20
1661	Ordered Silver and Copper Nanorod Arrays for Enhanced Raman Scattering Created via Guided Oblique Angle Deposition on Polymer. 2014 , 118, 4878-4884	26
1660	Ordered arrays of Au-nanobowls loaded with Ag-nanoparticles as effective SERS substrates for rapid detection of PCBs. 2014 , 25, 145605	32
1659	Magnetically assembled Ni@Ag urchin-like ensembles with ultra-sharp tips and numerous gaps for SERS applications. 2014 , 10, 2564-9	17
1658	The use of Au@SiO ₂ shell-isolated nanoparticle-enhanced Raman spectroscopy for human breast cancer detection. 2014 , 406, 5425-32	33
1657	Silicon nanohybrid-based surface-enhanced Raman scattering sensors. 2014 , 10, 4455-68	61
1656	Bifunctional AgCl/Ag composites for SERS monitoring and low temperature visible light photocatalysis degradation of pollutant. 2014 , 38, 7-12	9
1655	Growing gold nanoparticles on a flexible substrate to enable simple mechanical control of their plasmonic coupling. 2014 , 2, 7927-7933	69
1654	Three-dimensional and time-ordered surface-enhanced Raman scattering hotspot matrix. 2014 , 136, 5332-41	250
1653	Large area uniform deposition of silver nanoparticles through bio-inspired polydopamine coating on silicon nanowire arrays for practical SERS applications. 2014 , 2, 4894-4900	68
1652	Functionalized Gold Nanoparticles Coated Polymer Spheres as SERS Substrate for the Detection of TNT Explosives. 2014 , 924, 366-370	6
1651	Photoluminescence Plasmonic Enhancement of Single Quantum Dots Coupled to Gold Microplates. 2014 , 118, 8514-8520	29
1650	Evolution of interfacial intercalation chemistry on epitaxial graphene/SiC by surface enhanced Raman spectroscopy. 2014 , 320, 441-447	10
1649	An ink-jet printed, surface enhanced Raman scattering paper for food screening. 2014 , 4, 40487-40493	25
1648	Enhanced light-matter interaction of graphene-gold nanoparticle hybrid films for high-performance SERS detection. 2014 , 2, 4683-4691	70
1647	Gold nanoparticles with tipped surface structures as substrates for single-particle surface-enhanced Raman spectroscopy: concave nanocubes, nanotrisoctahedra, and nanostars. 2014 , 6, 17255-67	107
1646	One-step detection of melamine in milk by hollow gold chip based on surface-enhanced Raman scattering. 2014 , 122, 80-4	40

1645	Tip-enhanced Raman spectroscopy [An interlaboratory reproducibility and comparison study. 2014 , 45, 22-31	82
1644	Size controllable synthesis of ultrafine spherical gold particles and their simulation of plasmonic and SERS behaviors. 2014 , 438, 22-28	8
1643	CO Oxidation on Pt(100): New Insights based on Combined Voltammetric, Microscopic and Spectroscopic Experiments. 2014 , 133, 132-145	21
1642	Mildly O2 plasma treated CVD graphene as a promising platform for molecular sensing. 2014 , 76, 212-219	26
1641	Controlled assembly of gold nanorods on nanopatterned surfaces: Effects of surface materials, pH and surfactant. 2014 , 121, 76-79	4
1640	Carbon cloth surface-decorated with silver nanoparticles for surface-enhanced Raman scattering. 2014 , 584, 635-639	14
1639	Optimal dimensions of gold nanoshells for light backscattering and absorption based applications. 2014 , 146, 468-474	7
1638	In situ SERS monitoring of photocatalytic organic decomposition using recyclable TiO ₂ -coated Ag nanowire arrays. 2014 , 301, 351-357	47
1637	Resonant Mirror Enhanced Raman Spectroscopy. 2014 , 118, 13099-13106	6
1636	Plasmonic Coupling in Single Silver Nanosphere Assemblies by Polarization-Dependent Dark-Field Scattering Spectroscopy. 2014 , 118, 13801-13808	29
1635	Nano-petri-dish array assisted glancing angle sputtering for Ag-NP assembled bi-nanoring arrays as effective SERS substrates. 2014 , 6, 7991-5	19
1634	Highly Intensified Surface Enhanced Raman Scattering by Using Monolayer Graphene as the Nanospacer of Metal Film/Metal Nanoparticle Coupling System. 2014 , 24, 3114-3122	151
1633	Multifunctional Fe ₃ O ₄ @TiO ₂ @Au magnetic microspheres as recyclable substrates for surface-enhanced Raman scattering. 2014 , 6, 5971-9	67
1632	Few-Layer Graphene-Encapsulated Metal Nanoparticles for Surface-Enhanced Raman Spectroscopy. 2014 , 118, 8993-8998	101
1631	Highly sensitive, uniform, and reproducible surface-enhanced Raman spectroscopy from hollow Au-Ag alloy nanourchins. 2014 , 26, 2431-9	212
1630	Functionalized aligned silver nanorod arrays for glucose sensing through surface enhanced Raman scattering. 2014 , 4, 23382	41
1629	Biosynthesis of Ag nanoparticles using pedicellamide and its photocatalytic activity: an eco-friendly approach. 2014 , 132, 687-91	34
1628	The surface adsorption of 2,2'-bipyridine and benzoin on Cu electrode interface probed by surface-enhanced Raman spectroscopy. 2014 , 726, 44-50	2

1627	Surface sol-gel growth of ultrathin SiO ₂ films on roughened Au electrodes: Extending borrowed SERS to a SERS inactive material. 2014 , 608, 35-39	8
1626	High-temperature surface enhanced Raman spectroscopy for in situ study of solid oxide fuel cell materials. 2014 , 7, 306-310	51
1625	Engineered inorganic core/shell nanoparticles. 2014 , 543, 163-197	80
1624	Plasmonic gas and chemical sensing. 2014 , 3, 157-180	74
1623	Effects of atomic geometry and electronic structure of platinum surfaces on molecular adsorbates studied by gap-mode SERS. 2014 , 136, 10299-307	67
1622	Facile synthesis of gold coated copper(II) hydroxide pine-needle-like micro/nanostructures for surface-enhanced Raman scattering. 2014 , 311, 666-671	7
1621	Progress of nanoscience in China. 2014 , 9, 257-288	19
1620	Critical Importance of a Gap Mode in Surface Enhanced Raman Scattering. 2014 , 35, 345-350	
1619	Using Ambient Ion Beams to Write Nanostructured Patterns for Surface Enhanced Raman Spectroscopy. 2014 , 126, 12736-12739	15
1618	Using ambient ion beams to write nanostructured patterns for surface enhanced Raman spectroscopy. 2014 , 53, 12528-31	23
1617	Activation of Oxygen on Gold and Silver Nanoparticles Assisted by Surface Plasmon Resonances. 2014 , 126, 2385-2389	43
1616	Rough surface Au@Ag core-shell nanoparticles to fabricating high sensitivity SERS immunochromatographic sensors. 2015 , 13, 81	34
1615	Self-assembly of Au nanoparticle arrays by porous anodic alumina templates leads to surface-enhanced Raman scattering. 2015 , 19, S1-286-S1-289	
1614	Selectable Nanopattern Arrays for Nanolithographic Imprint and Etch-Mask Applications. 2015 , 2, 1500016	14
1613	Nanoelectrochemistry of Carbon. 2015 , 308-371	
1612	Tunable double-resonance dimer structure for surface-enhanced Raman scattering substrate in near-infrared region. 2015 , 3, 313	7
1611	Strongly hybridized plasmon-photon modes in optoplasmonic microtubular cavities. 2015 , 92,	14
1610	Active magneto-optical control of spontaneous emission in graphene. 2015 , 92,	43

1609	Boron nitride encapsulated copper nanoparticles: a facile one-step synthesis and their effect on thermal decomposition of ammonium perchlorate. 2015 , 5, 16736	38
1608	Highly ordered graphene-isolated silver nanodot arrays as SERS substrate for detection of urinary nucleosides. 2015 , 25, 115601	8
1607	Whispering-gallery nanocavity plasmon-enhanced Raman spectroscopy. 2015 , 5, 15012	34
1606	A New Strategy of Lithography Based on Phase Separation of Polymer Blends. 2015 , 5, 15947	26
1605	Innovative Strategy on Hydrogen Evolution Reaction Utilizing Activated Liquid Water. 2015 , 5, 16263	21
1604	Anisotropic surroundings effects on photo absorption of partially embedded Au nanospheroids in silica glass substrate. 2015 , 5, 027112	2
1603	Electromagnetic field redistribution induced selective plasmon driven surface catalysis in metal nanowire-film systems. 2015 , 5, 17223	6
1602	Near-field mapping of three-dimensional surface charge poles for hybridized plasmon modes. 2015 , 5, 107221	16
1601	A Surface-Enhanced Raman Scattering Sensor Integrated with Battery-Controlled Fluidic Device for Capture and Detection of Trace Small Molecules. 2015 , 5, 12865	17
1600	Internal-Modified Dithiol DNA-Directed Au Nanoassemblies: Geometrically Controlled Self-Assembly and Quantitative Surface-Enhanced Raman Scattering Properties. 2015 , 5, 16715	8
1599	Characterization and noninvasive diagnosis of bladder cancer with serum surface enhanced Raman spectroscopy and genetic algorithms. 2015 , 5, 9582	64
1598	Compact Shielding of Graphene Monolayer Leads to Extraordinary SERS-Active Substrate with Large-Area Uniformity and Long-Term Stability. 2015 , 5, 17167	29
1597	Multiple weak interaction-assisted SERS detection platform for triadimefon. 2015 , 46, 54-58	6
1596	Large scale synthesis of pinhole-free shell-isolated nanoparticles (SHINs) using improved atomic layer deposition (ALD) method for practical applications. 2015 , 46, 1200-1204	23
1595	Solar-Energy-Driven Photoelectrochemical Biosensing Using TiO ₂ Nanowires. 2015 , 21, 11288-99	36
1594	Interfacial Effect of Novel Core-Shell Triple Shell Structured Au@SiO ₂ @Ag@SiO ₂ with Ultrathin SiO ₂ Passivation Layer between the Metal Interfaces on Efficient Dye-Sensitized Solar Cells. 2015 , 2, 1500383	14
1593	Reliable Quantitative SERS Analysis Facilitated by Core-Shell Nanoparticles with Embedded Internal Standards. 2015 , 127, 7416-7420	40
1592	Relevance of Gap Mode Raman Spectroscopy to Various Substrates. 2015 , 36, 363-368	

1591	Research Trends in Electroless Plating Process. 2015 , 66, 438-442	3
1590	Site-Selective Trimetallic Heterogeneous Nanostructures for Enhanced Electrocatalytic Performance. 2015 , 27, 5573-7	41
1589	Ultrabroadband Metasurface for Efficient Light Trapping and Localization: A Universal Surface-Enhanced Raman Spectroscopy Substrate for All Excitation Wavelengths. 2015 , 2, 1500142	44
1588	Gold-based SERS tags for biomedical imaging. 2015 , 17, 114002	59
1587	Facile Preparation of Ultrasmall Void Metallic Nanogap from Self-Assembled Gold-Silica Core-Shell Nanoparticles Monolayer via Kinetic Control. 2015 , 27, 4344-50	69
1586	Spherical Nanoparticle Arrays with Tunable Nanogaps and Their Hydrophobicity Enhanced Rapid SERS Detection by Localized Concentration of Droplet Evaporation. 2015 , 2, 1500031	65
1585	Plasmo-fluidics: Merging Light and Fluids at the Micro-/Nanoscale. 2015 , 11, 4423-44	51
1584	Au nanoparticle-based sensor for apomorphine detection in plasma. 2015 , 6, 2224-32	9
1583	Review of Recent Progress of Plasmonic Materials and Nano-Structures for Surface-Enhanced Raman Scattering. 2015 , 8, 3024-3052	147
1582	RAMAN AND SURFACE ENHANCED RAMAN SIGNALS OF THE SENSOR 1-(4-MERCAPTOPHENYL)-2,4,6-TRIPHENYLPYRIDINIUM PERCHLORATE. 2015 , 60, 2944-2948	2
1581	Highly Stable Surface-Enhanced Raman Spectroscopy Substrates Using Few-Layer Graphene on Silver Nanoparticles. 2015 , 2015, 1-7	11
1580	Thickness-dependent SERS activities of gold nanosheets controllably synthesized via photochemical reduction in lamellar liquid crystals. 2015 , 51, 5116-9	24
1579	Surface-Enhanced Electrochemiluminescence of Ru@SiO ₂ for Ultrasensitive Detection of Carcinoembryonic Antigen. 2015 , 87, 5966-72	126
1578	Band-Edge Bilayer Plasmonic Nanostructure for Surface Enhanced Raman Spectroscopy. 2015 , 2, 1546-1551	10
1577	A durable surface-enhanced Raman scattering substrate: ultrathin carbon layer encapsulated Ag nanoparticle arrays on indium-tin-oxide glass. 2015 , 17, 14849-55	6
1576	Hydrophobic gold nanostructures via electrochemical deposition for sensitive SERS detection of persistent toxic substances. 2015 , 5, 13443-13450	18
1575	A Poly Adenine-Mediated Assembly Strategy for Designing Surface-Enhanced Resonance Raman Scattering Substrates in Controllable Manners. 2015 , 87, 6631-8	43
1574	Surface-Enhanced Raman Scattering-Based Bioimaging. 2015 , 325-346	

1573	Electron beam lithography tri-layer lift-off to create ultracompact metal/metal oxide 2D patterns on CaF ₂ substrate for surface-enhanced infrared spectroscopy. 2015 , 141, 87-91	5
1572	A multimodal imaging agent for intrinsic surface enhanced Raman scattering of biological tissue. 2015 ,	
1571	Chemically synthesized noble metal nanostructures for plasmonics. 2015 , 4,	14
1570	Jellyfish mesoglea as a matrix for the synthesis of extremely high content silver dendrites. 2015 , 454, 14-9	10
1569	Atomic-layer-deposited silver and dielectric nanostructures for plasmonic enhancement of Raman scattering from nanoscale ultrathin films. 2015 , 26, 265702	10
1568	Highly-reproducible Raman scattering of NaYF ₄ :Yb,Er@SiO ₂ @Ag for methylamphetamine detection under near-infrared laser excitation. 2015 , 140, 5268-75	12
1567	The field enhancement and optical sensing in the surface photonic crystal. 2015 ,	1
1566	Plasmonics in Analytical Spectroscopy. 2015 , 269-301	
1565	Probing a dip-coated layer of organic molecules by an aerosol nanoparticle sensor with sub-100 nm resolution based on surface-enhanced Raman scattering. 2015 , 5, 5158-5163	3
1564	Gold Nanorod Rotary Motors Driven by Resonant Light Scattering. 2015 , 9, 12542-51	82
1563	Controlled stepwise-synthesis of core-shell Au@MIL-100 (Fe) nanoparticles for sensitive surface-enhanced Raman scattering detection. 2015 , 140, 8165-71	38
1562	Optical integrated chips with micro and nanostructures for refractive index and SERS-based optical label-free sensing. 2015 , 4, 419-436	9
1561	3-Mercapto-1-Propanesulfonate for Cu Electrodeposition Studied by in Situ Shell-Isolated Nanoparticle-Enhanced Raman Spectroscopy, Density Functional Theory Calculations, and Cyclic Voltammetry. 2015 , 119, 23453-23462	28
1560	Protected hollow metal nanoresonators for Raman analysis of surfaces. 2015 ,	
1559	Recent advances in plasmonic nanostructures for sensing: a review. 2015 , 54, 100902	72
1558	Broadband plasmon-induced transparency in terahertz metamaterials via constructive interference of electric and magnetic couplings. 2015 , 23, 27361-8	44
1557	Hierarchical porous plasmonic metamaterials for reproducible ultrasensitive surface-enhanced Raman spectroscopy. 2015 , 27, 1090-6	162
1556	Rapid Au recovery from aqueous solution by a microorganism-mediated, surfactant-directed approach: Effect of surfactants and SERS of bio-Au. 2015 , 267, 43-50	10

1555	Urchin-like LaVO ₃ /Au composite microspheres for surface-enhanced Raman scattering detection. 2015 , 443, 80-7	16
1554	Analysis of polycyclic aromatic hydrocarbons in water with gold nanoparticles decorated hydrophobic porous polymer as surface-enhanced Raman spectroscopy substrate. 2015 , 139, 214-21	25
1553	Au/Ag bimetal nanogap arrays with tunable morphologies for surface-enhanced Raman scattering. 2015 , 5, 7454-7460	17
1552	Ultrasensitive SERS assay of lysozyme using a novel and unique four-way helical junction molecule probe for signal amplification. 2015 , 51, 907-10	15
1551	Free radical-quenched SERS probes for detecting H ₂ O ₂ and glucose. 2015 , 140, 2741-6	23
1550	Optofluidic microsystem with quasi-3 dimensional gold plasmonic nanostructure arrays for online sensitive and reproducible SERS detection. 2015 , 863, 41-8	18
1549	Plasmonics-enhanced metal-organic framework nanoporous films for highly sensitive near-infrared absorption. 2015 , 3, 2763-2767	33
1548	Plasmonics of multifaceted metallic nanoparticles, field enhancement, and TERS. 2015 , 252, 56-71	9
1547	Sailing into uncharted waters: recent advances in the in situ monitoring of catalytic processes in aqueous environments. 2015 , 5, 3035-3060	36
1546	A sensitive SERS substrate based on Au/TiO ₂ /Au nanosheets. 2015 , 142, 50-4	19
1545	Fabrication of Au nanorod-coated Fe ₃ O ₄ microspheres as SERS substrate for pesticide analysis by near-infrared excitation. 2015 , 46, 470-475	48
1544	Facile synthesis of Fe ₂ O ₃ @SnO ₂ core-shell heterostructure nanotubes for high performance gas sensors. 2015 , 213, 27-34	89
1543	Electromagnetic Enhancement in Shell-Isolated Nanoparticle-Enhanced Raman Scattering from Gold Flat Surfaces. 2015 , 119, 5246-5251	33
1542	Facile fabrication of a silver dendrite-integrated chip for surface-enhanced Raman scattering. 2015 , 7, 2931-6	42
1541	SERS-Enabled Lab-on-a-Chip Systems. 2015 , 3, 618-633	72
1540	Electrochemical shell-isolated nanoparticle-enhanced Raman spectroscopy: correlating structural information and adsorption processes of pyridine at the Au(hkl) single crystal/solution interface. 2015 , 137, 2400-8	79
1539	Critical assessment of enhancement factor measurements in surface-enhanced Raman scattering on different substrates. 2015 , 17, 21294-301	28
1538	Highly sensitive surface-enhanced Raman scattering based on multi-dimensional plasmonic coupling in Au-graphene-Ag hybrids. 2015 , 51, 866-9	53

1537	Ultrasound-mediated method for rapid delivery of nano-particles into cells for intracellular surface-enhanced Raman spectroscopy and cancer cell screening. 2015 , 26, 065101	25
1536	Magnetically optimized SERS assay for rapid detection of trace drug-related biomarkers in saliva and fingerprints. 2015 , 68, 350-357	61
1535	Prospects for plasmonic hot spots in single molecule SERS towards the chemical imaging of live cells. 2015 , 17, 21072-93	197
1534	Preparation of surface-enhanced Raman scattering(SERS)-active optical fiber sensor by laser-induced Ag deposition and its application in bioidentification of biotin/avidin. 2015 , 31, 25-30	7
1533	Facile and generalized encapsulations of inorganic nanocrystals with nitrogen-doped carbonaceous coating for multifunctionality. 2015 , 7, 3254-62	10
1532	Three-dimensional nanostructured $\text{NiO} \cdot 3(\text{VO}_4)_2$ compound on nickel foam as pseudocapacitive electrodes for electrochemical capacitors. 2015 , 627, 313-319	15
1531	Plasmonic core-shell nanoparticles for SERS detection of the pesticide thiram: size- and shape-dependent Raman enhancement. 2015 , 7, 2862-8	122
1530	Facile and sensitive glucose sandwich assay using in situ-generated Raman reporters. 2015 , 87, 2016-21	53
1529	Controlled formation of core-shell structures with uniform AlPO_4 nanoshells. 2015 , 51, 2943-2945	15
1528	CTAB micelles assisted rGO-AgNP hybrids for SERS detection of polycyclic aromatic hydrocarbons. 2015 , 17, 21158-63	16
1527	Surface-enhanced Raman spectroscopy + support vector machine: a new noninvasive method for prostate cancer screening?. 2015 , 15, 5-7	8
1526	Size-controlled synthesis of Pd nanosheets for tunable plasmonic properties. 2015 , 17, 1833-1838	63
1525	Fabrication of highly-specific SERS substrates by co-precipitation of functional nanomaterials during the self-sedimentation of silver nanowires into a nanoporous film. 2015 , 51, 1309-12	22
1524	Applications of shell-isolated nanoparticles in surface-enhanced Raman spectroscopy and fluorescence. 2015 , 66, 103-117	32
1523	Surpassingly competitive electromagnetic field enhancement at the silica/silver interface for selective intracellular surface enhanced Raman scattering detection. 2015 , 9, 2820-35	22
1522	Tuning interior nanogaps of double-shelled Au/Ag nanoboxes for surface-enhanced Raman scattering. 2015 , 5, 8382	33
1521	Study on surface-enhanced Raman scattering substrates structured with hybrid Ag nanoparticles and few-layer graphene. 2015 , 87, 385-394	37
1520	Optical super-resolution microscopy and its applications in nano-catalysis. 2015 , 8, 441-455	16

1519	Plasmonic Absorption Enhancement of a Single Quantum Dot. 2015 , 10, 955-962	3
1518	Exploitation of desilylation chemistry in tailor-made functionalization on diverse surfaces. 2015 , 6, 6403	22
1517	A Ag-molecularly imprinted polymer composite for efficient surface-enhanced Raman scattering activities under a low-energy laser. 2015 , 140, 3239-43	23
1516	Conductive Lewis Base Matrix to Recover the Missing Link of Li ₂ S ₈ during the Sulfur Redox Cycle in Li ₂ S Battery. 2015 , 27, 2048-2055	258
1515	Microchip-Based Surface Enhanced Raman Spectroscopy for the Determination of Sodium Thiocyanate in Milk. 2015 , 48, 1930-1940	13
1514	Methods of photoelectrode characterization with high spatial and temporal resolution. 2015 , 8, 2863-2885	42
1513	Bio-inspired synthesis of metal nanomaterials and applications. 2015 , 44, 6330-74	317
1512	Fast assembling microarrays of superparamagnetic Fe ₃ O ₄ @Au nanoparticle clusters as reproducible substrates for surface-enhanced Raman scattering. 2015 , 7, 13427-37	28
1511	Dielectric shell modulated plasmonic crystal for novel light absorption meta-surface. 2015 , 158, 262-265	2
1510	In Situ Monitoring of Electrooxidation Processes at Gold Single Crystal Surfaces Using Shell-Isolated Nanoparticle-Enhanced Raman Spectroscopy. 2015 , 137, 7648-51	89
1509	A SERS study of oxidation of glutathione under plasma irradiation. 2015 , 5, 57847-57852	13
1508	Polyethylenimine-interlayered silver-shell magnetic-core microspheres as multifunctional SERS substrates. 2015 , 3, 8684-8693	44
1507	DNA-hybrid-gated functional mesoporous silica for sensitive DNA methyltransferase SERS detection. 2015 , 51, 13983-5	27
1506	Geometrical and morphological optimizations of plasmonic nanoarrays for high-performance SERS detection. 2015 , 7, 15487-94	30
1505	Graphene-based hybrid films for plasmonic sensing. 2015 , 7, 14561-76	37
1504	Recent progress in the applications of graphene in surface-enhanced Raman scattering and plasmon-induced catalytic reactions. 2015 , 3, 9024-9037	100
1503	Monolithic nanoporous gold disks with large surface area and high-density plasmonic hot-spots. 2015 ,	
1502	Dimeric Core-shell Ag ₂ @TiO ₂ Nanoparticles for Off-Resonance Raman Study of the TiO ₂ /Ag Interface. 2015 , 119, 18396-18403	16

1501	Gallium/gold composite microspheres fixed on a silicon substrate for surface enhanced Raman scattering. 2015 , 5, 67134-67140	4
1500	How Far Can We Probe by SERS?. 2015 , 119, 20057-20064	39
1499	Fabrication of ordered mullite nanowhisker array with surface enhanced Raman scattering effect. 2015 , 5, 9690	9
1498	Hot electron-induced reduction of small molecules on photorecycling metal surfaces. 2015 , 6, 7570	171
1497	Thickness of a metallic film, in addition to its roughness, plays a significant role in SERS activity. 2015 , 5, 11644	57
1496	In situ SERS detection of multi-class insecticides on plant surfaces. 2015 , 7, 6325-6330	48
1495	Silicon dioxide covered Au and Ag nanoparticles for shell-isolated nanoparticle enhanced spectroscopies in the near-infrared. 2015 , 5, 59373-59378	7
1494	A graphene-interlayered magnetic composite as a multifunctional SERS substrate. 2015 , 5, 62101-62109	10
1493	Gold Nanoparticles for In Vitro Diagnostics. 2015 , 115, 10575-636	598
1492	Quantitative Plasmon Mode and Surface-Enhanced Raman Scattering Analyses of Strongly Coupled Plasmonic Nanotrimers with Diverse Geometries. 2015 , 15, 4628-36	43
1491	Effect of adsorbed molecules on surface-enhanced Raman scattering of metal/molecule/metal junctions. 2015 , 5, 55720-55726	1
1490	Terahertz plasmon-polariton modes in graphene driven by electric field inside a Fabry-Pérot cavity. 2015 , 117, 223104	11
1489	Fabrication and robotization of ultrasensitive plasmonic nanosensors for molecule detection with Raman scattering. 2015 , 15, 10422-51	11
1488	Plasmonic Ag Core-Satellite Nanostructures with a Tunable Silica-Spaced Nanogap for Surface-Enhanced Raman Scattering. 2015 , 31, 8129-37	31
1487	Strong Dependence in Surface-Enhanced Raman Scattering of Pyridine on Stable 13-Atom Silver-Caged Bimetallic Clusters. 2015 , 119, 17429-17437	15
1486	Wavelength-Selective Photocatalysis Using GoldPlatinum Nanorattles. 2015 , 119, 18618-18626	12
1485	Sensing using plasmonic nanostructures and nanoparticles. 2015 , 26, 322001	169
1484	Spectroscopic Imaging. 2015 , 69, 339-384	4

1483	Fabrication of superstable gold nanorod-carbon nanocapsule as a molecule loading material. 2015 , 60, 1101-1107	15
1482	Lighting up the Raman signal of molecules in the vicinity of graphene related materials. 2015 , 48, 1862-70	115
1481	Growth graphene on silver-copper nanoparticles by chemical vapor deposition for high-performance surface-enhanced Raman scattering. 2015 , 353, 63-70	36
1480	Separation of Silver Nanocrystals for Surface-enhanced Raman Scattering Using Density Gradient Centrifugation. 2015 , 31, 834-839	
1479	TiO ₂ hollow spheres with nanoporous structures fabricated by anodization of Ti particles. 2015 , 5, 41830-41834	
1478	"Elastic" property of mesoporous silica shell: for dynamic surface enhanced Raman scattering ability monitoring of growing noble metal nanostructures via a simplified spatially confined growth method. 2015 , 7, 7516-25	45
1477	Improvement of surface-enhanced Raman scattering by dipolar resonance mode of silver half-shell array. 2015 , 120, 11-16	4
1476	Laser hybrid micro/nano-structuring of Si surfaces in air and its applications for SERS detection. 2014 , 4, 6657	31
1475	In situ growth of three-dimensional graphene coatings on arbitrary-shaped micro/nano materials and its mechanism studies. 2015 , 92, 84-95	15
1474	Explosive and chemical threat detection by surface-enhanced Raman scattering: a review. 2015 , 893, 1-13	205
1473	Structures, stabilities and properties of hollow (Al ₂ O ₃) _n clusters (n=10, 12, 16, 18, 24 and 33): Studied with density functional theory. 2015 , 1063, 29-34	5
1472	Surface- and Tip-Enhanced Raman Spectroscopy as Operando Probes for Monitoring and Understanding Heterogeneous Catalysis. 2015 , 145, 40-57	49
1471	Improved properties of gold nanorods coated with thin multilayer of small organic molecules by fast and facile method for surface enhanced Raman scattering. 2015 , 47, 2759-2766	
1470	Guided formation of sub-5 nm interstitial gaps between plasmonic nanodisks. 2015 , 7, 8338-42	11
1469	Oxidative unzipping of stacked nitrogen-doped carbon nanotube cups. 2015 , 7, 10734-41	9
1468	Reliable Quantitative SERS Analysis Facilitated by Core-Shell Nanoparticles with Embedded Internal Standards. 2015 , 54, 7308-12	272
1467	Silica-coated gold nanostars for surface-enhanced resonance Raman spectroscopy mapping of integrins in breast cancer cells. 2015 ,	3
1466	Silicon-nanoparticles isolated by in situ grown polycrystalline graphene hollow spheres for enhanced lithium-ion storage. 2015 , 3, 7810-7821	37

1465	Hybrid nanostructures for SERS: materials development and chemical detection. 2015 , 17, 21046-71	123
1464	Self-assembled plasmonic templates produced by microwave annealing: applications to surface-enhanced Raman scattering. 2015 , 26, 205603	12
1463	Graphene/Cu nanoparticle hybrids fabricated by chemical vapor deposition as surface-enhanced Raman scattering substrate for label-free detection of adenosine. 2015 , 7, 10977-87	140
1462	Plasmonic Silver Supercrystals with Ultrasmall Nanogaps for Ultrasensitive SERS-Based Molecule Detection. 2015 , 3, 404-411	51
1461	SERS-based approaches toward genetic profiling. 2015 , 7, 263-78	11
1460	Electrochemical synthesis of mesoporous gold films toward mesospace-stimulated optical properties. 2015 , 6, 6608	151
1459	ZnO-nanotaper array sacrificial templated synthesis of noble-metal building-block assembled nanotube arrays as 3D SERS-substrates. 2015 , 8, 957-966	59
1458	Comparison of the plasmonic performances between lithographically fabricated and chemically grown gold nanorods. 2015 , 17, 10861-70	39
1457	Dimer-on-mirror SERS substrates with attogram sensitivity fabricated by colloidal lithography. 2015 , 7, 9405-10	89
1456	Fiber-optic SERS microfluidic chip based on light-induced gold nano-particle aggregation. 2015 , 352, 148-154	7
1455	Optical response and SERS properties of individual large scale supracrystals made of small silver nanocrystals. 2015 , 8, 1615-1626	17
1454	Engineering of SERS Substrates Based on Noble Metal Nanomaterials for Chemical and Biomedical Applications. 2015 , 50, 499-525	62
1453	Semiconductor-enhanced Raman scattering for highly robust SERS sensing: the case of phosphate analysis. 2015 , 51, 7641-4	48
1452	Selective and sensitive SERS sensor for detection of Hg ²⁺ in environmental water base on rhodamine-bonded and amino group functionalized SiO ₂ -coated Au@Ag core-shell nanorods. 2015 , 5, 32168-32174	28
1451	Quantitative SHINERS analysis of temporal changes in the passive layer at a gold electrode surface in a thiosulfate solution. 2015 , 87, 3791-9	30
1450	Rolling-circle amplification detection of thrombin using surface-enhanced Raman spectroscopy with core-shell nanoparticle probe. 2015 , 21, 6817-22	19
1449	Plasmon-free SERS self-monitoring of catalysis reaction on Au nanoclusters/TiO ₂ photonic microarray. 2015 , 51, 8813-6	45
1448	Plasmonics and Ultrasensitive Detection. 2015 , 21-44	

1447	Probing zeolites by vibrational spectroscopies. 2015 , 44, 7262-341	241
1446	Surface-enhanced Raman scattering on a silver film-modified Au nanoparticle-decorated SiO ₂ mask array. 2015 , 5, 66096-66103	2
1445	A nanotweezer system for evanescent wave excited surface enhanced Raman spectroscopy (SERS) of single nanoparticles. 2015 , 23, 6793-802	31
1444	Pursuing shell-isolated nanoparticle-enhanced Raman spectroscopy (SHINERS) for concomitant detection of breast lesions and microcalcifications. 2015 , 7, 16960-8	33
1443	Dielectric shell isolated and graphene shell isolated nanoparticle enhanced Raman spectroscopies and their applications. 2015 , 44, 8399-409	104
1442	Magnetically Assisted Surface-Enhanced Raman Spectroscopy for the Detection of Staphylococcus aureus Based on Aptamer Recognition. 2015 , 7, 20919-29	127
1441	Nanooptics of Plasmonic Nanomatryoshkas: Shrinking the Size of a Core-Shell Junction to Subnanometer. 2015 , 15, 6419-28	106
1440	Control of localized surface plasmon resonance energy in monolayer structures of gold and silver nanoparticles. 2015 , 17, 27077-81	9
1439	Solution processed nanomanufacturing of SERS substrates with random Ag nanoholes exhibiting uniformly high enhancement factors. 2015 , 5, 85019-85027	6
1438	Plasmon resonances of Ag capped Si nanopillars fabricated using mask-less lithography. 2015 , 23, 12965-78	45
1437	Planar monolithic porous polymer layers functionalized with gold nanoparticles as large-area substrates for sensitive surface-enhanced Raman scattering sensing of bacteria. 2015 , 896, 111-9	18
1436	A portable microcolumn based on silver nanoparticle functionalized glass fibers and its SERS application. 2015 , 140, 7934-8	11
1435	Metal Nanoparticle-Nanowire Assisted SERS on Film. 2015 , 119, 19376-19381	22
1434	Highly Symmetric Gold Nanostars: Crystallographic Control and Surface-Enhanced Raman Scattering Property. 2015 , 137, 10460-3	206
1433	Plasmon-induced resonance energy transfer for solar energy conversion. 2015 , 9, 601-607	446
1432	Molten salt synthesis of mullite nanowhiskers using different silica sources. 2015 , 22, 884-891	9
1431	"Smart" Ag Nanostructures for Plasmon-Enhanced Spectroscopies. 2015 , 137, 13784-7	132
1430	Surface-Enhanced Raman Scattering Based on Controllable-Layer Graphene Shells Directly Synthesized on Cu Nanoparticles for Molecular Detection. 2015 , 16, 2953-60	19

1429	Large-Scale Hot Spot Engineering for Quantitative SERS at the Single-Molecule Scale. 2015 , 137, 13698-705	252
1428	Top-down patterning and self-assembly of flower-like gold arrays for surface enhanced Raman spectroscopy. 2015 , 356, 1314-1319	13
1427	Fiber-optic SERS detection enabled by light-induced gold nano-particle aggregation. 2015 ,	
1426	Large-Scale Plasmonic nanoCones Array For Spectroscopy Detection. 2015 , 7, 23597-604	28
1425	Nanogap effects on near- and far-field plasmonic behaviors of metallic nanoparticle dimers. 2015 , 17, 29293-8	49
1424	High performance SERS active substrates fabricated by directly growing graphene on Ag nanoparticles. 2015 , 5, 90457-90465	28
1423	Oxidative Etching and Metal Overgrowth of Gold Nanorods within Mesoporous Silica Shells. 2015 , 27, 7196-7203	30
1422	Polyethylenimine-interlayered core-shell-satellite 3D magnetic microspheres as versatile SERS substrates. 2015 , 7, 18694-707	54
1421	Silica-Protected Hollow Silver and Gold Nanoparticles: New Material for Raman Analysis of Surfaces. 2015 , 119, 20030-20038	28
1420	Portable SERS-enabled micropipettes for microarea sampling and reliably quantitative detection of surface organic residues. 2015 , 87, 9217-24	71
1419	Plasmomechanics: A Colour-Changing Device Based on the Plasmonic Coupling of Gold Nanoparticles. 2015 , 614, 20-29	9
1418	Gold Nanomaterials at Work in Biomedicine. 2015 , 115, 10410-88	818
1417	Controllable synthesis of tetrapod gold nanocrystals with precisely tunable near-infrared plasmon resonance towards highly efficient surface enhanced Raman spectroscopy bioimaging. 2015 , 3, 7377-7385	26
1416	SERS Nanoparticles in Medicine: From Label-Free Detection to Spectroscopic Tagging. 2015 , 115, 10489-529	576
1415	Electrochemical Tip-Enhanced Raman Spectroscopy. 2015 , 137, 11928-31	193
1414	Surface-enhanced Raman scattering effect of ordered gold nanoparticle array for rhodamine B with different morphologies. 2015 , 33, 1470-1476	9
1413	Characterization of a Self-Assembled Monolayer of 1-Thio- β -D-Glucose with Electrochemical Surface Enhanced Raman Spectroscopy Using a Nanoparticle Modified Gold Electrode. 2015 , 31, 10076-86	14
1412	Plasmon-Enhanced Second-Harmonic Generation Nanorulers with Ultrahigh Sensitivities. 2015 , 15, 6716-21	69

1411	Rapid separation and on-line detection by coupling high performance liquid chromatography with surface-enhanced Raman spectroscopy. 2015 , 5, 47640-47646	35
1410	Fabrication of a Au/polystyrene sphere substrate with three-dimensional nanostructures for surface-enhanced Raman spectroscopy. 2015 , 355, 1168-1174	18
1409	Nanomaterials and Nanoarchitectures. 2015 ,	5
1408	Target-induced nanocatalyst deactivation facilitated by core@shell nanostructures for signal-amplified headspace-colorimetric assay of dissolved hydrogen sulfide. 2015 , 87, 10153-60	75
1407	Nitrogen-doped graphene network supported copper nanoparticles encapsulated with graphene shells for surface-enhanced Raman scattering. 2015 , 7, 17079-87	25
1406	Surface-enhanced Raman spectroscopy on single Fe ₂ O ₃ @Au spindle nanoparticle: polarization dependence and FDTD simulation. 2015 , 17, 114014	4
1405	Intensity enhancement of vibrational sum frequency generation by gap-mode plasmon resonance. 2015 , 639, 83-87	5
1404	Selective plasmon driven surface catalysis in metal triangular nanoplate-molecule-film sandwich structure. 2015 , 639, 47-51	6
1403	In situ monitoring of palladacycle-mediated carbonylation by surface-enhanced Raman spectroscopy. 2015 , 5, 97734-97737	3
1402	Preparation of sensitive and recyclable porous Ag/TiO ₂ composite films for SERS detection. 2015 , 359, 853-859	25
1401	Synthesis of surface-imprinted Ag nanoplates for detecting organic pollutants in water environments based on surface enhanced Raman scattering. 2015 , 5, 99914-99919	19
1400	Vibrational Spectroscopic Observation of Atomic-Scale Local Surface Sites Using Site-Selective Signal Enhancement. 2015 , 15, 7982-6	22
1399	Reversible gating of smart plasmonic molecular traps using thermoresponsive polymers for single-molecule detection. 2015 , 6, 8797	67
1398	Hydrogen-Induced Tuning of Plasmon Resonance in Palladium/Silver Layered Nanodimer Arrays. 2015 , 2, 66-72	10
1397	Biosynthesis of Silver and Gold Nanoparticles Using Huangdan (Camellia sinensis) Leaf Extract. 2015 , 45, 941-946	8
1396	Headspace thin-film microextraction coupled with surface-enhanced Raman scattering as a facile method for reproducible and specific detection of sulfur dioxide in wine. 2015 , 87, 633-40	46
1395	Highly uniform and reproducible surface enhanced Raman scattering on air-stable metallic glassy nanowire array. 2014 , 4, 5835	78
1394	Extraction of absorption and scattering contribution of metallic nanoparticles toward rational synthesis and application. 2015 , 87, 1058-65	40

1393	Fabrication of graphene-isolated-Au-nanocrystal nanostructures for multimodal cell imaging and photothermal-enhanced chemotherapy. 2014 , 4, 6093	83
1392	A highly-ordered and uniform sunflower-like dendritic silver nanocomplex array as reproducible SERS substrate. 2015 , 5, 3860-3867	5
1391	Silver nano-dendritic crystal film: a rapid dehydration SERS substrate of totally new concept. 2015 , 5, 4578-4585	11
1390	Shell-isolated nanoparticle-enhanced fluorescence (SHINEF) of CdTe quantum dots. 2015 , 151, 351-356	8
1389	Gold-nanoparticle, functionalized-porous-polymer monolith enclosed in capillary for on-column SERS detection. 2015 , 7, 1349-1357	16
1388	Highly reproducible SERS arrays directly written by inkjet printing. 2015 , 7, 421-5	73
1387	Plasmon-driven surface catalysis in hybridized plasmonic gap modes. 2014 , 4, 7087	47
1386	Gold nanoparticle-doped silk film as biocompatible SERS substrate. 2015 , 5, 1937-1942	19
1385	SERS-based pesticide detection by using nanofinger sensors. 2015 , 26, 015502	63
1384	Plasmonic nanorod arrays of a two-segment dimer and a coaxial cable with 1 nm gap for large field confinement and enhancement. 2015 , 7, 1463-70	17
1383	Hierarchically assembled NiCo@SiO ₂ @Ag magnetic core-shell microspheres as highly efficient and recyclable 3D SERS substrates. 2015 , 140, 440-8	12
1382	A theoretical and experimental approach to shell-isolated nanoparticle-enhanced Raman spectroscopy of single-crystal electrodes. 2015 , 631, 73-80	26
1381	Smart liquid SERS substrates based on Fe ₃ O ₄ /Au nanoparticles with reversibly tunable enhancement factor for practical quantitative detection. 2014 , 4, 7204	33
1380	The effect of dielectric constants on noble metal/semiconductor SERS enhancement: FDTD simulation and experiment validation of Ag/Ge and Ag/Si substrates. 2014 , 4, 4052	59
1379	Graphene oxide shell-isolated Ag nanoparticles for surface-enhanced Raman scattering. 2015 , 81, 767-772	82
1378	Physical deposition improved SERS stability of morphology controlled periodic micro/nanostructured arrays based on colloidal templates. 2015 , 11, 844-53	112
1377	The electronic structure of metal-molecule hybrids in charged interfaces: surface-enhanced Raman selection rules derived from plasmon-like resonances. 2015 , 17, 2326-9	16
1376	Principles and applications of Raman spectroscopy in pharmaceutical drug discovery and development. 2015 , 10, 187-206	26

1375	Innovative strategy with potential to increase hemodialysis efficiency and safety. 2014 , 4, 4425	28
1374	Synthesis and characterization of vinyl-functionalized magnetic nanofibers for protein imprinting. 2015 , 51, 202-5	27
1373	Sensitive detection of point mutation using exponential strand displacement amplification-based surface enhanced Raman spectroscopy. 2015 , 65, 191-7	29
1372	Released plasmonic electric field of ultrathin tetrahedral-amorphous-carbon films coated Ag nanoparticles for SERS. 2014 , 4, 4494	20
1371	Enhancing effects of gold nanorods on luminescence of dyes. 2015 , 157, 126-130	7
1370	One-step shell polymerization of inorganic nanoparticles and their applications in SERS/nonlinear optical imaging, drug delivery, and catalysis. 2014 , 4, 5593	35
1369	Nanoparticle characterization based on STM and STS. 2015 , 44, 970-87	61
1368	Self-assembled vertically aligned gold nanorod superlattices for ultra-high sensitive detection of molecules. 2015 , 8, 907-919	22
1367	Linear and nonlinear optical properties of hybrid metallic-dielectric plasmonic nanoantennas. 2016 , 7, 111-20	22
1366	Metal-enhanced fluorescence of single shell-isolated alloy metal nanoparticle. 2016 , 55, 9131-9136	10
1365	Plasmon-driven surface catalysis on photochemically deposited-based SERS substrates. 2016 , 55, 8468-8471	3
1364	Aptamer-Based Technologies in Foodborne Pathogen Detection. 2016 , 7, 1426	46
1363	A Nanostructured SERS Switch Based on Molecular Beacon-Controlled Assembly of Gold Nanoparticles. 2016 , 6,	7
1362	Synthesis of Ball-Like Ag Nanorod Aggregates for Surface-Enhanced Raman Scattering and Catalytic Reduction. 2016 , 6,	4
1361	Surface-enhanced Raman scattering activities of graphene-wrapped Cu particles by chemical vapor deposition assisted with thermal annealing. 2016 , 24, 24551-24566	4
1360	Silver Nanoparticle-Embedded Thin Silica-Coated Graphene Oxide as an SERS Substrate. 2016 , 6,	11
1359	Development of a Loop Mediated Isothermal Amplification (LAMP) - Surface Enhanced Raman spectroscopy (SERS) Assay for the Detection of Salmonella Enterica Serotype Enteritidis. 2016 , 6, 522-32	45
1358	Potential dependent thiocyanate adsorption on gold electrodes: a comparison study between SERS and SHINERS. 2016 , 47, 1207-1212	12

1357	Highly Ordered Ag/Cu Hybrid Nanostructure Arrays for Ultrasensitive Surface-Enhanced Raman Spectroscopy. 2016 , 3, 1600115	19
1356	Bacterial Nanocellulose-Based Flexible Surface Enhanced Raman Scattering Substrate. 2016 , 3, 1600214	49
1355	Plasmonic AgAl Bimetallic Alloy Nanoparticle/Al ₂ O ₃ Nanocermet Thin Films with Robust Thermal Stability for Solar Thermal Applications. 2016 , 3, 1600248	20
1354	Probing single molecules and molecular aggregates: Raman spectroscopic advances. 2016 , 47, 623-635	12
1353	Active Gap SERS for the Sensitive Detection of Biomacromolecules with Plasmonic Nanostructures on Hydrogels. 2016 , 4, 259-263	37
1352	Fabrication and surface enhanced Raman spectroscopy of single Au@SiO ₂ dimers linked by benzenedithiol. 2016 , 47, 537-544	3
1351	Synthesis of hierarchical carbon sphere@NiMoO ₄ composite materials for supercapacitor electrodes. 2016 , 42, 15694-15700	39
1350	Review of surface enhanced Raman spectroscopic (SERS) detection of synthetic chemical pesticides. 2016 , 85, 73-82	251
1349	Surface-Enhanced Raman Scattering Active Plasmonic Nanoparticles with Ultrasmall Interior Nanogap for Multiplex Quantitative Detection and Cancer Cell Imaging. 2016 , 88, 7828-36	63
1348	Highly sensitive and reproducible silicon-based surface-enhanced Raman scattering sensors for real applications. 2016 , 141, 5010-9	27
1347	Creating SERS hot spots on length adjustable AgVO ₃ nanobelts. 2016 , 677, 12-17	7
1346	Boron Nitride Nanosheets Improve Sensitivity and Reusability of Surface-Enhanced Raman Spectroscopy. 2016 , 55, 8405-9	58
1345	Plasmonic Indium Nanoparticle-Induced High-Performance Photoswitch for Blue Light Detection. 2016 , 4, 291-296	25
1344	Boron Nitride Nanosheets Improve Sensitivity and Reusability of Surface-Enhanced Raman Spectroscopy. 2016 , 128, 8545-8549	12
1343	A monolayer of hierarchical silver hemi-mesoparticles with tunable surface topographies for highly sensitive surface-enhanced Raman spectroscopy. 2016 , 144, 074703	6
1342	Hybridized plasmon modes and near-field enhancement of metallic nanoparticle-dimer on a mirror. 2016 , 6, 30011	66
1341	Hexagonal Boron Nitride/Au Substrate for Manipulating Surface Plasmon and Enhancing Capability of Surface-Enhanced Raman Spectroscopy. 2016 , 10, 11156-11162	44
1340	Magnetic-Polaron-Induced Enhancement of Surface Raman Scattering. 2016 , 6, 19025	10

1339	A hybrid system with highly enhanced graphene SERS for rapid and tag-free tumor cells detection. 2016 , 6, 25134	37
1338	Template Synthesis of Noble Metal Nanocrystals with Unusual Crystal Structures and Their Catalytic Applications. 2016 , 49, 2841-2850	139
1337	Plasmon Enhanced Raman Scattering from Molecular Adsorbates on Atomically Defined Planar Metal Surfaces. 2016 , 41-55	
1336	FDTD simulation study of size/gap and substrate-dependent SERS activity study of Au@SiO ₂ nanoparticles. 2016 , 25, 083301	12
1335	Surface-Enhanced Raman Scattering of Biological Materials. 2016 , 1-29	2
1334	Hotspot-engineered quasi-3D metallic network for surface-enhanced Raman scattering based on colloid monolayer templating. 2016 , 109, 121108	15
1333	Wavelength modulated SERS hot spot distribution in 1D nanostructures on metal film. 2016 , 49, 425301	5
1332	Research on the photochemical kinetics process of gold nanoparticle-doped photopolymer system using Raman spectroscopy. 2016 ,	
1331	Surface chemical bonds, surface-enhanced Raman scattering, and dielectric constant of SiO ₂ nanospheres in-situ decorated with Ag-nanoparticles by electron-irradiation. 2016 , 120, 234901	8
1330	Synthesis and improved SERS performance of silver nanoparticles-decorated surface mesoporous silica microspheres. 2016 , 378, 181-190	20
1329	Heterodimer Nanostructures Induced Energy Focusing on Metal Film. 2016 , 120, 7778-7784	16
1328	Sequential determination of trace 4-aminoazobenzene in multiple textiles based on nanoarrayed functionalized polystyrene substrate by surface enhanced Raman spectroscopy. 2016 , 154, 346-53	6
1327	Single nanowire on graphene (SNOG) as an efficient, reproducible, and stable SERS-active platform. 2016 , 8, 8878-86	21
1326	Silver nanoparticles on cotton swabs for improved surface-enhanced Raman scattering, and its application to the detection of carbaryl. 2016 , 183, 1307-1313	49
1325	Hybrid nanostructures of metal/two-dimensional nanomaterials for plasmon-enhanced applications. 2016 , 45, 3145-87	281
1324	Structural and optical control of DNA-mediated Janus plasmonic nanostructures. 2016 , 8, 9337-42	6
1323	Surface enhanced Raman scattering (SERS) fabrics for trace analysis. 2016 , 386, 296-302	37
1322	Investigation of amorphous SiO _x layer on gold surface for Surface Plasmon Resonance measurements. 2016 , 163, 43-48	9

1321	Recent topics on single-molecule fluctuation analysis using blinking in surface-enhanced resonance Raman scattering: clarification by the electromagnetic mechanism. 2016 , 141, 5000-9	31
1320	Observation of gold electrode surface response to the adsorption and oxidation of thiocyanate in acidic electrolyte with broadband sum-frequency generation spectroscopy. 2016 , 85, 122-127	8
1319	Superhydrophobic SERS chip based on a Ag coated natural taro-leaf. 2016 , 8, 11487-93	64
1318	Improved H ₂ S gas sensing properties of ZnO nanorods via decoration of nano-porous SiO ₂ thin layers. 2016 , 6, 45660-45663	5
1317	Deviating from the nanorod shape: Shape-dependent plasmonic properties of silver nanorice and nanocarrot structures. 2016 , 11, 1	11
1316	Experimental and Theoretical Study on Isotopic Surface-Enhanced Raman Spectroscopy for the Surface Catalytic Coupling Reaction on Silver Electrodes. 2016 , 120, 11956-11965	27
1315	Porous Au-Ag Nanospheres with High-Density and Highly Accessible Hotspots for SERS Analysis. 2016 , 16, 3675-81	322
1314	Utilizing in Situ Electrochemical SHINERS for Oxygen Reduction Reaction Studies in Aprotic Electrolytes. 2016 , 7, 2119-24	67
1313	Quantum Mechanical Description of Raman Scattering from Molecules in Plasmonic Cavities. 2016 , 10, 6291-8	97
1312	Atomic layer depositionSequential self-limiting surface reactions for advanced catalyst Bottom-upSynthesis. 2016 , 71, 410-472	195
1311	Ag-Au alloy nanoparticles: Synthesis and in situ monitoring SERS of plasmonic catalysis. 2016 , 231, 609-614	83
1310	Polymer nanopillar array with Au nanoparticle inlays as a flexible and transparent SERS substrate. 2016 , 6, 35527-35531	18
1309	Synthesis in situ of gold nanoparticles by a dialkynyl Fischer carbene complex anchored to glass surfaces. 2016 , 383, 375-381	6
1308	Surface- and Tip-Enhanced Raman Spectroscopy in Catalysis. 2016 , 7, 1570-84	121
1307	Ion beam induced optical and surface modification in plasmonic nanostructures. 2016 , 379, 42-47	6
1306	Identifying Enclosed Chemical Reaction and Dynamics at the Molecular Level Using Shell-Isolated Miniaturized Plasmonic Liquid Marble. 2016 , 7, 1501-6	29
1305	Au nanocluster arrays on self-assembled block copolymer thin films as highly active SERS substrates with excellent reproducibility. 2016 , 6, 38716-38723	8
1304	Highly Sensitive Detection of Hormone Estradiol E ₂ Using Surface-Enhanced Raman Scattering Based Immunoassays for the Clinical Diagnosis of Precocious Puberty. 2016 , 8, 10665-72	57

1303	Real-Time and in Situ Monitoring of Pesticide Penetration in Edible Leaves by Surface-Enhanced Raman Scattering Mapping. 2016 , 88, 5243-50	72
1302	Structure-Function Relationships for Surface-Enhanced Raman Spectroscopy-Active Plasmonic Paper. 2016 , 120, 20789-20797	25
1301	Facile synthesis of hierarchical Mo-doped S/BiOCl heterostructured spheres and its excellent photo/thermocatalytic activity under near room temperature. 2016 , 673, 93-101	16
1300	Highly sensitive multifunctional recyclable Ag@TiO ₂ nanorod SERS substrates for photocatalytic degradation and detection of dye molecules. 2016 , 6, 45120-45126	40
1299	Surface enhanced Raman spectroscopy platform based on graphene with one-year stability. 2016 , 604, 74-80	16
1298	Near-field dielectric scattering promotes optical absorption by platinum nanoparticles. 2016 , 10, 473-482	236
1297	The artificial control of enhanced optical processes in fluorescent molecules on high-emittance metasurfaces. 2016 , 8, 11099-107	15
1296	Advanced cathode materials for lithium-ion batteries using nanoarchitectonics. 2016 , 1, 423-444	88
1295	HD DVD substrates for surface enhanced Raman spectroscopy analysis: fabrication, theoretical predictions and practical performance. 2016 , 6, 44163-44169	9
1294	Plasmonic gold nanodiscs fabricated into a photonic-crystal nanocavity. 2016 , 27, 225203	5
1293	Chemical Production of Thin Protective Coatings on Optical Nanotips for Tip-Enhanced Raman Spectroscopy. 2016 , 120, 20828-20832	27
1292	SERS detection of polycyclic aromatic hydrocarbons using a bare gold nanoparticles coupled film system. 2016 , 141, 4359-65	35
1291	Self-Assembled Large-Scale Monolayer of Au Nanoparticles at the Air/Water Interface Used as a SERS Substrate. 2016 , 32, 4530-7	92
1290	Engineering aggregation-induced SERS-active porous Au@ZnS multi-yolk-shell structures for visualization of guest species loading. 2016 , 6, 38690-38696	6
1289	Investigating the effect of Ag nanocube polydispersity on gap-mode SERS enhancement factors. 2016 , 141, 3916-24	12
1288	Graphene-Based Enhanced Raman Scattering toward Analytical Applications. 2016 , 28, 6426-6435	92
1287	A rapid SERS method for label-free bacteria detection using polyethylenimine-modified Au-coated magnetic microspheres and Au@Ag nanoparticles. 2016 , 141, 6226-6238	95
1286	Nanostructured plasmonic substrates for use as SERS sensors. 2016 , 3, 18	66

1285	A Single Nanoprobe for Ratiometric Imaging and Biosensing of Hypochlorite and Glutathione in Live Cells Using Surface-Enhanced Raman Scattering. 2016 , 88, 9518-9523	76
1284	Au-MPY/DTNB@SiO ₂ SERS nanoprobe for immunosorbent assay. 2016 , 87, 34-39	1
1283	Adsorption of Dye Molecules on Single Crystalline Semiconductor Surfaces: An Electrochemical Shell-Isolated Nanoparticle Enhanced Raman Spectroscopy Study. 2016 , 120, 22500-22507	14
1282	Hotspots engineering by grafting Au@Ag core-shell nanoparticles on the Au film over slightly etched nanoparticles substrate for on-site paraquat sensing. 2016 , 86, 944-950	25
1281	A facile synthesis of gold micro/nanostructures at the interface of 1,3-dibutylimidazolium bis(trifluoromethylsulfonyl)imide and water. 2016 , 480, 30-38	10
1280	Green, Multi-Gram One-Step Synthesis of Core-Shell Nanocomposites in Water and Their Catalytic Application to Chemoselective Hydrogenations. 2016 , 22, 17962-17966	13
1279	Plasmonic coupling in single flower-like gold nanoparticle assemblies. 2016 , 26, 449-454	4
1278	Emerging tools for studying single entity electrochemistry. 2016 , 193, 9-39	64
1277	Fabrication of flexible silicon nanowires by self-assembled metal assisted chemical etching for surface enhanced Raman spectroscopy. 2016 , 6, 93649-93659	32
1276	Precisely Controllable Core-Shell Ag@Carbon Dots Nanoparticles: Application to in Situ Super-Sensitive Monitoring of Catalytic Reactions. 2016 , 8, 27956-27965	75
1275	In-situ monitoring of redox processes of viologen at Au(hkl) single-crystal electrodes using electrochemical shell-isolated nanoparticle-enhanced Raman spectroscopy. 2016 , 72, 131-134	5
1274	Highly Reproducible Ag NPs/CNT-Intercalated GO Membranes for Enrichment and SERS Detection of Antibiotics. 2016 , 8, 28180-28186	58
1273	An ordered array of hierarchical spheres for surface-enhanced Raman scattering detection of traces of pesticide. 2016 , 27, 384001	16
1272	Plasmonically Engineered Nanoprobes for Biomedical Applications. 2016 , 138, 14509-14525	149
1271	Tuneable 2D self-assembly of plasmonic nanoparticles at liquid liquid interfaces. 2016 , 8, 19229-19241	43
1270	Preparation of large-area controllable patterned silver nanocrystals for high sensitive and stable surface-enhanced Raman spectroscopy. 2016 , 32, 428-432	3
1269	Evaluation of the Penetration of Multiple Classes of Pesticides in Fresh Produce Using Surface-Enhanced Raman Scattering Mapping. 2016 , 81, T2891-T2901	35
1268	Stable Graphene-Isolated-Au-Nanocrystal for Accurate and Rapid Surface Enhancement Raman Scattering Analysis. 2016 , 88, 10611-10616	39

1267	Induced SERS activity in Ag@SiO ₂ /Ag core-shell nanosphere arrays with tunable interior insulator. 2016 , 47, 1200-1206	11
1266	Simultaneous preconcentration and ultrasensitive on-site SERS detection of polycyclic aromatic hydrocarbons in seawater using hexanethiol-modified silver decorated graphene nanomaterials. 2016 , 8, 7587-7596	18
1265	Nanoparticles and intracellular applications of surface-enhanced Raman spectroscopy. 2016 , 141, 5037-55	76
1264	Growth of gold nanostructures on a Si wafer by concerted mechanisms of photoreduction and galvanic displacement. 2016 , 18, 6683-6688	3
1263	3D Cross-Point Plasmonic Nanoarchitectures Containing Dense and Regular Hot Spots for Surface-Enhanced Raman Spectroscopy Analysis. 2016 , 28, 8695-8704	127
1262	Semiconductor materials in analytical applications of surface-enhanced Raman scattering. 2016 , 47, 51-58	97
1261	Tip-Enhanced Raman Spectroscopy. 2016 , 88, 9328-9346	144
1260	Optimization of the particle density to maximize the SERS enhancement factor of periodic plasmonic nanostructure array. 2016 , 24, 20613-20	16
1259	Surface-enhanced Raman scattering sensing of trace fenthion coupled with stable silver colloids and OH stretching band of water as an internal standard. 2016 , 71, 891-895	5
1258	An optical fiber SERS sensor based on GO/AgNPs/rGO sandwich structure hybrid films. 2016 , 6, 81750-81756	7
1257	Fe ₃ O ₄ @polydopamine Composite Theranostic Superparticles Employing Preassembled Fe ₃ O ₄ Nanoparticles as the Core. 2016 , 8, 22942-52	89
1256	Electrochemical Double Layers in Ionic Liquids Investigated by Broadband Impedance Spectroscopy and Other Complementary Experimental Techniques. 2016 , 157-192	
1255	Synthesis of Sn(10)Fex@FeySn(10)Oz nanohybrids via a simple programmed microfluidic process. 2016 , 6, 84255-84261	12
1254	"Atomic Force Masking" Induced Formation of Effective Hot Spots along Grain Boundaries of Metal Thin Films. 2016 , 8, 32094-32101	4
1253	Current advancement in analysis of agonists. 2016 , 85, 1-16	24
1252	Probing Low-Copy-Number Proteins in a Single Living Cell. 2016 , 128, 13409-13412	16
1251	Probing Low-Copy-Number Proteins in a Single Living Cell. 2016 , 55, 13215-13218	88
1250	Improvement in surface-enhanced Raman spectroscopy from cubic SiC semiconductor nanowhiskers by adjustment of energy levels. 2016 , 18, 27572-27576	6

1249	Facile synthesis of dendritic Cu by electroless reaction of Cu-Al alloys in multiphase solution. 2016 , 387, 805-811	3
1248	Shell-Isolated Nanoparticle-Enhanced Raman Spectroscopy at Single-Crystal Electrode Surfaces. 2016 , 4, 1144-1158	17
1247	Determination of chemical hazards in foods using surface-enhanced Raman spectroscopy coupled with advanced separation techniques. 2016 , 54, 103-113	37
1246	Elucidating the interfacial interactions of copper and ammonia with the sulfur passive layer during thiosulfate mediated gold leaching. 2016 , 210, 925-934	24
1245	Autoenhanced Raman Spectroscopy via Plasmonic Trapping for Molecular Sensing. 2016 , 88, 7633-8	20
1244	Surface-Enhanced Raman Spectroscopy on Liquid Interfacial Nanoparticle Arrays for Multiplex Detecting Drugs in Urine. 2016 , 88, 8145-51	70
1243	Nanomanipulation and controlled self-assembly of metal nanoparticles and nanocrystals for plasmonics. 2016 , 45, 5672-5716	122
1242	Simple electrochemical synthesis of an AuAgCu trimetallic nanodendrite and its use as a SERS substrate. 2016 , 6, 75943-75950	9
1241	Facile Synthesis of Au-Coated Magnetic Nanoparticles and Their Application in Bacteria Detection via a SERS Method. 2016 , 8, 19958-67	143
1240	Enhanced Raman Scattering with Dielectrics. 2016 , 116, 14921-14981	350
1239	Silver Nanoparticle-Decorated Shape-Memory Polystyrene Sheets as Highly Sensitive Surface-Enhanced Raman Scattering Substrates with a Thermally Inducible Hot Spot Effect. 2016 , 88, 10908-10915	24
1238	Excitation of the Tunable Longitudinal Higher-Order Multipole SPR Modes by Strong Coupling in Large-Area Metal Sub-10 nm-Gap Array Structures and Its Application. 2016 , 120, 24932-24940	10
1237	Nanostructure-based plasmon-enhanced Raman spectroscopy for surface analysis of materials. 2016 , 1,	819
1236	Weakening Circular Dichroism of Plasmonic Nanospirals Induced by Surface Grafting with Alkyl Ligands. 2016 , 12, 6698-6702	16
1235	Comparison of Four Types of Raman Spectroscopy for Noninvasive Determination of Carotenoids in Agricultural Products. 2016 , 237-247	1
1234	Nanoantenna effect of surface-enhanced Raman scattering: managing light with plasmons at the nanometer scale. 2016 , 1, 492-521	8
1233	Sonochemical synthesis of highly branched flower-like FeO@SiO@Ag microcomposites and their application as versatile SERS substrates. 2016 , 8, 19816-19828	46
1232	High-sensitivity pesticide detection using particle-enhanced resonant Raman scattering. 2016 , 9, 032401	2

1231	Electrochemically grafted single molecule junctions exploiting a chemical protection strategy. 2016 , 220, 436-443	11
1230	Reproducible Ultrahigh SERS Enhancement in Single Deterministic Hotspots Using Nanosphere-Plane Antennas Under Radially Polarized Excitation. 2016 , 6, 33218	22
1229	Purcell effect at the percolation transition. 2016 , 94,	8
1228	Applications and Spectral Examples for Raman Spectroscopy. 2016 , 173-228	
1227	Use of Single-Layer g-CN/Ag Hybrids for Surface-Enhanced Raman Scattering (SERS). 2016 , 6, 34599	37
1226	The size effect of silver nanocubes on gap-mode surface enhanced Raman scattering substrate. 2016 , 69, 146-150	9
1225	Plasmonic Nanogap-Enhanced Raman Scattering with Nanoparticles. 2016 , 49, 2746-2755	227
1224	Highly Controlled Synthesis and Super-Radiant Photoluminescence of Plasmonic Cube-in-Cube Nanoparticles. 2016 , 16, 7962-7967	35
1223	Important impact of the experimental platform on the efficient control of electronic and vibrational properties of molecular junctions. 2016 , 13, 685	2
1222	Intermediate stages of electrochemical oxidation of single-crystalline platinum revealed by in situ Raman spectroscopy. 2016 , 7, 12440	127
1221	Multiscale conformal pattern transfer. 2016 , 6, 28490	7
1220	Polyhedron Cu ₂ O@Ag composite microstructures: synthesis, mechanism analysis and structure-dependent SERS properties. 2016 , 6, 99105-99113	10
1219	All-metal meta-surfaces for narrowband light absorption and high performance sensing. 2016 , 49, 445104	23
1218	Effects of substrate and polarization on plasmon driven surface catalysis in nanowire-film hybrid system. 2016 , 100, 886-891	7
1217	The Third Way in Analytical Nanoscience and Nanotechnology. 2016 , 1-26	2
1216	Photo-induced enhanced Raman spectroscopy for universal ultra-trace detection of explosives, pollutants and biomolecules. 2016 , 7, 12189	143
1215	Noble Metal Nanoparticles as SERS Tags: Fundamentals and Biomedical Applications. 2016 , 67-101	
1214	Laser-induced synthesis of nanostructured metal-carbon clusters and complexes. 2016 , 48, 1	9

1213	Transmission-type plasmonic sensor for surface-enhanced Raman spectroscopy. 2016 , 9, 122002	5
1212	Silicon Asymmetric Membranes for Efficient Lithium Storage: A Scalable Method. 2016 , 4, 502-509	6
1211	Design considerations for SERS detection in colloidal solution: reduce spectral intensity fluctuation. 2016 , 47, 395-401	7
1210	Drawing-fabrication of multifarious nanoplasmonic platform on PLLA paper for optimized SERS performance. 2016 , 47, 687-691	6
1209	Photochemical growth of silver nanoparticles with mixed-light irradiation. 2016 , 294, 911-916	10
1208	Laser Power Threshold of Chemical Transformation on Highly Uniform Plasmonic and Catalytic Nanosurface. 2016 , 120, 12163-12169	21
1207	Surface-enhanced Raman scattering of silver thin films on as-roughened substrate by reactive ion etching. 2016 , 122, 1	6
1206	Universal Near-Field Interference Patterns of Fano Resonances in Two-Dimensional Plasmonic Crystals. 2016 , 11, 1377-1383	25
1205	Boron Nitride Nanosheet-Veiled Gold Nanoparticles for Surface-Enhanced Raman Scattering. 2016 , 8, 15630-6	41
1204	Mercury species induced frequency-shift of molecular orientational transformation based on SERS. 2016 , 141, 4782-8	23
1203	Plasmonic Metasurfaces for Nonlinear Optics and Quantitative SERS. 2016 , 3, 1371-1384	59
1202	Nitrate reduction pathways on Cu single crystal surfaces: Effect of oxide and Cl ⁻ . 2016 , 29, 457-465	52
1201	Rapid on-site detection of paraquat in biologic fluids by iodide-facilitated pinhole shell-isolated nanoparticle-enhanced Raman spectroscopy. 2016 , 6, 59919-59926	14
1200	Alteration of the Nonsystemic Behavior of the Pesticide Ferbam on Tea Leaves by Engineered Gold Nanoparticles. 2016 , 50, 6216-23	44
1199	Ultrastrong Freestanding Graphene Oxide Nanomembranes with Surface-Enhanced Raman Scattering Functionality by Solvent-Assisted Single-Component Layer-by-Layer Assembly. 2016 , 10, 6702-15	37
1198	Plasmon-Driven Dynamic Response of a Hierarchically Structural Silver-Decorated Nanorod Array for Sub-10 nm Nanogaps. 2016 , 8, 15623-9	17
1197	Visually monitoring the etching process of gold nanoparticles by KI/I ₂ at single-nanoparticle level using scattered-light dark-field microscopic imaging. 2016 , 9, 1125-1134	45
1196	Sensitive Glycoprotein Sandwich Assays by the Synergistic Effect of In Situ Generation of Raman Probes and Plasmonic Coupling of Ag Core-Au Satellite Nanostructures. 2016 , 8, 10683-9	11

1195	Surface enhanced Raman spectroscopy hyphenated with surface microextraction for in-situ detection of polycyclic aromatic hydrocarbons on food contact materials. 2016 , 158, 322-329	27
1194	Annealing Effects on Structure and Optical Properties of Diamond-Like Carbon Films Containing Silver. 2016 , 11, 146	30
1193	Rapid and direct detection of illicit dyes on tainted fruit peel using a PVA hydrogel surface enhanced Raman scattering substrate. 2016 , 8, 4816-4820	18
1192	Noble-Metal-Free Materials for Surface-Enhanced Raman Spectroscopy Detection. 2016 , 17, 2630-9	42
1191	Ultrathin Carbon Film Protected Silver Nanostructures for Surface-Enhanced Raman Scattering. 2016 , 70, 1751-1758	2
1190	Multilayer Graphene with a Rippled Structure as a Spacer for Improving Plasmonic Coupling. 2016 , 26, 5093-5101	28
1189	Recent advances in transition metal phosphide nanomaterials: synthesis and applications in hydrogen evolution reaction. 2016 , 45, 1529-41	2040
1188	Orientation-dependent nanostructure arrays based on anisotropic silicon wet-etching for repeatable surface-enhanced Raman scattering. 2016 , 8, 4672-80	23
1187	The fabrication of plasmonic nanoparticle-containing multilayer films via a bio-inspired polydopamine coating. 2016 , 6, 12638-12641	18
1186	Engineered "hot" core-shell nanostructures for patterned detection of chloramphenicol. 2016 , 78, 67-72	31
1185	Self-assembly of subwavelength nanostructures with symmetry breaking in solution. 2016 , 8, 2951-9	9
1184	Transfer printing for preparing nanostructured PDMS film as flexible SERS active substrate. 2016 , 84, 222-227	42
1183	Revealing Intermolecular Interaction and Surface Restructuring of an Aromatic Thiol Assembling on Au(111) by Tip-Enhanced Raman Spectroscopy. 2016 , 88, 915-21	35
1182	Multifunctional Fe ₃ O ₄ @SiO ₂ -Au Satellite Structured SERS Probe for Charge Selective Detection of Food Dyes. 2016 , 8, 3056-62	62
1181	Flexible and Adhesive Surface Enhance Raman Scattering Active Tape for Rapid Detection of Pesticide Residues in Fruits and Vegetables. 2016 , 88, 2149-55	277
1180	Nonresonant chemical mechanism in surface-enhanced Raman scattering of pyridine on M@Au ₁₂ clusters. 2016 , 8, 4086-93	24
1179	Sensitive DNA detection and SNP discrimination using ultrabright SERS nanorattles and magnetic beads for malaria diagnostics. 2016 , 81, 8-14	75
1178	Nanochemistry and Nanomedicine for Nanoparticle-based Diagnostics and Therapy. 2016 , 116, 2826-85	962

1177	Highly dispersed Ag nanoparticles embedded in alumina nanobelts as excellent surface-enhanced Raman scattering substrates. 2016 , 6, 8580-8583	2
1176	Single functional magnetic-bead as universal biosensing platform for trace analyte detection using SERS-nanobioprobe. 2016 , 79, 661-8	32
1175	Highly sensitive fibre surface-enhanced Raman scattering probes fabricated using laser-induced self-assembly in a meniscus. 2016 , 8, 10607-14	26
1174	Plasmonic MoO ₃ -x@MoO ₃ nanosheets for highly sensitive SERS detection through nanoshell-isolated electromagnetic enhancement. 2016 , 52, 2893-6	116
1173	Dipping into a drink: Basil-seed supported silver nanoparticles as surface-enhanced Raman scattering substrates for toxic molecule detection. 2016 , 223, 447-452	21
1172	The Ag shell thickness effect of Au@Ag@SiO ₂ core-shell nanoparticles on the optoelectronic performance of dye sensitized solar cells. 2016 , 52, 2390-3	17
1171	Advanced removal of in bioaerosols by simultaneous adsorption and photocatalytic oxidation of Cu-doped TiO ₂ /PU under visible irradiation. 2016 , 286, 377-386	25
1170	Research on the influence of alkyl ammonium bromides on the properties of Ag/AgBr/GO composites. 2016 , 40, 1323-1329	5
1169	Shell-isolated graphene@Cu nanoparticles on graphene@Cu substrates for the application in SERS. 2016 , 98, 526-533	52
1168	Dielectrophoresis-enabled surface enhanced Raman scattering on gold-decorated polystyrene microparticle in micro-optofluidic devices for high-sensitive detection. 2016 , 230, 94-100	20
1167	Application of monitoring methodology in carbon complex contained solution using surface-enhanced Raman spectroscopy (SERS). 2016 , 51, 500-511	1
1166	Formation mechanism of plasmonic silver nanohexagonal particles made by galvanic displacement reaction. 2016 , 6, 31454-31461	9
1165	Structural controls of AuNR@mSiO ₂ : tuning of the SPR, and manipulation of the silica shell thickness and structure. 2016 , 4, 2614-2620	13
1164	High resolution scanning near field mapping of enhancement on SERS substrates: comparison with photoemission electron microscopy. 2016 , 18, 9405-11	15
1163	Determination of melamine in milk using surface plasma effect of aggregated Au@SiO ₂ nanoparticles by SERS technique. 2016 , 68, 14-19	41
1162	Metal-Catalyzed Chemical Reaction of Single Molecules Directly Probed by Vibrational Spectroscopy. 2016 , 138, 4673-84	123
1161	Stable and unique graphitic Raman internal standard nanocapsules for surface-enhanced Raman spectroscopy quantitative analysis. 2016 , 9, 1418-1425	38
1160	Simulated localized surface plasmon spectra of single gold and silver nanobars. 2016 , 127, 3466-3470	5

1159	Shell-isolated nanoparticle-enhanced Raman spectroscopy study of the adsorption behaviour of DNA bases on Au(111) electrode surfaces. 2016 , 141, 3731-6	22
1158	Oxidative Coupling or Reductive Coupling? Effect of Surroundings on the Reaction Route of the Plasmonic Photocatalysis of Nitroaniline. 2016 , 120, 1570-1579	13
1157	Single Particle Deformation and Analysis of Silica-Coated Gold Nanorods before and after Femtosecond Laser Pulse Excitation. 2016 , 16, 1818-25	47
1156	In situ Raman spectroscopy of carbon-coated ZnFe ₂ O ₄ anode material in Li-ion batteries - investigation of SEI growth. 2016 , 52, 3970-3	54
1155	Highly effective and uniform SERS substrates fabricated by etching multi-layered gold nanoparticle arrays. 2016 , 8, 5928-37	43
1154	Structure Sensitivity in Catalytic Hydrogenation at Platinum Surfaces Measured by Shell-Isolated Nanoparticle Enhanced Raman Spectroscopy (SHINERS). 2016 , 6, 1822-1832	53
1153	Non-resonant Raman spectroscopy of individual ZnO nanowires via Au nanorod surface plasmons. 2016 , 4, 1651-1657	7
1152	Highly uniform indicator-mediated SERS sensor platform for the detection of Zn ²⁺ . 2016 , 6, 16555-16560	7
1151	Gold nanoparticles as sensitive optical probes. 2016 , 141, 1611-26	67
1150	Recent progress in detection of mercury using surface enhanced Raman spectroscopy--A review. 2016 , 39, 134-143	57
1149	Fibrous-Root-Inspired Design and Lithium Storage Applications of a Co-Zn Binary Synergistic Nanoarray System. 2016 , 10, 2500-8	36
1148	Gradual plasmon evolution and huge infrared near-field enhancement of metallic bridged nanoparticle dimers. 2016 , 18, 2319-23	18
1147	MnO ₂ -protected silver nanoparticles: New electromagnetic nanoresonators for Raman analysis of surfaces in basis environment. 2016 , 388, 704-709	20
1146	SERS activity with tenfold detection limit optimization on a type of nanoporous AAO-based complex multilayer substrate. 2016 , 8, 5920-7	20
1145	Surface Enhanced Infrared Studies of 4-Methoxypyridine Adsorption on Gold Film Electrodes. 2016 , 32, 2184-91	15
1144	Few-layer MoS ₂ -encapsulated Cu nanoparticle hybrids fabricated by two-step annealing process for surface enhanced Raman scattering. 2016 , 230, 645-652	32
1143	Noble metal plasmonic nanostructure related chromisms. 2016 , 3, 203-217	10
1142	Raman scattering enhanced within the plasmonic gap between an isolated Ag triangular nanoplate and Ag film. 2016 , 27, 165401	10

1141	Floating silver film: A flexible surface-enhanced Raman spectroscopy substrate for direct liquid phase detection at gas/liquid interfaces. 2016 , 9, 1148-1158	25
1140	In-situ electrochemical shell-isolated Ag nanoparticles-enhanced Raman spectroscopy study of adenine adsorption on smooth Ag electrodes. 2016 , 199, 388-393	9
1139	Raman spectrum of graphene with its versatile future perspectives. 2016 , 80, 125-131	86
1138	Silver Nanoshell Plasmonically Controlled Emission of Semiconductor Quantum Dots in the Strong Coupling Regime. 2016 , 10, 4154-63	45
1137	Magnetic properties of a hexagonal prismatic nanoparticle with ferrimagnetic core-shell structure. 2016 , 78, 115-122	55
1136	Pinhole-Containing, Subnanometer-Thick Al ₂ O ₃ Shell-Coated Ag Nanorods as Practical Substrates for Quantitative Surface-Enhanced Raman Scattering. 2016 , 120, 606-615	36
1135	Basics of Surface-Enhanced Raman Scattering (SERS). 2016 , 21-59	1
1134	Bioanalytical SERS Applications. 2016 , 61-91	1
1133	Dual-primer self-generation SERS signal amplification assay for PDGF-BB using label-free aptamer. 2016 , 79, 130-5	24
1132	Large scale synthesis of surface-enhanced Raman scattering nanoprobes with high reproducibility and long-term stability. 2016 , 33, 22-27	24
1131	Surface Plasmon Catalytic Aerobic Oxidation of Aromatic Amines in Metal/Molecule/Metal Junctions. 2016 , 120, 944-955	32
1130	Design of Core-Pd/Shell-Ag Nanocomposite Catalyst for Selective Semihydrogenation of Alkynes. 2016 , 6, 666-670	107
1129	Plasmonic nanostructures for surface enhanced spectroscopic methods. 2016 , 141, 756-93	138
1128	Copper nanoparticle@graphene composite arrays and their enhanced catalytic performance. 2016 , 105, 59-67	53
1127	Polarization State of Light Scattered from Quantum Plasmonic Dimer Antennas. 2016 , 10, 1580-8	56
1126	Three-dimensional SERS hot spots for chemical sensing: Towards developing a practical analyzer. 2016 , 80, 364-372	51
1125	Identification and distinction of non-small-cell lung cancer cells by intracellular SERS nanoprobes. 2016 , 6, 5401-5407	22
1124	Ultrasensitive surface-enhanced Raman scattering detection in common fluids. 2016 , 113, 268-73	463

1123	Increasing the Enhancement Factor in Plasmon-Enhanced Fluorescence with Shell-Isolated Nanoparticles. 2016 , 120, 20530-20535	22
1122	How To Light Special Hot Spots in Multiparticle-Film Configurations. 2016 , 10, 581-7	61
1121	3D ordered silver nanoshells silica photonic crystal beads for multiplex encoded SERS bioassay. 2016 , 52, 284-7	41
1120	Ascertaining Plasmonic Hot Electrons Generation from Plasmon Decay in Hybrid Plasmonic Modes. 2016 , 11, 909-915	4
1119	Optimizing the figure of merit of gold nanoshell-based refractive index sensing. 2016 , 127, 250-253	8
1118	Gold nanoparticle-coated silicon cone array for surface-enhanced Raman spectroscopy. 2016 , 49, 51-55	2
1117	Tuning the surface enhanced Raman scattering and catalytic activities of gold nanorods by controlled coating of platinum. 2016 , 463, 180-7	25
1116	Graphene isolated Au nanoparticle arrays with high reproducibility for high-performance surface-enhanced Raman scattering. 2016 , 222, 1175-1183	102
1115	Experimental and density functional theory study of Raman and SERS spectra of 5-amino-2-mercaptobenzimidazole. 2016 , 153, 344-8	16
1114	Nanocap array of Au:Ag composite for surface-enhanced Raman scattering. 2016 , 152, 461-7	24
1113	Recent progress on colloidal metal nanoparticles as signal enhancers in nanosensing. 2016 , 233, 255-270	47
1112	Polarization-Induced Tunability of Plasmonic Light Absorption in Arrays of Sub-Wavelength Elliptical Disks. 2016 , 11, 79-86	1
1111	High-Quality Plasmon Sensing with Excellent Intensity Contrast by Dual Narrow-Band Light Perfect absorbers. 2017 , 12, 65-68	9
1110	Prussian Blue as a Highly Sensitive and Background-Free Resonant Raman Reporter. 2017 , 89, 1551-1557	57
1109	Hand-Held Femtogram Detection of Hazardous Picric Acid with Hydrophobic Ag Nanopillar SERS Substrates and Mechanism of Elasto-Capillarity. 2017 , 2, 198-202	67
1108	An Au NP doped buffer layer in a slab waveguide for enhancement of organic amplified spontaneous emission. 2017 , 5, 1356-1362	2
1107	A Plasmonic Coupling Substrate Based on Sandwich Structure of Ultrathin Silica-Coated Silver Nanocubes and Flower-Like Alumina-Coated Etched Aluminum for Sensitive Detection of Biomarkers in Urine. 2017 , 6, 1601290	9
1106	Large-scale Ag-nanoparticles/Al ₂ O ₃ /Au-nanograting hybrid nanostructure for surface-enhanced Raman scattering. 2017 , 172, 1-7	10

1105	Ultrasensitive SERS aptasensor for the detection of oxytetracycline based on a gold-enhanced nano-assembly. 2017 , 165, 412-418	40
1104	Mapping Infrared Enhancement around Gold Nanoparticles Using Polyelectrolytes. 2017 , 121, 2355-2363	7
1103	Ratiometric SERS imaging and selective biosensing of nitric oxide in live cells based on trisoctahedral gold nanostructures. 2017 , 53, 1880-1883	33
1102	Multicolor Gold-Silver Nano-Mushrooms as Ready-to-Use SERS Probes for Ultrasensitive and Multiplex DNA/miRNA Detection. 2017 , 89, 2531-2538	161
1101	Synergizing the multiple plasmon resonance coupling and quantum effects to obtain enhanced SERS and PEC performance simultaneously on a noble metal-semiconductor substrate. 2017 , 9, 2376-2384	21
1100	Plasmon-dominated photoelectrodes for solar water splitting. 2017 , 5, 4233-4253	49
1099	Synergistic Effects of Wrinkled Graphene and Plasmonics in Stretchable Hybrid Platform for Surface-Enhanced Raman Spectroscopy. 2017 , 5, 1600715	19
1098	Highly Selective and Repeatable Surface-Enhanced Resonance Raman Scattering Detection for Epinephrine in Serum Based on Interface Self-Assembled 2D Nanoparticles Arrays. 2017 , 9, 7772-7779	43
1097	Rapidly fabricating large-scale plasmonic silver nanosphere arrays with sub-20 nm gap on Si-pyramids by inverted annealing for highly sensitive SERS detection. 2017 , 7, 11578-11584	6
1096	Silver Nanoparticle Generators: Silicon Dioxide Microspheres. 2017 , 23, 6244-6248	6
1095	Attenuated Total Reflection Surface-Enhanced Infrared Absorption Spectroscopy: a Powerful Technique for Bioanalysis. 2017 , 1, 1	11
1094	Advances in surface-enhanced vibrational spectroscopy at electrochemical interfaces. 2017 , 2, 188-209	26
1093	Uptake of silver nanoparticles by DHA-treated cancer cells examined by surface-enhanced Raman spectroscopy in a microfluidic chip. 2017 , 17, 1306-1313	21
1092	Enhancement of Surface Raman Spectroscopy Performance by Silver Nanoparticles on Resin Nanorods Arrays from Anodic Aluminum Oxide Template. 2017 , 164, B3081-B3086	13
1091	Core-Shell Nanoparticle-Enhanced Raman Spectroscopy. 2017 , 117, 5002-5069	577
1090	On-chip laser processing for the development of multifunctional microfluidic chips. 2017 , 11, 1600116	47
1089	Patterning of triblock copolymer film and its application for surface-enhanced Raman scattering. 2017 , 35, 623-630	2
1088	Highly reproducible and uniform SERS substrates based on Ag nanoparticles with optimized size and gap. 2017 , 23, 58-63	12

1087	High sensitivity and homogeneity of surface enhanced Raman scattering on three-dimensional array/film hybrid platform. 2017 , 110, 081605	3
1086	Green in Situ Synthesis of Clean 3D Chestnutlike Ag/WO Nanostructures for Highly Efficient, Recyclable and Sensitive SERS Sensing. 2017 , 9, 7436-7446	67
1085	Lasing Enhanced Surface Plasmon Resonance Sensing. 2017 , 6, 472-478	46
1084	SERS-based ultrasensitive sensing platform: An insight into design and practical applications. 2017 , 337, 1-33	66
1083	Identification of Al on the Colloid Surface Using Surface-Enhanced Raman Spectroscopy. 2017 , 51, 2899-2906	10
1082	Microfluidic Synthesis of Nanohybrids. 2017 , 13, 1604084	53
1081	Non-Resonant Large Format Surface Enhanced Raman Scattering Substrates for Selective Detection and Quantification of Xylene Isomers. 2017 , 29, 1994-1998	11
1080	Nanoparticle-on-mirror cavity modes for huge and/or tunable plasmonic field enhancement. 2017 , 28, 105203	26
1079	Shell-Isolated Nanoparticle-Enhanced Raman Spectroscopy (SHINERS) of Electrode Surfaces. 2017 , 339-372	1
1078	Contact Forces between Single Metal Oxide Nanoparticles in Gas-Phase Applications and Processes. 2017 , 33, 2477-2484	10
1077	Building Electromagnetic Hot Spots in Living Cells via Target-Triggered Nanoparticle Dimerization. 2017 , 11, 3532-3541	89
1076	Design of Hybrid Nanostructural Arrays to Manipulate SERS-Active Substrates by Nanosphere Lithography. 2017 , 9, 7710-7716	35
1075	A capillary force-induced Au nanoparticle/Ag nanowire single hot spot platform for SERS analysis. 2017 , 5, 3229-3237	23
1074	In situ observation of the formation process for free-standing Au nanowires with a scanning electron microscope. 2017 , 28, 105707	2
1073	Tunable Synthesis of Ag Films at the Interface of Ionic Liquids and Water by Changing Cationic Structures of Ionic Liquids. 2017 , 17, 990-999	18
1072	In Situ Hot-Spot Assembly as a General Strategy for Probing Single Biomolecules. 2017 , 89, 4776-4780	31
1071	Photonics and spectroscopy in nanojunctions: a theoretical insight. 2017 , 46, 4000-4019	34
1070	Introduction: Vibrational Nanoscopy. 2017 , 117, 4943-4944	6

1069	Fabrication of Monodispersed Au@SiO ₂ Nanoparticles with Highly Stable Silica Layers by Ultrasound-Assisted Stober Method. 2017 , 121, 9543-9551	39
1068	Optical modulator based on propagating surface plasmon coupled fluorescent thin film: proof-of-concept studies. 2017 , 5, 024006	7
1067	A metallic molybdenum dioxide with high stability for surface enhanced Raman spectroscopy. 2017 , 8, 14903	153
1066	Continuous fabrication of microcapsules with controllable metal covered nanoparticle arrays using droplet microfluidics for localized surface plasmon resonance. 2017 , 17, 1970-1979	28
1065	Au@1,4-benzenedithiol@Au core-shell SERS immunosensor for ultra-sensitive and high specific biomarker detection. 2017 , 90, 56-62	8
1064	Non-symmetric hybrids of noble metal-semiconductor: Interplay of nanoparticles and nanostructures in formation dynamics and plasmonic applications. 2017 , 27, 157-168	17
1063	Surface passivation of aluminum hydride particles via atomic layer deposition. 2017 , 35, 03E111	13
1062	A green, reusable SERS film with high sensitivity for in-situ detection of thiram in apple juice. 2017 , 416, 704-709	70
1061	Graphene for flexible and wearable device applications. 2017 , 120, 244-257	113
1060	In Situ Quantitative Graphene-Based Surface-Enhanced Raman Spectroscopy. 2017 , 1, 1700126	28
1059	Fabrication of self-organized precisely tunable plasmonic SERS substrates via glancing angle deposition. 2017 , 214, 1700088	2
1058	Further expanding versatility of surface-enhanced Raman spectroscopy: from non-traditional SERS-active to SERS-inactive substrates and single shell-isolated nanoparticle. 2017 , 205, 457-468	9
1057	Simultaneous Surface-Enhanced Raman Spectroscopy Detection of Multiplexed MicroRNA Biomarkers. 2017 , 89, 6120-6128	126
1056	Fabrication of SERS substrates containing dense hot spots by assembling star-shaped nanoparticles on superhydrophobic surfaces. 2017 , 41, 5028-5033	7
1055	Uniform Microgels Containing Agglomerates of Silver Nanocubes for Molecular Size-Selectivity and High SERS Activity. 2017 , 13, 1604048	16
1054	Sensitive surface enhanced Raman spectroscopy (SERS) detection of methotrexate by core-shell-satellite magnetic microspheres. 2017 , 171, 152-158	13
1053	Carboxyl-functionalized Ag@SiO ₂ nanoparticle films for highly sensitive and selective surface-enhanced Raman scattering applications. 2017 , 201, 152-155	4
1052	Stable and conductive lead halide perovskites facilitated by X-type ligands. 2017 , 9, 7252-7259	55

1051	Raman of indigo on a silver surface. Raman and theoretical characterization of indigo deposited on silicon dioxide-coated and uncoated silver nanoparticles. 2017 , 50, 316-321	2
1050	Surface-enhanced Raman scattering using monolayer graphene-encapsulated Ag nanoparticles as a substrate for sensitive detection of 2,4,6-trinitrotoluene. 2017 , 9, 3105-3113	17
1049	Largely improved dimensional stability of short carbon fiber reinforced polyethersulfone composites by graphene oxide coating at a low content. 2017 , 119, 339-349	27
1048	Reliable molecular trace-detection based on flexible SERS substrate of graphene/Ag-nanoflowers/PMMA. 2017 , 249, 439-450	59
1047	Shell isolated nanoparticles for enhanced Raman spectroscopy studies in lithium-oxygen cells. 2017 , 205, 469-490	20
1046	Radiation pressure on core-shell nanoparticles in Rayleigh regime. 2017 ,	0
1045	SERS Detection of Biomolecules by Highly Sensitive and Reproducible Raman-Enhancing Nanoparticle Array. 2017 , 12, 344	30
1044	Quantitative detection using two-dimension shell-isolated nanoparticle film. 2017 , 48, 919-924	16
1043	On the Thermodynamics and Experimental Control of Twinning in Metal Nanocrystals. 2017 , 129, 8773-8777	6
1042	Plasmon-enhanced fluorescence spectroscopy. 2017 , 46, 3962-3979	278
1041	Plasmonic substrates for surface enhanced Raman scattering. 2017 , 984, 19-41	65
1040	Split-orientation-modulated plasmon coupling in disk/sector dimers. 2017 , 121, 213105	2
1039	Use of Standing Gold Nanorods for Detection of Malachite Green and Crystal Violet in Fish by SERS. 2017 , 82, 1640-1646	39
1038	Preparation of a self-cleanable molecularly imprinted sensor based on surface-enhanced Raman spectroscopy for selective detection of R6G. 2017 , 409, 4627-4635	15
1037	Probing Gap Plasmons Down to Subnanometer Scales Using Collapsible Nanofingers. 2017 , 11, 5836-5843	22
1036	SERS-Activated Platforms for Immunoassay: Probes, Encoding Methods, and Applications. 2017 , 117, 7910-7963	332
1035	Investigation of degradation and penetration behaviors of dimethoate on and in spinach leaves using in situ SERS and LC-MS. 2017 , 237, 305-311	19
1034	Silver Nanoparticles with Many Sharp Apexes and Edges as Efficient Nanoresonators for Shell-Isolated Nanoparticle-Enhanced Raman Spectroscopy. 2017 , 121, 12383-12391	23

1033	Single-molecule detection of dihydroazulene photo-thermal reaction using break junction technique. 2017 , 8, 15436	72
1032	In situ dynamic tracking of heterogeneous nanocatalytic processes by shell-isolated nanoparticle-enhanced Raman spectroscopy. 2017 , 8, 15447	132
1031	SERS-active metal-organic frameworks with embedded gold nanoparticles. 2017 , 142, 2640-2647	51
1030	Analytical plasmon dispersion in subwavelength closely spaced Au nanorod arrays from planar metal-insulator-metal waveguides. 2017 , 5, 6079-6085	14
1029	Highly Enhanced Raman Scattering on Carbonized Polymer Films. 2017 , 9, 21457-21463	6
1028	Controlled preparation of Ag nanoparticles on graphene with different amount of defects for surface-enhanced Raman scattering. 2017 , 7, 27105-27112	3
1027	Facile fabrication of silver nanoparticle-coated silica-C18 core-shell microspheres and their applications in SERS detection. 2017 , 7, 19262-19266	3
1026	On the Thermodynamics and Experimental Control of Twinning in Metal Nanocrystals. 2017 , 56, 8647-8651	14
1025	Synergetic SERS Enhancement in a Metal-Like/Metal Double-Shell Structure for Sensitive and Stable Application. 2017 , 9, 13564-13570	17
1024	Synthesis and characterization of platinum nano sized particles by laser ablation in C ₂ H ₆ O ₂ solution. 2017 , 49, 1	4
1023	Controlled Design and Fabrication of SERS/EF Multifunctional Nanoparticles for Nanoprobe Applications: Morphology-Dependent SERS Phenomena. 2017 , 121, 8070-8076	19
1022	Silica-encapsulated gold nanoparticle dimers for organelle-targeted cellular delivery. 2017 , 53, 5009-5012	8
1021	Plasmonic Enhancement of Molecule-Doped Core-Shell and Nanoshell on Molecular Fluorescence. 2017 , 37-72	
1020	Performance Enhancement of Tri-Cation and Dual-Anion Mixed Perovskite Solar Cells by Au@SiO ₂ Nanoparticles. 2017 , 27, 1606545	43
1019	In situ SERS and SHINERS study of electrochemical hydrogenation of p-ethynylaniline in nonaqueous solvents. 2017 , 78, 16-20	12
1018	Niobium pentoxide: a promising surface-enhanced Raman scattering active semiconductor substrate. 2017 , 3,	45
1017	Metal-enhanced luminescence: Current trend and future perspectives- A review. 2017 , 971, 1-13	29
1016	Plasmon-Enhanced Luminescence with Shell-Isolated Nanoparticles. 2017 , 257-270	1

1015	Long-term fluidization of titania nanoparticle agglomerates. 2017 , 316, 441-445	5
1014	The effect of excitation wavelength and metallic nanostructure on SERS spectra of C60. 2017 , 48, 829-836	6
1013	SERS-active liposome@Ag/Au nanocomposite for NIR light-driven drug release. 2017 , 154, 150-159	13
1012	A ternary functional Ag@GO@Au sandwiched hybrid as an ultrasensitive and stable surface enhanced Raman scattering platform. 2017 , 409, 306-313	33
1011	Femtosecond Laser Direct Writing of Plasmonic Ag/Pd Alloy Nanostructures Enables Flexible Integration of Robust SERS Substrates. 2017 , 2, 1600270	22
1010	One-pot synthesis of a DNA-anchored SERS nanoprobe with simultaneous nanostructural tuning and Raman reporter encoding. 2017 , 7, 5063-5066	5
1009	Plasmonic nanoparticles in chemical analysis. 2017 , 7, 17559-17576	92
1008	Fundamentals and applications of SERS-based bioanalytical sensing. 2017 , 6, 831-852	104
1007	Prosperity to challenges: recent approaches in SERS substrate fabrication. 2017 , 36,	21
1006	Silver nanoparticles decorated nanoporous gold for surface-enhanced Raman scattering. 2017 , 28, 055301	14
1005	Fabrication of Fe ₃ O ₄ @SiO ₂ @Ag magnetic plasmonic nanospindles as highly efficient SERS active substrates for label-free detection of pesticides. 2017 , 41, 1582-1590	20
1004	Probing electrochemical interfaces using shell-isolated nanoparticles-enhanced Raman spectroscopy. 2017 , 1, 16-21	20
1003	Application of Au based nanomaterials in analytical science. 2017 , 12, 64-97	58
1002	Improving the sensitivity of immunoassay based on MBA-embedded Au@SiO nanoparticles and surface enhanced Raman spectroscopy. 2017 , 175, 262-268	9
1001	Plasmonic nanoholes as SERS devices for biosensing applications: An easy route for nanostructures fabrication on glass substrates. 2017 , 175, 30-33	12
1000	Plasmon-Enhanced Spectroscopies with Shell-Isolated Nanoparticles. 2017 , 13, 1601598	7
999	The fabrication of polymer-nanocone-based 3D Au nanoparticle array and its SERS performance. 2017 , 123, 1	7
998	{110}-Terminated Square-Shaped Gold Nanoplates and Their Electrochemical Surface Reactivity. 2017 , 4, 557-564	5

997	A ratiometric nanoarchitecture for the simultaneous detection of pH and halide ions using UV plasmon-enhanced fluorescence. 2017 , 53, 755-758	13
996	Low-adhesive superhydrophobic surface-enhanced Raman spectroscopy substrate fabricated by femtosecond laser ablation for ultratrace molecular detection. 2017 , 5, 777-784	44
995	Plasmonic nanohole array for enhancing the SERS signal of a single layer of graphene in water. 2017 , 7, 14044	18
994	Plasmon enhanced quantum dots fluorescence and energy conversion in water splitting using shell-isolated nanoparticles. 2017 , 42, 232-240	17
993	Ultrathin Oxide Layer-Wrapped Noble Metal Nanoparticles via Colloidal Electrostatic Self-Assembly for Efficient and Reusable Surface Enhanced Raman Scattering Substrates. 2017 , 33, 12934-12942	7
992	Near-Electric-Field Tuned Plasmonic Au@SiO ₂ and Ag@SiO ₂ Nanoparticles for Efficient Utilization in Luminescence Enhancement and Surface-Enhanced Spectroscopy. 2017 , 121, 23062-23071	24
991	Optimizing silver-capped silicon nanopillars to simultaneously realize macroscopic, practical-level SERS signal reproducibility and high enhancement at low costs. 2017 , 48, 1808-1818	15
990	High reliable and robust ultrathin-layer gold coating porous silver substrate via galvanic-free deposition for solid phase microextraction coupled with surface enhanced Raman spectroscopy. 2017 , 994, 56-64	13
989	Controllable Shrinking of Glass Capillary Nanopores Down to sub-10 nm by Wet-Chemical Silanization for Signal-Enhanced DNA Translocation. 2017 , 2, 1452-1457	24
988	SERS-Based Lateral Flow Strip Biosensor for Simultaneous Detection of <i>Listeria monocytogenes</i> and <i>Salmonella enterica</i> Serotype Enteritidis. 2017 , 65, 10290-10299	97
987	Qualitative and quantitative determination of coumarin using surface-enhanced Raman spectroscopy coupled with intelligent multivariate analysis. 2017 , 7, 49097-49101	15
986	Plasmonic MoO Nanospheres as a Highly Sensitive and Stable Non-Noble Metal Substrate for Multicomponent Surface-Enhanced Raman Analysis. 2017 , 89, 11765-11771	46
985	Mesoporous Copper Nanoparticle Networks Decorated by Graphite Layers for Surface-Enhanced Raman Scattering Detection of Trace Analytes. 2017 , 82, 1290-1297	
984	Gold Nanoparticles: A Versatile Platform for Cancer Diagnosis, Imaging and Therapy. 2017 , 83-137	
983	Molecular-level understanding of electric double layer in ionic liquids. 2017 , 4, 105-111	22
982	Facile synthesis of gold nanomaterials with unusual crystal structures. 2017 , 12, 2367-2378	56
981	Au nanoparticle-modified WO ₃ nanoflowers/TiO ₂ nanotubes used for the SERS detection of dyes. 2017 , 41, 13968-13973	12
980	Three-Dimensional SERS Substrates Formed with Plasmonic Core-Satellite Nanostructures. 2017 , 7, 13066	26

979	Insights into the heterogeneous distribution of SERS effect in plasmonic hot spots between Au@SiO ₂ monolayer film and gold single crystal plates. 2017 , 7, 48544-48553	1
978	SERS-microfluidic systems: A potential platform for rapid analysis of food contaminants. 2017 , 70, 114-126	88
977	Inelastic electron tunneling spectroscopy in molecular junctions showing quantum interference. 2017 , 95,	9
976	Synthesis and characterization of binaphthalene-2,2'-diamine-functionalized gold nanoparticles. 2017 , 19, 1	2
975	Electrochemical THz-SERS Observation of Thiol Monolayers on Au(111) and (100) Using Nanoparticle-assisted Gap-Mode Plasmon Excitation. 2017 , 8, 4236-4240	20
974	Mace-like gold hollow hierarchical micro/nanostructures fabricated by co-effect of catalytic etching and electrodeposition and their SERS performance. 2017 , 4, 095009	4
973	Plasmonic band-edge modulated surface-enhanced Raman scattering. 2017 , 111, 051601	2
972	Optical-signal-enhancing metasurface platforms for fluorescent molecules at water-transparent near-infrared wavelengths. 2017 , 7, 37076-37085	5
971	Ordered Arrangement and Optical Properties of Silica-Stabilized Gold Nanoparticle-PNIPAM Core-Satellite Clusters for Sensitive Raman Detection. 2017 , 13, 1701095	13
970	In Vitro Isothermal Nucleic Acid Amplification Assisted Surface-Enhanced Raman Spectroscopic for Ultrasensitive Detection of <i>Vibrio parahaemolyticus</i> . 2017 , 89, 9775-9780	38
969	Long-range surface plasmon resonance and surface-enhanced Raman scattering on X-shaped gold plasmonic nanohole arrays. 2017 , 19, 24126-24134	15
968	Size-Controllable Gold Nanopores with High SERS Activity. 2017 , 89, 10407-10413	33
967	Poly-cytosine-mediated nanotags for SERS detection of Hg. 2017 , 9, 14184-14191	46
966	Leakage-free polypyrrole-Au nanostructures for combined Raman detection and photothermal cancer therapy. 2017 , 5, 7949-7962	20
965	In situ observation of Pt oxides on the low index planes of Pt using surface enhanced Raman spectroscopy. 2017 , 19, 27570-27579	22
964	Silver nanoflowers for single-particle SERS with 10 pM sensitivity. 2017 , 28, 465705	20
963	Corrosion-Protected Hybrid Nanoparticles. 2017 , 4, 1700234	12
962	Molecular Wires Bridging Gaps between Gold Surfaces and Their Influence on SERS Intensities. 2017 , 121, 20937-20946	9

961	Increasing local field by interfacial coupling in nanobowl arrays. 2017 , 7, 43671-43680	7
960	The nature of the AuN bond in gold(III) complexes with aromatic nitrogen-containing heterocycles: the influence of Au(III) ions on the ligand aromaticity. 2017 , 41, 12407-12415	13
959	Tunable SERS Platforms from Small Nanoparticle 3D Superlattices: A Comparison between Gold, Silver, and Copper. 2017 , 18, 3066-3075	11
958	Effect of TiO ₂ nanoparticles on newly synthesized phenothiazine derivative-CPTA dye and its applications as dye sensitized solar cell. 2017 , 244, 97-102	18
957	A facile solvent mediated self-assembly silver nanoparticle mirror substrate for quantitatively improved surface enhanced Raman scattering. 2017 , 142, 4075-4082	9
956	Smart supramolecular sensing with cucurbit[n]urils: probing hydrogen bonding with SERS. 2017 , 205, 505-515	13
955	Improving the stability of LiNi _{0.80} Co _{0.15} Al _{0.05} O ₂ by AlPO ₄ nanocoating for lithium-ion batteries. 2017 , 60, 1230-1235	37
954	High performance graphene/semiconductor van der Waals heterostructure optoelectronic devices. 2017 , 40, 122-148	67
953	Near infrared surface-enhanced Raman scattering based on star-shaped gold/silver nanoparticles and hyperbolic metamaterial. 2017 , 7, 5446	65
952	SERS polarization dependence of Ag nanorice dimer on metal and dielectric film. 2017 , 684, 373-377	5
951	In Situ Two-Step Photoreduced SERS Materials for On-Chip Single-Molecule Spectroscopy with High Reproducibility. 2017 , 29, 1702893	50
950	A sensitive Galvanic replacement reaction-SERS method for Au(III) with Victoria blue B molecular probes in silver nanosol substrate. 2017 , 251, 404-409	5
949	Silica-Coated Core-Shell Structured Polystyrene Nanospheres and Their Size-Dependent Mechanical Properties. 2017 , 33, 8225-8232	26
948	Tailoring Amino-Functionalized Graphitic Carbon-Encapsulated Gold Core/Shell Nanostructures for the Sensitive and Selective Detection of Copper Ions. 2017 , 27, 1702232	16
947	Rapid signal enhancement method for nanoprobe-based biosensing. 2017 , 7, 6837	11
946	Au-Pt alloy nanoparticles obtained by nanosecond laser irradiation of gold and platinum bulk targets in an ethylene glycol solution. 2017 , 132, 1	6
945	Innovative sandwich assay with dual optical and SERS sensing mechanisms for bacterial detection. 2017 , 9, 4732-4739	27
944	Self-assembly of Ag nanoparticles on the woven cotton fabrics as mechanical flexible substrates for surface enhanced Raman scattering. 2017 , 726, 484-489	21

943	Blocking Hot Electron Emission by SiO ₂ Coating Plasmonic Nanostructures. 2017 , 121, 18795-18799	7
942	Real-time monitoring of plasmon-induced proton transfer of hypoxanthine in serum. 2017 , 9, 12307-12310	9
941	Chemical Functionalization of Plasmonic Surface Biosensors: A Tutorial Review on Issues, Strategies, and Costs. 2017 , 9, 29394-29411	93
940	Simultaneous detection of clenbuterol and ractopamine based on multiplexed competitive surface enhanced Raman scattering (SERS) immunoassay. 2017 , 41, 10407-10414	19
939	Ultrathin polydopamine film coated gold nanoparticles: a sensitive, uniform, and stable SHINERS substrate for detection of benzotriazole. 2017 , 142, 3459-3467	25
938	Nanogapped Au Antennas for Ultrasensitive Surface-Enhanced Infrared Absorption Spectroscopy. 2017 , 17, 5768-5774	131
937	Semiconductor SERS enhancement enabled by oxygen incorporation. 2017 , 8, 1993	184
936	Controllable fabrication of metallic photonic crystals for ultra-sensitive SERS and photodetectors. 2017 , 7, 55851-55858	3
935	Ultrasensitive Detection of Capsaicin in Oil for Fast Identification of Illegal Cooking Oil by SERRS. 2017 , 2, 8401-8406	12
934	Controllable fabrication of Ag-nanoplate-decorated PAN-nanopillar arrays and their application in surface-enhanced Raman scattering. 2017 , 7, 53157-53163	8
933	Bioinspired Synthesis of Mesoporous Gold-silica Hybrid Microspheres as Recyclable Colloidal SERS Substrates. 2017 , 7, 14728	25
932	Liquid magnetic competitive immunoassay of clenbuterol based on surface-enhanced Raman spectroscopy. 2017 , 48, 1307-1317	6
931	Optimally designed gold nanorattles with strong built-in hotspots and weak polarization dependence. 2017 , 28, 495201	6
930	Free-standing Ag triangle arrays a configurable vertical gap for surface enhanced Raman spectroscopy. 2017 , 28, 385401	9
929	Remarkable SERS Activity Observed from Amorphous ZnO Nanocages. 2017 , 56, 9851-9855	163
928	A high-performance and low cost SERS substrate of plasmonic nanopillars on plastic film fabricated by nanoimprint lithography with AAO template. 2017 , 7, 065205	14
927	Remarkable SERS Activity Observed from Amorphous ZnO Nanocages. 2017 , 129, 9983-9987	33
926	Differentiated interactions in phosphate solutions: Comparing Ag(111) and Ag(100) surfaces. 2017 , 799, 487-496	2

925	Revealing the Role of Interfacial Properties on Catalytic Behaviors by in Situ Surface-Enhanced Raman Spectroscopy. 2017 , 139, 10339-10346	89
924	Immunoassay quantification using surface-enhanced fluorescence (SEF) tags. 2017 , 142, 2717-2724	17
923	A simple and sensitive surface-enhanced Raman spectroscopic discriminative detection of organophosphorous nerve agents. 2017 , 409, 5091-5099	9
922	Atomic-Layer-Deposition Assisted Formation of Wafer-Scale Double-Layer Metal Nanoparticles with Tunable Nanogap for Surface-Enhanced Raman Scattering. 2017 , 7, 5161	14
921	Long-Range Plasmon Field and Plasmoelectric Effect on Catalysis Revealed by Shell-Thickness-Tunable Pinhole-Free 2 Core-Shell Nanoparticles: A Case Study of p-Nitrophenol Reduction. 2017 , 7, 5391-5398	54
920	Iron layer-dependent surface-enhanced raman scattering of hierarchical nanocap arrays. 2017 , 423, 1124-1133	13
919	Plasmon-enhanced spectroscopy of absorption and spontaneous emissions explained using cavity quantum optics. 2017 , 46, 3904-3921	89
918	Electromagnetic theories of surface-enhanced Raman spectroscopy. 2017 , 46, 4042-4076	662
917	Nonlinear optical properties of Au/Ag core-shell nanorods for all-optical switching. 2017 , 50, 355302	11
916	A study of plasmonic field enhancement in bimetallic and active core-shell nanoparticles/nanorods. 2017 ,	0
915	The Oxygen Reduction Reaction on Kinked Stepped Surfaces of Pt. 2017 , 8, 46-50	15
914	Nanoparticle assisted Raman information acquisition from metal encapsulated sandwich structure. 2017 , 48, 443-447	4
913	Surface-enhanced Raman scattering from plasmonic Ag-nanocube@Au-nanospheres core@satellites. 2017 , 48, 217-223	6
912	Graphene oxide-Ag nanoparticles-pyramidal silicon hybrid system for homogeneous, long-term stable and sensitive SERS activity. 2017 , 396, 1130-1137	22
911	Electrochemical SERS observation of molecular adsorbates on Ru/Pt-modified Au(111) surfaces using sphere-plane type gap-mode plasmon excitation. 2017 , 800, 151-155	8
910	Chemical Coupling SERS Properties of Pyridine on Silver-Caged Metal Clusters M@Ag ₁₂ (M = V, Nb, Ta, Cr, Mo, W, Mn ⁺ , Tc ⁺ , Re ⁺). 2017 , 46, 3904-3909	2
909	Multifunctional satellite Fe ₃ O ₄ -Au@TiO ₂ nano-structure for SERS detection and photo-reduction of Cr(VI). 2017 , 513, 234-240	22
908	SERS-based ultrasensitive detection of organophosphorus nerve agents via substrate's surface modification. 2017 , 324, 194-202	36

907	Theoretical study of normal Raman spectra and SERS of benzyl chloride and benzyl radical on silver electrodes. 2017 , 48, 53-63	7
906	A simple drop-and-detect method using porous alumina ceramics as platforms for rapid surface-enhanced Raman spectroscopy. 2017 , 48, 89-96	3
905	Hydrothermal reduction of graphene oxide; effect on surface-enhanced Raman scattering. 2017 , 48, 97-103	50
904	Ultrathin tin oxide layer-wrapped gold nanoparticles induced by laser ablation in solutions and their enhanced performances. 2017 , 489, 92-99	12
903	Design and Fabrication of Plasmonic Nanomaterials Based on Gold Nanorod Supercrystals. 2017 , 29, 15-25	47
902	Shell-isolated nanoparticle-enhanced Raman spectroscopy characterization of oxide ores during thiosulfate-mediated gold leaching. 2017 , 48, 197-203	2
901	Ag nanoparticles cladded with parylene for high-stability microfluidic surface-enhanced Raman scattering (SERS) biochemical sensing. 2017 , 242, 1171-1176	15
900	Hierarchical Ag mesostructures for single particle SERS substrate. 2017 , 393, 197-203	12
899	Coupling shell-isolated nanoparticle enhanced Raman spectroscopy with paper chromatography for multi-components on-site analysis. 2017 , 162, 52-56	13
898	Hierarchical Branched Vanadium Oxide Nanorod@Si Nanowire Architecture for High Performance Supercapacitors. 2017 , 13, 1603076	17
897	Real-Time Probing Nanopore-in-Nanogap Plasmonic Coupling Effect on Silver Supercrystals with Surface-Enhanced Raman Spectroscopy. 2017 , 27, 1603233	45
896	Ultrasensitive SERS Detection by Defect Engineering on Single Cu O Superstructure Particle. 2017 , 29, 1604797	223
895	3.7 Raman Spectroscopy. 2017 , 108-127	
894	The role of ion irradiation in activating silent Raman modes via tuning in plasmonic behaviour and surface disorder of Au/ZnO/Pt NFG system. 2017 , 119, 66002	2
893	Graphene for surface enhanced Raman scattering (SERS) molecular sensors. 2017 ,	
892	Electrospray surface-enhanced Raman spectroscopy (ES-SERS) for probing surface chemical compositions of atmospherically relevant particles. 2017 , 17, 14025-14037	20
891	Analytical Nanoscience and Nanotechnology. 2017 , 1-28	
890	An Ordered AgNWs@GO-AgNPs Film as the Sensitive, Stable and Multifunctional Surface-Enhanced Raman Scattering Substrate. 2017 , 164, B747-B752	6

889	Laser-induced construction of multi-branched CuS nanodendrites with excellent surface-enhanced Raman scattering spectroscopy in repeated applications. 2017 , 25, 16204-16213	9
888	Ag gyruis-nanostructure supported on graphene/Au film with nanometer gap for ideal surface enhanced Raman scattering. 2017 , 25, 20631-20641	34
887	Second harmonic generation enhancement from a nonlinear nanocrystal integrated hyperbolic metamaterial cavity. 2017 , 25, 21342-21348	10
886	Synthesis of three-dimensional honeycomb-like Au nanoporous films by laser induced modification and its application for surface enhanced Raman spectroscopy. 2017 , 7, 1557	3
885	Modulation of hot regions in waveguide-based evanescent-field-coupled localized surface plasmons for plasmon-enhanced spectroscopy. 2017 , 5, 527	15
884	Surface regeneration and signal increase in surface-enhanced Raman scattering substrates. 2017 , 56, B198-B213	14
883	Quantitatively extracting the contribution of asymmetric local-field to $\langle E \rangle$ in cross-shaped Ag nanoholes. 2017 , 25, 1296-1307	4
882	Surface-Enhanced Raman Scattering. 2017 ,	2
881	Surface-Enhanced Raman Spectroscopy: A Tool for All Classes of Food Contaminants. 2017 ,	1
880	Synthesis of Au NP@MoS ₂ Quantum Dots Core@Shell Nanocomposites for SERS Bio-Analysis and Label-Free Bio-Imaging. 2017 , 10,	17
879	SERS Taper-Fiber Nanoprobe Modified by Gold Nanoparticles Wrapped with Ultrathin Alumina Film by Atomic Layer Deposition. 2017 , 17,	12
878	Pt-Based Nanostructures for Observing Genuine SERS Spectra of p-Aminothiophenol (PATP) Molecules. 2017 , 7, 953	4
877	A Review of Three-Dimensional Scanning Near-Field Optical Microscopy (3D-SNOM) and Its Applications in Nanoscale Light Management. 2017 , 7, 973	63
876	A Novel Method to Directly Analyze Dissolved Acetic Acid in Transformer Oil without Extraction Using Raman Spectroscopy. 2017 , 10, 967	11
875	Supercritical angle Raman microscopy: a surface-sensitive nanoscale technique without field enhancement. 2017 , 6, e17066	5
874	Surface-Enhanced Spectroscopy for Surface Characterization. 2017 , 115-154	
873	Graphene-Ag Hybrids on Laser-Textured Si Surface for SERS Detection. 2017 , 17,	19
872	Development of graphene oxide-wrapped gold nanorods as robust nanoplatform for ultrafast near-infrared SERS bioimaging. 2017 , 12, 4349-4360	20

871	Synthesis and characterization of noble metal-titania core-shell nanostructures with tunable shell thickness. 2017 , 8, 2083-2093	11
870	Amphiphilic Functionalized Acupuncture Needle as SERS Sensor for In Situ Multiphase Detection. 2018 , 90, 3826-3832	33
869	3D Plasmon Coupling Assisted Sers on Nanoparticle-Nanocup Array Hybrids. 2018 , 8, 3002	15
868	Mechanistic Insights on Plasmon-Driven Photocatalytic Oxidative Coupling of Thiophenol Derivatives: Evidence for Steady-State Photoactivated Oxygen. 2018 , 122, 5686-5697	28
867	A polydopamine-based molecularly imprinted polymer on nanoparticles of type SiO@rGO@Ag for the detection of Ecyhalothrin via SERS. 2018 , 185, 193	20
866	Plasmon-Induced Magnetic Resonance Enhanced Raman Spectroscopy. 2018 , 18, 2209-2216	70
865	Surface enhanced Raman spectroscopy (SERS): A novel reliable technique for rapid detection of common harmful chemical residues. 2018 , 75, 10-22	120
864	Surface-Enhanced Raman Scattering Detection of Pesticide Residues Using Transparent Adhesive Tapes and Coated Silver Nanorods. 2018 , 10, 9129-9135	87
863	3D silver nanoparticles with multilayer graphene oxide as a spacer for surface enhanced Raman spectroscopy analysis. 2018 , 10, 5897-5905	112
862	Probing of sub-picometer vertical differential resolutions using cavity plasmons. 2018 , 9, 801	63
861	Plasmon-enhanced scattering and charge transfer in few-layer graphene interacting with buried printed 2D-pattern of silver nanoparticles. 2018 , 29, 175301	2
860	Effect of nanostructured silicon on surface enhanced Raman scattering.. 2018 , 8, 6629-6633	11
859	Experimental and theoretical investigation for a hierarchical SERS activated platform with 3D dense hot spots. 2018 , 263, 408-416	22
858	Cellulose Microfiber-Supported TiO2@Ag Nanocomposites: A Dual-Functional Platform for Photocatalysis and in Situ Reaction Monitoring. 2018 , 57, 4277-4286	20
857	Design of SERS nanoprobe for Raman imaging: materials, critical factors and architectures. 2018 , 8, 381-389	42
856	In situ formation of SERS hot spots by a bis-quaternized perylene dye: a simple strategy for highly sensitive detection of heparin over a wide concentration range. 2018 , 143, 1899-1905	15
855	Classifying low-grade and high-grade bladder cancer using label-free serum surface-enhanced Raman spectroscopy and support vector machine. 2018 , 28, 035603	13
854	Ultrahigh sensitive metal-free SERS platforms by functional-groups. 2018 , 263, 258-265	6

853	Zero-Mode Waveguide Nanophotonic Structures for Single Molecule Characterization. 2018 , 51, 193001	15
852	CdS core-Au plasmonic satellites nanostructure enhanced photocatalytic hydrogen evolution reaction. 2018 , 49, 363-371	85
851	Raman photostability of off-resonant gap-enhanced Raman tags.. 2018 , 8, 14434-14444	18
850	Miniaturized dielectric barrier discharge-atomic emission spectrometer for pesticide: Sensitive determination of thiram after derivatization with mercurial ion. 2018 , 138, 457-464	9
849	Surface-enhanced Raman spectroscopy (SERS): an adventure from plasmonic metals to organic semiconductors as SERS platforms. 2018 , 6, 5314-5335	129
848	ReviewSurface-Enhanced Raman Scattering Sensors for Food Safety and Environmental Monitoring. 2018 , 165, B3098-B3118	88
847	Raman spectroscopy probing of redox states and mechanism of flavin coenzyme. 2018 , 49, 1311-1322	6
846	Platinum nanoparticles: a non-toxic, effective and thermally stable alternative plasmonic material for cancer therapy and bioengineering. 2018 , 10, 9097-9107	55
845	Surface-enhanced Raman spectroscopy solution and solid substrates with built-in calibration for quantitative applications. 2018 , 49, 659-667	15
844	Electrochemical Dynamics of a Single Platinum Nanoparticle Collision Event for the Hydrogen Evolution Reaction. 2018 , 130, 3522-3526	29
843	Facile On-Site Aqueous Pollutant Monitoring Using a Flexible, Ultralight, and Robust Surface-Enhanced Raman Spectroscopy Substrate: Interface Self-Assembly of Au@Ag Nanocubes on a Polyvinyl Chloride Template. 2018 , 52, 5812-5820	40
842	Electrochemical fabrication of pyramid-shape silver microstructure as effective and reusable SERS substrate. 2018 , 274, 242-249	26
841	Shell-Isolated Tip-Enhanced Raman and Fluorescence Spectroscopy. 2018 , 130, 7645-7649	10
840	Silver microspheres coated with a molecularly imprinted polymer as a SERS substrate for sensitive detection of bisphenol A. 2018 , 185, 242	37
839	Facile Amplification of Solution-State Surface-Enhanced Raman Scattering of Small Molecules Using Spontaneously Formed 3D Nanoplasmonic Wells. 2018 , 90, 5023-5031	16
838	Rhodium nanocubes and nanotripods for highly sensitive ultraviolet surface-enhanced Raman spectroscopy. 2018 , 143, 2310-2322	6
837	Both Cationic and Anionic Co-(de)intercalation into a Metal-Oxide Material. 2018 , 2, 1134-1145	70
836	Smart-Dust-Nanorice for Enhancement of Endogenous Raman Signal, Contrast in Photoacoustic Imaging, and T2-Shortening in Magnetic Resonance Imaging. 2018 , 14, e1703683	6

835	Surface-Enhanced Raman Spectroscopy for Bioanalysis: Reliability and Challenges. 2018 , 118, 4946-4980	746
834	Shell-Isolated Tip-Enhanced Raman and Fluorescence Spectroscopy. 2018 , 57, 7523-7527	29
833	Density-matrix evaluation of the enhancement to resonant Raman scattering and fluorescence of molecules confined in metallic nanoparticle dimers. 2018 , 8, 1832	9
832	Localized surface plasmon resonance based biosensing. 2018 , 18, 279-296	42
831	Direct Visualization of the Reversible O /O Redox Process in Li-Rich Cathode Materials. 2018 , 30, e1705197	190
830	Conductive nitrides: Growth principles, optical and electronic properties, and their perspectives in photonics and plasmonics. 2018 , 123, 1-55	128
829	Label-free SERS in biological and biomedical applications: Recent progress, current challenges and opportunities. 2018 , 197, 56-77	100
828	Rapid and ultrasensitive surface-enhanced Raman spectroscopy detection of mercury ions with gold film supported organometallic nanobelts. 2020 , 31, 155501	6
827	Unraveling the Mechanism of Water-Mediated Sulfur Tolerance via Operando Surface-Enhanced Raman Spectroscopy. 2020 , 12, 2370-2379	12
826	Voltage-manipulating graphene-mediated surface-enhanced Raman scattering (G-SERS): principle and applications. 2020 , 55, 558-573	5
825	Water oxidation intermediates on iridium oxide electrodes probed by in situ electrochemical SHINERS. 2020 , 56, 1129-1132	19
824	Identifying Anionic Redox Activity within the Related O3- and P2-Type Cathodes for Sodium-Ion Battery. 2020 , 12, 851-857	13
823	Controlled fabrication of gold nanobipyramids/polypyrrole for shell-isolated nanoparticle-enhanced Raman spectroscopy to detect β -aminobutyric acid. 2020 , 229, 117890	11
822	Upconversion Nanoparticle-Assisted Payload Delivery from TiO under Near-Infrared Light Irradiation for Bacterial Inactivation. 2020 , 14, 337-346	50
821	Crystal-Amorphous Core-Shell Structure Synergistically Enabling TiO Nanoparticles' Remarkable SERS Sensitivity for Cancer Cell Imaging. 2020 , 12, 4204-4211	31
820	Surface Plasmon Field-Enhanced Raman Scattering Based on Evanescent Field Excitation of Waveguide-Coupled Surface Plasmon Resonance Configuration. 2020 , 124, 1640-1645	3
819	A review on recent advances in the applications of surface-enhanced Raman scattering in analytical chemistry. 2020 , 1097, 1-29	159
818	Plexciton for surface enhanced Raman scattering and emission. 2020 , 51, 476-482	7

817	Enhanced sensing of sulfur hexafluoride decomposition components based on noble-metal-functionalized cerium oxide. 2020 , 187, 108391	10
816	Ag@TiO Nanoprisms with Highly Efficient Near-Infrared Photothermal Conversion for Melanoma Therapy. 2020 , 15, 148-155	15
815	Silver Nanoparticles SERS Sensors Using Rapid Thermal CVD Nanoscale Graphene Islands as Templates. 2020 , 19, 25-33	3
814	Few-layered vdW MoO ₃ for sensitive, uniform and stable SERS applications. 2020 , 507, 145116	13
813	Probing Hot Electron Behaviors by Surface-Enhanced Raman Spectroscopy. 2020 , 1, 100184	13
812	Distance-Dependence Study of Plasmon Resonance Energy Transfer with DNA Spacers. 2020 , 92, 14278-14283	7
811	Portable and multiplexed lateral flow immunoassay reader based on SERS for highly sensitive point-of-care testing. 2020 , 168, 112524	28
810	Surface-enhanced Raman scattering holography. 2020 , 15, 1005-1011	28
809	Ultrasensitive and Remote SERS Enabled by Oxygen-free Integrated Plasmonic Field Transmission. 2020 , 1, 100189	2
808	Observing a Chemical Reaction at a Buried Solid/Solid Interface in Situ. 2020 , 92, 14145-14152	12
807	Probing the Mechanisms of Strong Fluorescence Enhancement in Plasmonic Nanogaps with Sub-nanometer Precision. 2020 , 14, 14769-14778	15
806	Theoretical and Experimental Studies of TiC MXene for Surface-Enhanced Raman Spectroscopy-Based Sensing. 2020 , 5, 26486-26496	17
805	Recent progress in use and observation of surface hydrogen migration over metal oxides. 2020 , 22, 22852-22863	14
804	Surface coordination layer passivates oxidation of copper. <i>Nature</i> , 2020 , 586, 390-394	50-4 54
803	Carbon Monoxide Gas Induced 4H-to- Phase Transformation of Gold As Revealed by Transmission Electron Microscopy. 2020 , 59, 14415-14423	1
802	Shell isolated nanoparticle enhanced Raman spectroscopy for renewable energy electrocatalysis. 2020 , 44, 19953-19960	5
801	Polarization- and Wavelength-Dependent Shell-Isolated-Nanoparticle-Enhanced Sum-Frequency Generation with High Sensitivity. 2020 , 125, 047401	11
800	Trends in luminescence thermometry. 2020 , 128, 040902	122

799	A Bifunctional Photo-Assisted Li-O Battery Based on a Hierarchical Heterostructured Cathode. 2020 , 32, e1907098	36
798	Sensitive and reproducible surface-enhanced raman spectroscopy (SERS) with arrays of dimer-nanopillars. 2020 , 322, 128563	16
797	Plasmonics under Attack: Protecting Copper Nanostructures from Harsh Environments. 2020 , 32, 6788-6799	7
796	UV Irradiation-Induced SERS Enhancement in Randomly Distributed Au Nanostructures. 2020 , 20,	1
795	Introduction and overview. 2020 , 1-40	0
794	Surface-enhanced Raman scattering (SERS) and applications. 2020 , 349-386	2
793	Shell-isolated nanoparticle-enhanced Raman spectroscopy: a review. 2020 , 387-414	
792	2D materials: Excellent substrates for surface-enhanced Raman scattering (SERS) in chemical sensing and biosensing. 2020 , 130, 115983	30
791	Spectroscopic Probe Molecule Selection Using Quantum Theory, First-Principles Calculations, and Machine Learning. 2020 ,	4
790	The moveable "hot spots" effect in an Au nanoparticles-Au plate coupled system. 2020 , 12, 23789-23798	3
789	Nanoparticles Engineering by Pulsed Laser Ablation in Liquids: Concepts and Applications. 2020 , 10,	43
788	A high-capacity cathode for rechargeable K-metal battery based on reversible superoxide-peroxide conversion. 2021 , 8, nwaa287	6
787	Beyond Adsorption Descriptors in Hydrogen Electrocatalysis. 2020 , 10, 14747-14762	30
786	Intrinsic electrocatalytic activity of a single IrO nanoparticle towards oxygen evolution reaction. 2020 , 12, 22014-22021	5
785	Single-Molecule Sensing of Interfacial Acid-Base Chemistry. 2020 , 11, 10023-10028	11
784	Atomically precise alloy nanoclusters: syntheses, structures, and properties. 2020 , 49, 6443-6514	186
783	SERS methods based on nanomaterials as a diagnostic tool of cancer. 2020 , 189-211	
782	Bulk Phase-Encoded Gold Nanoparticles: The Fourth-Generation Surface-Enhanced Raman Scattering Tag for Hg ²⁺ Ion Detection. 2020 , 124, 19267-19272	3

781	Observation of inhomogeneous plasmonic field distribution in a nanocavity. 2020 , 15, 922-926	22
780	Physicochemical properties and structure of fluid at nano-/micro-interface: Progress in simulation and experimental study. 2020 , 5, 274-285	14
779	Facile Synthesis of an Economic 3D Surface-Enhanced Raman Scattering Platform for Ultrasensitive Detection of Antibiotics. 2020 , 13, 1947-1955	5
778	A Liquid Electrolyte with De-Solvated Lithium Ions for Lithium-Metal Battery. 2020 , 4, 1776-1789	62
777	Point-of-Use Rapid Detection of SARS-CoV-2: Nanotechnology-Enabled Solutions for the COVID-19 Pandemic. 2020 , 21,	61
776	Nanoscale optical imaging in chemistry. 2020 ,	24
775	IoT based detection of adulteration in Gold using ANN. 2020 , 764, 012018	
774	Highly efficient core-shell Ag@carbon dot modified TiO nanofibers for photocatalytic degradation of organic pollutants and their SERS monitoring.. 2020 , 10, 26639-26645	6
773	Low temperature synthesis of plasmonic molybdenum nitride nanosheets for surface enhanced Raman scattering. 2020 , 11, 3889	17
772	Rapid and Quantitative Detection of Aflatoxin B in Grain by Portable Raman Spectrometer. 2020 , 74, 1365-1373	3
771	Facile and versatile substrate fabrication for surface enhanced Raman spectroscopy using spark discharge generation of Au/Ag nanoparticles. 2020 , 531, 147268	7
770	Silica shell-isolated gold nanospheres: Synthesis, investigation of stability in organic solvents, and application in shell-isolated nanoparticle-enhanced Raman spectroscopy. 2020 , 29, 100497	2
769	Three-dimensional AuAg alloy NPs/graphene/AuAg alloy NP sandwiched hybrid nanostructure for surface enhanced Raman scattering properties. 2020 , 8, 12599-12606	9
768	Surface-enhanced electrochemiluminescence combined with resonance energy transfer for sensitive carcinoembryonic antigen detection in exhaled breath condensates. 2020 , 145, 6524-6531	3
767	ZIF-8-modified Au-Ag/Si nanoporous pillar array for active capture and ultrasensitive SERS-based detection of pentachlorophenol. 2020 , 12, 4064-4071	3
766	Programmable Organic-Free Negative Differential Resistance Memristor Based on Plasmonic Tunnel Junction. 2020 , 16, e2002727	7
765	Nano-substructured plasmonic pore arrays: a robust, low cost route to reproducible hierarchical structures extended across macroscopic dimensions. 2020 , 2, 4740-4756	2
764	Low temperature-boosted high efficiency photo-induced charge transfer for remarkable SERS activity of ZnO nanosheets. 2020 , 11, 9414-9420	22

763	Tin oxide subnanoparticles: a precisely-controlled synthesis, subnano-detection for their detailed characterisation and applications. 2020 , 49, 13512-13518	0
762	Design of Organic/Inorganic Hybrid Catalysts for Energy and Environmental Applications. 2020 , 6, 1916-1937	14
761	Ag-Nanoparticles@Bacterial Nanocellulose as a 3D Flexible and Robust Surface-Enhanced Raman Scattering Substrate. 2020 , 12, 50713-50720	24
760	Influence of cavity geometry towards plasmonic gap tolerance and respective near-field in nanoparticle-on-mirror. 2020 , 20, 1335-1341	2
759	Shining Light on Aluminum Nanoparticle Synthesis. 2020 , 53, 2020-2030	12
758	Observation of Substituent Effects in the Electrochemical Adsorption and Hydrogenation of Alkynes on Pt ₂ Using SHINERS. 2020 , 10, 10999-11010	6
757	Advances and challenges for experiment and theory for multi-electron multi-proton transfer at electrified solid-liquid interfaces. 2020 , 22, 19401-19442	18
756	A sensitive SERS-based sandwich immunoassay platform for simultaneous multiple detection of foodborne pathogens without interference. 2020 , 12, 4885-4891	10
755	Monolayer ZnS@Ag Nanospheres SERS Substrate for Highly Sensitive Dye Molecules Detection. 2020 , 15, 2050122	1
754	Vertically-Oriented WS Nanosheets with a Few Layers and Its Raman Enhancements. 2020 , 10,	4
753	Crystal Phase Control of Gold Nanomaterials by Wet-Chemical Synthesis. 2020 , 53, 2106-2118	34
752	Porous carbon nanowire array for surface-enhanced Raman spectroscopy. 2020 , 11, 4772	37
751	Selectively enhanced Raman/fluorescence spectra in photonic-plasmonic hybrid structures. 2020 , 2, 4682-4688	2
750	Electrochemical metamaterials. 2020 , 24, 2101-2111	1
749	Quantitative and Sensitive SERS Platform with Analyte Enrichment and Filtration Function. 2020 , 20, 7304-7312	80
748	Silica-Coated Silver Nanoparticles Decorated with Fluorescent CdTe Quantum Dots and DNA Aptamers for Detection of Tetracycline. 2020 , 3, 9796-9803	12
747	In Situ Raman Study of CO Electrooxidation on Pt(hkl) Single-Crystal Surfaces in Acidic Solution. 2020 , 132, 23760-23764	1
746	In Situ Raman Study of CO Electrooxidation on Pt(hkl) Single-Crystal Surfaces in Acidic Solution. 2020 , 59, 23554-23558	20

745	Photoinduced Enhanced Raman Spectroscopy with Hybrid 2 Nanosheets. 2020 , 124, 20350-20358	9
744	Atomistic Control of Metal-Molecule Junctions for Efficient Photo-Induced Uphill Charge Transfer. 2020 , 124, 18173-18180	5
743	Electronic and vibrational surface-enhanced Raman scattering: from atomically defined Au(111) and (100) to roughened Au. 2020 , 11, 9807-9817	11
742	Biosensing based on surface-enhanced Raman spectroscopy as an emerging/next-generation point-of-care approach for acute myocardial infarction diagnosis. 2020 , 40, 1191-1209	5
741	Operando characterization techniques for electrocatalysis. 2020 , 13, 3748-3779	83
740	. 2020 ,	1
739	Long-Range Surface Plasmon Resonance Configuration for Enhancing SERS with an Adjustable Refractive Index Sample Buffer to Maintain the Symmetry Condition. 2020 , 5, 32951-32958	2
738	Bridging the Gap in the Mechanistic Understanding of Electrocatalysis via In Situ Characterizations. 2020 , 23, 101776	7
737	A study of the diffusion behaviour of reactive dyes in cellulose fibres using confocal Raman microscopy. 2020 , 136, 503-511	4
736	Carbon based dots capped tin oxide nanosheets hybridizing with silver nanoparticles for ultra-sensitive surface enhanced raman scattering substrate. 2020 , 170, 270-276	8
735	Bimetallic Core-Shell Nanostars with Tunable Surface Plasmon Resonance for Surface-Enhanced Raman Scattering. 2020 , 3, 10885-10894	13
734	Surface-Enhanced Raman Spectroscopy: General Introduction. 2020 , 1-42	1
733	Recent advances on the synthesis of mesoporous metals for electrocatalytic methanol oxidation. 2020 , 3, 291-306	2
732	Operando vibrational spectroscopy for electrochemical biomass valorization. 2020 , 56, 8726-8734	13
731	Patterned Superhydrophobic SERS Substrates for Sample Pre-Concentration and Demonstration of Its Utility through Monitoring of Inhibitory Effects of Paraoxon and Carbaryl on AChE. 2020 , 25,	1
730	Synthesis of highly-branched Au@AgPd core/shell nanoflowers for in situ SERS monitoring of catalytic reactions. 2020 , 31, 2437-2441	5
729	Facile synthesis of Au nanoparticle-coated FeO magnetic composite nanospheres and their application in SERS detection of malachite green. 2020 , 241, 118532	18
728	Damping resonance and refractive index effect on the layer-by-layer sputtering of Ag and AlO on the polystyrene template. 2020 , 238, 118430	2

727	Mechanism Study of Molecular Deformation of 2,2',5',2''-Tetramethylated -Terphenyl-4,4''-dithiol Trapped in Gold Junctions. 2020 , 11, 4456-4461	3
726	Buoyant particulate strategy for few-to-single particle-based plasmonic enhanced nanosensors. 2020 , 11, 2603	16
725	Surface-enhanced Raman scattering based on hybrid surface plasmon excited by Au nanodisk and Au film coupling structure. 2020 , 384, 126544	22
724	Investigate on plasma catalytic reaction of 4-nitrobenzenethiol on Ag@SiO ₂ Core-Shell substrate via Surface-enhanced Raman scattering. 2020 , 237, 118362	6
723	Hotspots on the Move: Active Molecular Enrichment by Hierarchically Structured Micromotors for Ultrasensitive SERS Sensing. 2020 , 12, 28783-28791	20
722	Plasmonic and phononic properties of epitaxial conductive transition metal nitrides. 2020 , 22, 084001	12
721	Cross-plane transport in a single-molecule two-dimensional van der Waals heterojunction. 2020 , 6, eaba6714	19
720	Quantifying Optical Absorption of Single Plasmonic Nanoparticles and Nanoparticle Dimers Using Microstring Resonators. 2020 , 5, 2067-2075	1
719	Shining light on the solid-liquid interface: in situ/operando monitoring of surface catalysis. 2020 , 10, 5362-5385	7
718	SERS using two-photon polymerized nanostructures for mycotoxin detection.. 2020 , 10, 14274-14282	10
717	ZnO micron rods as single dielectric resonator for optical sensing. 2020 , 1109, 107-113	1
716	Roughened silver microtubes for reproducible and quantitative SERS using a template-assisted electrosynthesis approach. 2020 , 20, 100710	5
715	AuPtPd spherically self-assembled nano-sieves as SERS sensors. 2020 , 843, 155885	4
714	Molecular-level effects on cell membrane models to explain the phototoxicity of gold shell-isolated nanoparticles to cancer cells. 2020 , 194, 111189	11
713	Chemical selectivity in electrochemical surface oxidation enhanced Raman scattering. 2020 , 353, 136560	4
712	Ag-Embedded Silica Core-Shell Nanospheres for Surface Enhanced Raman Spectroscopy of High-Temperature Processes. 2020 , 92, 9566-9573	3
711	Plasmon-Enhanced Resonant Photoemission Using Atomically Thick Dielectric Coatings. 2020 , 14, 8806-8815	12
710	Preparation of Monolayer Photonic Crystals from Ag Nanobulge-Deposited SiO ₂ Particles as Substrates for Reproducible SERS Assay of Trace Thiol Pesticide. 2020 , 10,	4

- 709 Flower-like Ag coated with molecularly imprinted polymers as a surface-enhanced Raman scattering substrate for the sensitive and selective detection of glibenclamide. **2020**, 12, 2858-2864 13
- 708 Windowless thin layer electrochemical Raman spectroscopy of Ni-Fe oxide electrocatalysts during oxygen evolution reaction. **2020**, 871, 114282 10
- 707 Raman reporter-assisted Au nanorod arrays SERS nanoprobe for ultrasensitive detection of mercuric ion (Hg) with superior anti-interference performances. **2020**, 398, 122890 15
- 706 Silicon-Au nanowire resonators for high-Q multiband near-infrared wave absorption. **2020**, 31, 375201 3
- 705 White nanolight source for optical nanoimaging. **2020**, 6, eaba4179 18
- 704 Real-time detection of single-molecule reaction by plasmon-enhanced spectroscopy. **2020**, 6, eaba6012 17
- 703 A 500 Wh/kg Lithium-Metal Cell Based on Anionic Redox. **2020**, 4, 1445-1458 39
- 702 Thermal Stability of Unary to Quinary Noble-Metal/3d-Transition-Metal Alloy Nanoparticles from Molecular Dynamics Simulations: Implications for Multimetallic Catalysis. **2020**, 3, 5381-5389 5
- 701 Ultrasmall Ag Clusters Modified W18O49 Ultrathin Nanowires for Sensitive Surface Enhanced Raman Spectroscopy Detection. **2020**, 5, 3105-3112 1
- 700 Selective, Quantitative, and Multiplexed Surface-Enhanced Raman Spectroscopy Using Aptamer-Functionalized Monolithic Plasmonic Nanogrids Derived from Cross-Point Nano-Welding. **2020**, 30, 2000612 12
- 699 Quasi-metallic Tungsten Oxide Nanodendrites with High Stability for Surface-Enhanced Raman Scattering. **2020**, 1, 100031 4
- 698 Greater SERS Activity of Ligand-Stabilized Gold Nanostars with Sharp Branches. **2020**, 36, 3558-3564 24
- 697 Methods of inorganic pollutants detection in water. **2020**, 115-134
- 696 In-Situ Probing of Crystal-Phase-Dependent Photocatalytic Activities of Au Nanostructures by Surface-Enhanced Raman Spectroscopy. **2020**, 2, 409-414 14
- 695 . **2020**,
- 694 Sensitive and label-free shell isolated Ag NPs@Si architecture based SERS active substrate: FDTD analysis and in-situ cellular DNA detection. **2020**, 515, 145955 13
- 693 Cysteamine modified core-shell nanoparticles for rapid assessment of oxamyl and thiacloprid pesticides in milk using SERS. **2020**, 14, 2021-2029 28
- 692 Highly Efficient Gold Nano-Flower Optical Biosensor Doped in a Sol-Gel/PEG Matrix for the Determination of a Calcitonin Biomarker in Different Serum Samples. **2020**, 5, 5629-5637 13

691	In Situ Raman Monitoring and Manipulating of Interfacial Hydrogen Spillover by Precise Fabrication of Au/TiO ₂ /Pt Sandwich Structures. 2020 , 59, 10343-10347	30
690	In Situ Raman Monitoring and Manipulating of Interfacial Hydrogen Spillover by Precise Fabrication of Au/TiO ₂ /Pt Sandwich Structures. 2020 , 132, 10429-10433	5
689	Conductometric Response-Triggered Surface-Enhanced Raman Spectroscopy for Accurate Gas Recognition and Monitoring Based on Oxide-wrapped Metal Nanoparticles. 2020 , 5, 1641-1649	3
688	Trace detection of polycyclic aromatic hydrocarbons in environmental waters by SERS. 2020 , 234, 118250	15
687	The cascade structure of periodic micro/nanoscale Au nano-islands @ Ag-frustum arrays as effective SERS substrates. 2020 , 175, 109265	5
686	A Filter Supported Surface-Enhanced Raman Scattering "Nose" for Point-of-Care Monitoring of Gaseous Metabolites of Bacteria. 2020 , 92, 5055-5063	15
685	Shell-isolated nanoparticle-enhanced Raman spectroscopy for characterization of living yeast cells. 2020 , 240, 118560	9
684	Synthesis of a Gold-Metal Oxide Core-Satellite Nanostructure for In Situ SERS Study of CuO-Catalyzed Photooxidation. 2020 , 59, 18003-18009	14
683	Monolayer Assembly of MultiSpiked Gold Nanoparticles for Surface-Enhanced Raman Spectroscopy-Based Trace Detection of Dyes and Explosives. 2020 , 3, 6766-6773	9
682	Electrochemical SHINERS investigation of the adsorption of butyl xanthate and 2-mercaptobenzothiazole on pyrite. 2020 , 529, 147118	3
681	Molecular fingerprint of precancerous lesions in breast atypical hyperplasia. 2020 , 48, 300060520931616	2
680	Defining the plasmonic cavity performance based on mode transitions to realize highly efficient device design. 2020 , 1, 139-145	0
679	Synthesis of a Gold-Metal Oxide Core-Satellite Nanostructure for In Situ SERS Study of CuO-Catalyzed Photooxidation. 2020 , 132, 18159-18165	6
678	Reliable Quantification of pH Variation in Live Cells Using Prussian Blue-Caged Surface-Enhanced Raman Scattering Probes. 2020 , 92, 9574-9582	12
677	Ultrathin layer solid transformation-enabled-surface enhanced Raman spectroscopy for trace harmful small gaseous molecule detection. 2020 , 5, 739-746	9
676	Insights into plasmon induced keto-enol isomerization. 2020 , 12, 4334-4340	2
675	Core-Shell Nanostructure-Enhanced Raman Spectroscopy for Surface Catalysis. 2020 , 53, 729-739	65
674	Unveiling the size effect of Pt-on-Au nanostructures on CO and methanol electrooxidation by in situ electrochemical SERS. 2020 , 12, 5341-5346	9

673	In Situ Shell-Isolated Nanoparticle-Enhanced Raman Spectroscopy of Nickel-Catalyzed Hydrogenation Reactions. 2020 , 21, 625-632	11
672	Detect, remove and re-use: Sensing and degradation pesticides via 3D tilted ZMRs/Ag arrays. 2020 , 391, 122222	27
671	Surface-enhanced Raman spectroscopy for polychlorinated biphenyl detection: Recent developments and future prospects. 2020 , 125, 115836	16
670	Macroscopic two-dimensional monolayer films of gold nanoparticles: fabrication strategies, surface engineering and functional applications. 2020 , 12, 7433-7460	30
669	Practical SERS method for assessment of the washing durability of textiles containing silver nanoparticles. 2020 , 12, 1186-1196	1
668	Surface-Enhanced Raman Spectrum of TiO ₂ Nanoparticle for Biosensing (TiO ₂ Nanoparticle Served as SERS Sensing Substrate). 2020 , 133-152	0
667	Preparation of multi-functional magnetic-plasmonic nanocomposite for adsorption and detection of thiram using SERS. 2020 , 392, 122356	29
666	Preserving Plasmonic Nanostructures from Laser-Induced Deactivation by a Protective Dielectric Shell. 2020 , 124, 6385-6394	1
665	Interfacial effect of dual ultra-thin SiO ₂ core-triple shell Au@SiO ₂ @Ag@SiO ₂ for ultra-sensitive trinitrotoluene (TNT) detection.. 2020 , 10, 3826-3831	1
664	Design and modulation principles of molybdenum carbide-based materials for green hydrogen evolution. 2020 , 48, 398-423	19
663	3D Ultrasensitive Polymers-Plasmonic Hybrid Flexible Platform for In-Situ Detection. 2020 , 12,	5
662	SERS-encoded nanocomposites for dual pathogen bioassay. 2020 , 43, 161-167	5
661	Enhancing local electric fields at plasmonic nanogaps by optimal dielectric coatings. 2020 , 53, 155103	6
660	Mechanistic understanding of the electrocatalytic CO ₂ reduction reaction [New developments based on advanced instrumental techniques. 2020 , 31, 100835	42
659	Surface Changes of Li _{0.9} Ni _{0.1} Mn _{0.9} Co _{0.1} O ₂ in Li-Ion Batteries Using in Situ Surface-Enhanced Raman Spectroscopy. 2020 , 124, 4024-4031	13
658	Rapid and low-cost quantitative detection of creatinine in human urine with a portable Raman spectrometer. 2020 , 154, 112067	26
657	Ultrastable monodispersed lead halide perovskite nanocrystals derived from interfacial compatibility. 2020 , 71, 104554	9
656	Li-doping stabilized P2-Li _{0.2} Na _{1.0} Mn _{0.8} O ₂ sodium ion cathode with oxygen redox activity. 2020 , 44, 3253-3259	7

655	Fundamental Aspects of Electrocatalysis 1). 2020 , 773-890	8
654	Light extinction spectrometry for determining the size distribution and concentration of polydisperse gold nanospheres. 2020 , 204, 163676	1
653	Enzyme-Assist-Interference-Free Strategy for Raman Selective Determination of Sialic Acid. 2020 , 92, 3332-3339	4
652	Niobium pentoxide ultra-thin nanosheets: A photocatalytic degradation and recyclable surface-enhanced Raman scattering substrate. 2020 , 509, 145376	11
651	Surface-Modified Two-Dimensional Titanium Carbide Sheets for Intrinsic Vibrational Signal-Retained Surface-Enhanced Raman Scattering with Ultrahigh Uniformity. 2020 , 12, 23523-23531	15
650	Substrate for Surface-Enhanced Raman Spectroscopy Formed by Gold Nanoparticles Buried in Poly(methyl methacrylate). 2020 , 5, 10366-10373	6
649	Fundamental understanding and applications of plasmon-enhanced Raman spectroscopy. 2020 , 2, 253-271	128
648	Surface enhanced infrared absorption spectroscopy (SEIRA) as a green analytical chemistry approach: Coating of recycled aluminum TLC sheets with citrate capped silver nanoparticles for chemometric quantitative analysis of ternary mixtures as a green alternative to the traditional methods. 2020 , 1117, 60-73	11
647	Remarkable surface-enhanced Raman scattering of highly crystalline monolayer Ti3C2 nanosheets. 2020 , 63, 794-805	29
646	Light trapping induced flexible wrinkled nanocone SERS substrate for highly sensitive explosive detection. 2020 , 314, 128081	26
645	Reproducible and Bendable SERS Substrates with Tailored Wettability Using Block Copolymers and Anodic Aluminum Oxide Templates. 2020 , 41, e2000088	2
644	Surface plasmons and SERS application of Au nanodisk array and Au thin film composite structure. 2020 , 52, 1	24
643	Design of Magnetic-Plasmonic Nanoparticle Assemblies via Interface Engineering of Plasmonic Shells for Targeted Cancer Cell Imaging and Separation. 2020 , 16, e2001103	12
642	Speciation of Cu Surfaces During the Electrochemical CO Reduction Reaction. 2020 , 142, 9735-9743	70
641	Revisiting the Atomistic Structures at the Interface of Au(111) Electrode-Sulfuric Acid Solution. 2020 , 142, 9439-9446	22
640	Paper-based flexible surface enhanced Raman scattering platforms and their applications to food safety. 2020 , 100, 349-358	24
639	Controlled Synthesis of Palladium Nanocubes as an Efficient Nanocatalyst for Suzuki-Miyaura Cross-Coupling and Reduction of -Nitrophenol. 2020 , 36, 5208-5218	15
638	Convenient Construction of Orthogonal Dual Aptamer-Based Plasmonic Immunosandwich Assay for Probing Protein Disease Markers in Complex Samples and Living Animals. 2020 , 5, 1436-1444	10

- 637 Fabrication and Applications of 3D Nanoarchitectures for Advanced Electrocatalysts and Sensors. **2020**, 32, e1907500 10
- 636 Shell-Isolated Nanoparticle-Enhanced Luminescence of Metallic Nanoclusters. **2020**, 92, 7146-7153 5
- 635 Nanoscale Sensors in Catalysis: All Eyes on Catalyst Particles. **2020**, 14, 3725-3735 36
- 634 Quantum electrocatalysts: theoretical picture, electrochemical kinetic isotope effect analysis, and conjecture to understand microscopic mechanisms. **2020**, 22, 11219-11243 11
- 633 Raman study of the photoinduced behavior of dye molecules on TiO(γ) single crystal surfaces. **2020**, 11, 6431-6435 4
- 632 Combination of an Artificial Intelligence Approach and Laser Tweezers Raman Spectroscopy for Microbial Identification. **2020**, 92, 6288-6296 32
- 631 Restructuring effects of the chemical environment in metal nanocatalysis and single-atom catalysis. **2021**, 373, 80-97 17
- 630 Long-range surface plasmon enhanced Raman spectroscopy at highly damping platinum electrodes. **2021**, 52, 420-430 2
- 629 Plasmonic gold nanostars@ZIF-8 nanocomposite for the ultrasensitive detection of gaseous formaldehyde. **2021**, 56, 4151-4160 8
- 628 Wafer-scale SERS metallic nanotube arrays with highly ordered periodicity. **2021**, 329, 129132 8
- 627 Graphene-coated Au nanoparticle-enhanced Raman spectroscopy. **2021**, 52, 439-445 6
- 626 Surface-enhanced Raman scattering-active AuNR array cellulose films for multi-hazard detection. **2021**, 402, 123505 11
- 625 Attenuated total reflection-cascading nanostructure-enhanced Raman spectroscopy on flat surfaces: A nano-optical design. **2021**, 52, 446-457 1
- 624 Fabrication of colloidal platforms for surface-enhanced Raman spectroscopy on optically inert templates. **2021**, 52, 554-562 2
- 623 A nanozyme-based enhanced system for total removal of organic mercury and SERS sensing. **2021**, 405, 124642 10
- 622 Plasmon mediated photoelectrochemical transformations: The example of para-aminothiophenol. **2021**, 367, 137485 5
- 621 Electrokinetic Preseparation and Molecularly Imprinted Trapping for Highly Selective SERS Detection of Charged Phthalate Plasticizers. **2021**, 93, 946-955 14
- 620 Label-free SERS detection of Raman-Inactive protein biomarkers by Raman reporter indicator: Toward ultrasensitivity and universality. **2021**, 174, 112825 60

619	Local hot charge density regulation: Vibration-free pyroelectric nanogenerator for effectively enhancing catalysis and in-situ surface enhanced Raman scattering monitoring. 2021 , 81, 105585	105
618	2D to 3D transformation of gold nanosheets on human adipose-derived Elastin nanotemplates. 2021 , 95, 66-72	
617	Spectroscopic Verification of Adsorbed Hydroxy Intermediates in the Bifunctional Mechanism of the Hydrogen Oxidation Reaction. 2021 , 60, 5708-5711	24
616	Shell-Isolated Au Nanoparticles Functionalized with Rhodamine B Fluorophores in Helium Nanodroplets. 2021 , 12, 145-150	5
615	Fluorinated hexagonal boron nitride as a spacer with silver nanorods for surface enhanced Raman spectroscopy analysis. 2021 , 47, 6528-6534	2
614	Three-Dimensional Metamaterial for Plasmon-Enhanced Raman Scattering at any Excitation Wavelengths from the Visible to Near-Infrared Range. 2021 , 93, 1409-1415	3
613	Spectroscopic Verification of Adsorbed Hydroxy Intermediates in the Bifunctional Mechanism of the Hydrogen Oxidation Reaction. 2021 , 133, 5772-5775	2
612	Nanoporous FePd alloy as multifunctional ferromagnetic SERS-active substrate. 2021 , 543, 148759	7
611	Molecular Radiative Energy Shifts under Strong Oscillating Fields. 2021 , 17, e2007244	
610	Shell-Isolated Plasmonic Nanostructures for Biosensing, Catalysis, and Advanced Nanoelectronics. 2021 , 31, 2008031	7
609	Interface-Induced Ag Monolayer Film for Surface-Enhanced Raman Scattering Detection of Water-Insoluble Enrofloxacin. 2021 , 16, 349-358	4
608	Dual synergistic modulation of photo-induced electron transfer processes between molecules and gold nanopillars for ultrasensitive plasmon-enhanced Raman scattering. 2021 , 9, 8842-8848	2
607	Mechanical modulation of spontaneous emission of nearby nanostructured black phosphorus. 2021 , 29, 1037-1047	1
606	Single-molecule electrochemistry. 2021 , 253-293	0
605	Single-molecule surface-enhanced Raman spectroscopy (SM-SERS): characteristics and spectral information. 2021 , 70, 137401-137401	0
604	(Nano)tag-antibody conjugates in rapid tests. 2021 , 9, 5414-5438	3
603	Semiconducting Metal-Organic Polymer Nanosheets for a Photoinvolved Li-O Battery under Visible Light. 2021 , 143, 1941-1947	45
602	New advances in using Raman spectroscopy for the characterization of catalysts and catalytic reactions. 2021 , 50, 3519-3564	42

601 Nanoscavengers for the Waste Water Remediation. **2021**, 73-89

600 Plasmon-driven photocatalytic molecular transformations on metallic nanostructure surfaces: mechanistic insights gained from plasmon-enhanced Raman spectroscopy. **2021**, 6, 250-280 9

599 Recent advances and perspectives in photo-induced enhanced Raman spectroscopy. **2021**, 13, 8707-8721 6

598 Recent advances in understanding oxygen evolution reaction mechanisms over iridium oxide. **2021**, 8, 2900-2917 24

597 A Programmable DNA-Silicification-Based Nanocavity for Single-Molecule Plasmonic Sensing. **2021**, 33, e2005133 10

596 A universal polymer shell-isolated nanoparticle (SHIN) design for single particle spectro-electrochemical SERS sensing using different core shapes. 0

595 Functions and Applications of CoreShell Materials in Hydrogenation-Related Processes. **2021**, 41-59

594 Large-Area Nanogap-Controlled 3D Nanoarchitectures Fabricated Layer-by-Layer Nanoimprint. **2021**, 15, 503-514 7

593 Towards practical and sustainable SERS: a review of recent developments in the construction of multifunctional enhancing substrates. **2021**, 9, 11517-11552 11

592 surface-enhanced Raman spectroelectrochemistry reveals the molecular conformation of electrolyte additives in Li-ion batteries. **2021**, 9, 20024-20031 4

591 Charge-Transfer Resonance and Electromagnetic Enhancement Synergistically Enabling MXenes with Excellent SERS Sensitivity for SARS-CoV-2 S Protein Detection. **2021**, 13, 52 43

590 Au nanolenses for near-field focusing. **2021**, 12, 6355-6361 3

589 Rational Component and Structure Design of Noble-Metal Composites for Optical and Catalytic Applications. **2021**, 2, 2000138 12

588 Progress in the Applications of Raman Spectroscopy in Microbial Identification. **2021**, 33, 1183-1190

587 Vanadium dioxide nanostructures with remarkable surface-enhanced Raman scattering activity. **2021**, 57, 4815-4818 1

586 Recent advances in plasmon-enhanced Raman spectroscopy for catalytic reactions on bifunctional metallic nanostructures. **2021**, 13, 13962-13975 6

585 Radiative Decay Rate Enhancement and Quenching for Multiple Emitters near a Metal Nanoparticle Surface. **2021**, 125, 2531-2536 2


584 Controlling the immobilization process of an optically enhanced protein microarray for highly reproducible immunoassay. **2021**, 13, 4269-4277 1

583	Applications of Shell-Isolated Nanoparticle-Enhanced Raman Spectroscopy. 2021 , 8, 46	4
582	Nanometer-Thick Al ₂ O ₃ Layers on Ag/Al Nanostructures as Conductive Electrodes. 2021 , 4, 1270-1281	1
581	Nano-slit assisted high-Q photonic resonant perfect absorbers. 2021 , 29, 5270-5278	3
580	Curvature-Dependent Cavity-Nanoparticle Scaffold-Based Clusters with LSPR Enhancement as SERS Substrates. 2021 , 16, 1231-1239	1
579	Substrate-mediated hyperbolic phonon polaritons in MoO ₃ . 2021 , 10, 1517-1527	9
578	Highly Sensitive WO Mesocrystal Raman Scattering Substrate with Large-Area Signal Uniformity. 2021 , 93, 3138-3145	11
577	Composite Structure Based on Gold-Nanoparticle Layer and HMM for Surface-Enhanced Raman Spectroscopy Analysis. 2021 , 11,	5
576	Recent progress in in situ/operando analysis tools for oxygen electrocatalysis. 2021 , 54, 173001	6
575	Improve optical properties by modifying Ag nanoparticles on a razor clam SERS substrate. 2021 , 29, 5152-5165	28
574	General molten-salt route to three-dimensional porous transition metal nitrides as sensitive and stable Raman substrates. 2021 , 12, 1376	9
573	Advances in surface-enhanced Raman scattering bioprobes for cancer imaging. 2021 , 2, 20200146	3
572	Plasmonic nanoreactors regulating selective oxidation by energetic electrons and nanoconfined thermal fields. 2021 , 7,	14
571	The origin of ultrasensitive SERS sensing beyond plasmonics. 2021 , 16, 1	17
570	Controlling Infrared Plasmon Resonances in Inverse-Spinel Cadmium Stannate Nanocrystals via Site-Selective Cation-Exchange Reactions. 2021 , 33, 1954-1963	3
569	Eco-Friendly Nanoplatfoms for Crop Quality Control, Protection, and Nutrition. 2021 , 8, 2004525	8
568	Quantum nanophotonic and nanoplasmonic sensing: towards quantum optical bioscience laboratories on chip. 2021 , 10, 1387-1435	9
567	Plasmon-enhanced lateral photovoltaic effect observed in Ag-ZnO core-shell nanoparticles. 2021 , 118, 122101	8
566	An affordable option to Au single crystals through cathodic corrosion of a wire: Fabrication, electrochemical behavior, and applications in electrocatalysis and spectroscopy. 2021 , 372, 137867	5

565	Probing Single-Atom Catalysts and Catalytic Reaction Processes by Shell-Isolated Nanoparticle-Enhanced Raman Spectroscopy. 2021 , 60, 9306-9310	17
564	Probing Single-Atom Catalysts and Catalytic Reaction Processes by Shell-Isolated Nanoparticle-Enhanced Raman Spectroscopy. 2021 , 133, 9392-9396	3
563	CVD graphene-based flexible and transparent SERS substrate towards L-tyrosine detection. 2021 , 241, 111546	2
562	Plasmonic Core-Shell Nanoparticle Enhanced Spectroscopies for Surface Analysis. 2021 , 93, 6573-6582	4
561	Plasmonic SERS active nanostructured Ag ₂ SiO ₂ at optimum volume ratio synthesized via sol-gel technique. 2021 , 606, 412638	2
560	Electrochemical Tip-Enhanced Raman Spectroscopy: An In Situ Nanospectroscopy for Electrochemistry. 2021 , 72, 213-234	6
559	A silver trimesate organic framework as an ultrasensitive surface-enhanced Raman scattering substrate for detection of various organic pollutants. 2021 , 163, 105896	5
558	In Situ Surface-Enhanced Raman Spectroscopy Characterization of Electrocatalysis with Different Nanostructures. 2021 , 72, 331-351	13
557	Near-field characterization of surface plasmon polaritons on a nanofabricated transmission structure. 2021 , 103,	2
556	Many Birds, One Stone: A Smart Nanodevice for Ratiometric Dual-Spectrum Assay of Intracellular MicroRNA and Multimodal Synergetic Cancer Therapy. 2021 , 15, 6961-6976	15
555	Polarized SERS Controlled by Anisotropic Growth on Ordered Curvature Substrate. 2021 , 26,	
554	Design and synthesis of a sandwiched silver microsphere/TiO ₂ nanoparticles/molecular imprinted polymers structure for suppressing background noise interference in high sensitivity surface-enhanced Raman scattering detection. 2021 , 544, 148879	2
553	Plasmonic Core-Shell Nanomaterials and their Applications in Spectroscopies. 2021 , e2005900	11
552	Reduced cytotoxicity of CTAB-templated silica layer on gold nanorod using fluorescence dyes and its application in cancer theranostics. 2021 , 96, 202-212	7
551	Recent advances in development of devices and probes for sensing and imaging in the brain. 2021 , 64, 915-931	6
550	Large Area Patterning of Nanoparticles and Nanostructures: Current Status and Future Prospects. 2021 , 15, 5861-5875	16
549	Modeling Electrified Pt(111)-H ₂ O/Water Interfaces from Ab Initio Molecular Dynamics. 2021 , 1, 569-577	21
548	Ultrasensitive plasmon enhanced Raman scattering detection of nucleolin using nanochannels of 3D hybrid plasmonic metamaterial. 2021 , 178, 113040	4

547	Solid Electrolyte Interphase Instability in Operating Lithium-Ion Batteries Unraveled by Enhanced-Raman Spectroscopy. 2021 , 6, 1757-1763	14
546	Synthesis, Assembly, Optical Properties, and Sensing Applications of Plasmonic Gap Nanostructures. 2021 , 33, e2006966	15
545	Au@ZIF-8 Core-Shell Nanoparticles as a SERS Substrate for Volatile Organic Compound Gas Detection. 2021 , 93, 7188-7195	16
544	Rapid identification of pathogens by using surface-enhanced Raman spectroscopy and multi-scale convolutional neural network. 2021 , 413, 3801-3811	5
543	SERS Selective Enhancement on Monolayer MoS Enabled by a Pressure-Induced Shift from Resonance to Charge Transfer. 2021 , 13, 26551-26560	5
542	A high sensitive glucose sensor based on Ag nanodendrites/Cu mesh substrate via surface-enhanced Raman spectroscopy and electrochemical analysis. 2021 , 863, 158758	10
541	Recent progress on two-dimensional layered materials for surface enhanced Raman spectroscopy and their applications. 2021 , 18, 100378	10
540	Electrospun polymeric nanofiber decorated with sea urchin-like gold nanoparticles as an efficient and stable SERS platform. 2021 , 590, 125-133	10
539	Charactering and optimizing cathode electrolytes interface for advanced rechargeable batteries: Promises and challenges. 2021 ,	1
538	In-situ surface-enhanced Raman scattering based on MTi nanoflowers: Monitoring and degradation of contaminants. 2021 , 412, 125209	12
537	Application and mechanisms of microalgae harvesting by magnetic nanoparticles (MNPs). 2021 , 265, 118519	8
536	In situ/operando vibrational spectroscopy for the investigation of advanced nanostructured electrocatalysts. 2021 , 436, 213824	10
535	Probing Interfacial Electronic Effects on Single-Molecule Adsorption Geometry and Electron Transport at Atomically Flat Surfaces. 2021 , 60, 15452-15458	11
534	SHINERS in cultural heritage: Can SHINERS spectra always be compared with normal Raman spectra? A study of alizarin and its adsorption in the silicon dioxide shell. 2021 , 52, 1406-1417	0
533	Nucleation and Growth-Controlled Facile Fabrication of Gold Nanoporous Structures for Highly Sensitive Surface-Enhanced Raman Spectroscopy Applications. 2021 , 11,	1
532	Combined Paper Centrifugal Chromatographic Separation and SERS Detection for Multicomponent Substances. 2021 , 93, 8693-8697	2
531	Reduced Self-Aggregation and Improved Stability of Silica-Coated FeO/Ag SERS-Active Nanotags Functionalized With 2-Mercaptoethanesulfonate. 2021 , 9, 697595	1
530	Probing Interfacial Electronic Effects on Single-Molecule Adsorption Geometry and Electron Transport at Atomically Flat Surfaces. 2021 , 133, 15580-15586	1

529	Recent Progress on Metal-Enhanced Photocatalysis: A Review on the Mechanism. 2021 , 2021, 9794329	42
528	Ag-coated 3D Cu(OH) ₂ nanowires on the woven copper mesh as a cost-effective surface-enhanced Raman scattering substrate. 2021 , 415, 127132	5
527	In Situ Spectroscopy for Mechanistic Studies in Semiconductor Photocatalysis. 2021 , 51-75	
526	Electrokinetic and in situ spectroscopic investigations of CO electrochemical reduction on copper. 2021 , 12, 3264	29
525	Development of RGO@MoS ₂ @Ag ternary nanocomposites with tunable geometry structure for recyclable SERS detection. 2021 , 339, 129856	17
524	Zero- and Two-Dimensional Metal Nanostructures: An Overview on Methods of Preparation, Characterization, Properties, and Applications. 2021 , 11,	1
523	Role of dispersion relation effect in topological surface-enhanced Raman scattering. 2021 , 2, 100488	3
522	Plasmonic metal-organic frameworks.	7
521	Numerical Investigation of Enhanced and Quenched Radiative Decay Rate for One and Multiple Emitters near a Nanoparticle Surface. 2021 , 125, 16211-16219	0
520	Pinhole-Free Shell-Isolated Nanoparticle Enhanced Raman Spectroscopy for Interference-Free Probing of Electrochemical Reactions. 2021 , 12, 7046-7052	2
519	Insights into Fano-type resonance fluorescence from quantum-dot-metal-nanoparticle molecules with a squeezed vacuum. 2021 , 104,	1
518	Recent developments on gold nanostructures for surface enhanced Raman spectroscopy: Particle shape, substrates and analytical applications. A review. 2021 , 1168, 338474	16
517	A Novel Approach To Investigate Linear And Nonlinear Electrical Conductivity Of ????.	0
516	Core-Shell Plasmonic Nanostructures on Au Films as SERS Substrates: Thickness of Film and Quality Factor of Nanoparticle Matter. 2021 , 125, 16024-16032	1
515	Flexible nanocellulose-based SERS substrates for fast analysis of hazardous materials by spiral scanning. 2021 , 414, 125160	15
514	Femtosecond laser micro-nano structured Ag SERS substrates with unique sensitivity, uniformity and stability for food safety evaluation. 2021 , 139, 106969	11
513	Operando Shell-Isolated Nanoparticle-Enhanced Raman Spectroscopy of the NO Reduction Reaction over Rhodium-Based Catalysts. 2021 , 22, 1595-1602	3
512	Surface-Enhanced Raman Spectroscopic Evidence of Key Intermediate Species and Role of NiFe Dual-Catalytic Center in Water Oxidation. 2021 , 60, 19774-19778	22

511	Size- and composition-controlled intermetallic nanocrystals via amalgamation seeded growth. 2021 , 7,	3
510	Manipulation of Ultrafast Nonlinear Optical Response Based on Surface Plasmon Resonance. 2021 , 9, 2100847	3
509	Strong coupling of a plasmonic nanoparticle to a semiconductor nanowire. 2021 , 10, 2875-2881	0
508	Light-Trapped Nanocavities for Ultraviolet Surface-Enhanced Raman Scattering. 2021 , 125, 17241-17247	1
507	Investigating the potential of ZTO as an efficient and cheap SERS substrate for the identification of bacteria. 2021 , 11, 075012	
506	Design and optimization of bowtie nanoantenna for electromagnetic field enhancement. 2021 , 136, 1	0
505	Surface-Enhanced Raman Spectroscopic Evidence of Key Intermediate Species and Role of NiFe Dual-Catalytic Center in Water Oxidation. 2021 , 133, 19927-19931	5
504	Thickness control of mesoporous silica coated on gold nanorod. 2021 , 23, 1	0
503	Lasing-enhanced surface plasmon resonance spectroscopy and sensing. 2021 , 9, 1699	2
502	Synergistic SERS Enhancement in GaN-Ag Hybrid System toward Label-Free and Multiplexed Detection of Antibiotics in Aqueous Solutions. 2021 , 8, e2100640	4
501	Methods in Raman spectroscopy for saliva studies  review. 1-57	9
500	Oxygen electrochemistry in Li-O2 batteries probed by in situ surface-enhanced Raman spectroscopy. 2021 , 1, 345-358	7
499	Quantitative Study of Residual Strain and Geometrically Necessary Dislocation Density Using HR-EBSD Method. 2021 , 61, 1281	0
498	Noble Metallic Pyramidal Substrate for Surface-Enhanced Raman Scattering Detection of Plasmid DNA Based on Template Stripping Method. 2021 , 12,	
497	Advances of surface-enhanced Raman and IR spectroscopies: from nano/microstructures to macro-optical design. 2021 , 10, 161	24
496	Molecular Dynamics Simulations of Thermally Induced Surface and Shape Evolution of Concave Au Nanocubes: Implications for Catalysis. 2021 , 4, 9527-9535	0
495	Raman Scattering Methods for Monitoring the Electric Properties of the Postannealed Bulk Heterojunction. 2021 , 4, 8360-8367	
494	One-pot synthesis of Au@mSiO2 yolk-shell nanoparticles with enhanced catalytic and surface-enhanced Raman scattering (SERS) properties. 2021 , 871, 159631	2

493	Development of Highly Sensitive Raman Spectroscopy for Subnano and Single-Atom Detection. 2021 , 26,	0
492	Environment and food safety: a novel integrative review. 2021 , 28, 54511-54530	3
491	Operando toolbox for heterogeneous interface in electrocatalysis. 2021 , 1, 509-522	2
490	Preparation of silver with an ultrathin molecular imprinted layer for detection of carbendazim by SERS. 2021 , 75, 6477	2
489	Accessing Plasmonic Hotspots Using Nanoparticle-on-Foil Constructs. 2021 , 8, 2811-2817	4
488	Kinetic photovoltage along semiconductor-water interfaces. 2021 , 12, 4998	2
487	Detection of Off-Resonance Single-Walled Carbon Nanotubes by Enormous Surface-Enhanced Raman Scattering. 2100559	0
486	Sustainable Surface-Enhanced Raman Substrate with Hexagonal Boron Nitride Dielectric Spacer for Preventing Electric Field Cancellation at Au-Au Nanogap. 2021 , 13, 42176-42182	2
485	Three-Dimensional Au/Ag Nanoparticle/Crossed Carbon Nanotube SERS Substrate for the Detection of Mixed Toxic Molecules. 2021 , 11,	1
484	Reducing Water Activity by Zeolite Molecular Sieve Membrane for Long-Life Rechargeable Zinc Battery. 2021 , 33, e2102415	37
483	Solar water sterilization enabled by photothermal nanomaterials. 2021 , 87, 106158	11
482	Electrochemical impedance spectroscopy and Raman spectroscopy studies on electrochemical interface between Au(111) electrode and ethaline deep eutectic solvent. 2021 , 390, 138859	7
481	EMoN Yolk Microspheres with Ultrathin Nanosheets for a Wide-Spectrum, Sensitive, and Durable Surface-Enhanced Raman Scattering Substrate. 2021 , 93, 12360-12366	1
480	A Comprehensive Review on Raman Spectroscopy Applications. 2021 , 9, 262	21
479	Novel Methods and Approaches for Safety Evaluation of Nanoparticle Formulations: A Focus Towards Models and Adverse Outcome Pathways. 2021 , 12, 612659	14
478	A Highly Sensitive SERS Platform Based on Small-Sized Ag/GQDs Nanozyme for Intracellular Analysis. 2021 , 430, 132687	7
477	Calcium Alginate Gel Beads Containing Gold Nanobipyramids for Surface-Enhanced Raman Scattering Detection in Aqueous Samples.	1
476	Engineering Efficient Self-Assembled Plasmonic Nanostructures by Configuring Metallic Nanoparticle's Morphology. 2021 , 22,	2

475	General Microwave Route to Single-Crystal Porous Transition Metal Nitrides for Highly Sensitive and Stable Raman Scattering Substrates. 2021 , 21, 7724-7731	2
474	Nitrogen-Doped Titanium Monoxide Flexible Membrane for a Low-Cost, Biocompatible, and Durable Raman Scattering Substrate. 2021 , 93, 12776-12785	0
473	Improving the SERS effect of van der Waals material by intercalation strategy. 2021 , 559, 149834	2
472	Surface lattice engineering for fine-tuned spatial configuration of nanocrystals. 2021 , 12, 5661	4
471	Application of nanomaterials decorated with cyclodextrins as sensing elements for environment analysis. 2021 , 28, 59499-59518	1
470	Fe ₃ O ₄ -protected gold nanoparticles: New plasmonic-magnetic nanomaterial for Raman analysis of surfaces. 2021 , 562, 150220	6
469	Plasmonic paper substrates for point-of-need applications: Recent developments and fabrication methods. 2021 , 345, 130401	7
468	SMUTHI: A python package for the simulation of light scattering by multiple particles near or between planar interfaces. 2021 , 273, 107846	8
467	One-pot green synthesis of Ag@AgCl nanoparticles with excellent photocatalytic performance. 2021 , 9, 277-284	9
466	Ultrasensitive surface-enhanced Raman spectroscopy detection of gaseous sulfur-mustard simulant based on thin oxide-coated gold nanocone arrays. 2021 , 420, 126668	2
465	Enhance Raman scattering for probe methylene blue molecules adsorbed on ZnO microstructures due to charge transfer processes. 2021 , 120, 111460	4
464	Emerging core-shell nanostructures for surface-enhanced Raman scattering (SERS) detection of pesticide residues. 2021 , 424, 130323	13
463	Effective fabrication of porous Au-Ag alloy nanorods for in situ Raman monitoring catalytic oxidation and reduction reactions. 2021 , 91, 262-269	2
462	Stable SERS substrate based on highly reflective metal liquid-like films wrapped hydrogels for direct determination of small molecules in a high protein matrix. 2021 , 234, 122678	5
461	Shell-thickness control of hollow SiO ₂ nanoparticles through post-treatment using sol-gel technique toward efficient water confinement. 2021 , 629, 127501	0
460	Insertable and reusable SERS sensors for rapid on-site quality control of fish and meat products. 2021 , 426, 130733	5
459	Nanocomposite of Au and black phosphorus quantum dots as versatile probes for amphibious SERS spectroscopy, 3D photoacoustic imaging and cancer therapy. 2021 , 8, 100073	8
458	On-demand nanoparticle-on-mirror (NPoM) structure for cost-effective surface-enhanced Raman scattering substrates. 2021 , 263, 120193	0

- 457 Photo-reduced WO₃/PAN nanofiber membranes with deposited Ag nanoparticles as efficient SERS substrates. **2021**, 568, 150936 1
- 456 Full life cycle characterization strategies for spatiotemporal evolution of heterogeneous catalysts. **2021**, 42, 2141-2148 0
- 455 An efficient double template strategy to construct large-area and highly ordered silver "urchin-like" arrays for sensitive SERS analysis. **2021**, 570, 151069 4
- 454 Facet dependent catalytic activity of Pd nanocrystals for the remedy of organic Pollutant: A mechanistic study. **2021**, 570, 150775 1
- 453 Nanoplasmonic materials for surface-enhanced Raman scattering. **2022**, 33-79 1
- 452 Experimental aspects of surface-enhanced Raman scattering for biological applications. **2022**, 81-124
- 451 Principles of surface-enhanced Raman spectroscopy. **2022**, 1-32 0
- 450 Plasmonic Fano-type nanocavity for double resonance enhanced SERS and optical sensing. **2022**, 502, 127441 3
- 449 A facile microwave-assisted synthesis of Ag@SiO₂ nanoparticles for Raman spectroscopy. **2021**, 45, 10952-10958
- 448 A highly-efficient, stable, and flexible Kapton tape-based SERS chip. **2021**, 5, 6471-6475 2
- 447 Manipulating atomic defects in plasmonic vanadium dioxide for superior solar and thermal management. **2021**, 8, 1700-1710 4
- 446 Understanding electrochemical interfaces using in situ core-shell nanoparticle-enhanced Raman spectroscopy. **2021**, 18, 295-342
- 445 Recent progress in mycotoxins detection based on surface-enhanced Raman spectroscopy. **2021**, 20, 1887-1909 17
- 444 Surface-enhanced Raman spectroscopy for bioanalysis and diagnosis. **2021**, 13, 11593-11634 20
- 443 More Symmetrical "Hot Spots" Ensure Stronger Plasmon-Enhanced Fluorescence: From Au Nanorods to Nanostars. **2021**, 93, 2480-2489 14
- 442 Application of Nanomaterials to Separation of Glycosylated Proteins. **2021**, 179-296
- 441 Aortic aneurysm evaluation by scanning acoustic microscopy and Raman spectroscopy. **2021**, 13, 4683-4690 1
- 440 Peak-fitting assisted SERS strategy for accurate discrimination of carboxylic acid enantiomers. **2021**, 57, 11064-11067 2

439	Ag Nanoparticle-Decorated Mesoporous Silica as a Dual-Mode Raman Sensing Platform for Detection of Volatile Organic Compounds. 2021 , 4, 1019-1028	3
438	Probing electrosynthetic reactions with furfural on copper surfaces. 2021 , 57, 5127-5130	3
437	Zinc oxide nanostructures as effective pesticide controllers: Sensing and degradation of pesticides. 2021 , 181-201	
436	Pharmaceuticals and personal care products: occurrence, detection, risk, and removal technologies in aquatic environment. 2021 , 265-284	0
435	Recent progress of surface-enhanced Raman spectroscopy for subcellular compartment analysis. 2021 , 11, 4872-4893	11
434	Nanospheres from coordination polymers of Ag ⁺ with a highly hydrophilic thiol ligand formed in situ from dynamic covalent binding and a hydrophobic thiol.	0
433	Quantitative Detection of Pesticides Based on SERS and Gold Colloid. 2016 , 587-596	1
432	Quantitative Analysis of Disease Biomarkers Using Surface-Enhanced Raman Scattering Spectroscopy. 2014 , 401-417	1
431	Plasmonic Gas and Chemical Sensing. 2015 , 239-272	2
430	SERS Biosensing and Bioimaging: Design and Applications in Cancer Diagnostics. 2017 , 345-364	1
429	Reactivity and Catalysis by Nanoalloys. 2020 , 267-345	1
428	Laser fabrication of periodic arrays of microsquares on silicon for SERS application. 2018 , 427, 133-140	11
427	Modification of surfaces of silver nanoparticles for controlled deposition of silicon, manganese, and titanium dioxides. 2018 , 427, 334-339	10
426	In situ electrochemical surface-enhanced Raman spectroscopy study of CO electrooxidation on PtFe nanocatalysts. 2017 , 81, 38-42	18
425	Graphene-covered FePc as a model of the encapsulated type of catalyst for the oxygen reduction reaction. 2020 , 112, 106670	5
424	AFM tip-based mechanical nanomachining of 3D micro and nano-structures via the control of the scratching trajectory. 2017 , 248, 236-248	16
423	Plasmonic nanocavities fabricated by directed self-assembly lithography and nanotransfer printing and used as surface-enhanced Raman scattering substrates. 2020 , 227, 111309	1
422	Excellent Trace Detection of Proteins on TiO ₂ Nanotube Substrates through Novel Topography Optimization. 2020 , 124, 27790-27800	3

421	Quasi-Analytical Approach for Modeling of Surface-Enhanced Raman Scattering. 2015 , 119, 28992-28998	10
420	Insight of the Influence of Magnetic-Field Direction on Magneto-Plasmonic Interfaces for Tuning Photocatalytical Performance of Semiconductors. 2020 , 11, 9931-9937	7
419	Plasmon-Enhanced Fluorescence of Phosphors Using Shell-Isolated Nanoparticles for Display Technologies. 2020 , 3, 5846-5854	4
418	Substrate influence on the polarization dependence of SERS in crossed metal nanowires. 2017 , 5, 7028-7034	10
417	Spectroelectrochemistry, the future of visualizing electrode processes by hyphenating electrochemistry with spectroscopic techniques. 2020 , 145, 2482-2509	30
416	In situ optical spectroscopy characterization for optimal design of lithium-sulfur batteries. 2019 , 48, 5432-5453	3
415	Plasmon-enhanced nonlinear nanofocusing of gold nanoprisms driven via an ultrafast azimuthal vector beam. 2020 , 12, 7045-7050	4
414	Roadmap for single-molecule surface-enhanced Raman spectroscopy. 2020 , 2, 1	35
413	Instrumentation in Raman spectroscopy. 83-172	14
412	Surface-enhanced Raman scattering (SERS) spectroscopy: a versatile spectroscopic and analytical technique used in nanoscience and nanotechnology. 2013 , 1, 111-124	7
411	Facile synthesis of metal-phenolic-coated gold nanocuboids for surface-enhanced Raman scattering. 2020 , 59, 6124-6130	1
410	Active Surface Plasmon Sensor. 2014 ,	1
409	Near-field nanoprobe using Si tip-Au nanoparticle photoinduced force microscopy with 120:1 signal-to-noise ratio, sub-6-nm resolution. 2018 , 26, 26365-26376	23
408	Label-free rapid identification of tumor cells and blood cells with silver film SERS substrate. 2018 , 26, 33044-33056	10
407	Comparative analysis on Raman enhancement properties of waveguide coupled SERS probe. 2019 , 27, 35555-35564	1
406	Simultaneously performing optical and electrical responses from a plasmonic sensor based on gold/silicon Schottky junction. 2019 , 27, 38382-38390	11
405	Programmable field localization and enhancement effects on a non-structured planar surface with a permittivity gradient. 2020 , 28, 1051-1060	2
404	Twin-ZnSe nanowires as surface enhanced Raman scattering substrate with significant enhancement factor upon defect. 2020 , 28, 18843-18858	7

403	Compact conical beam shaper and freeform segmented reflector for SERS analysis. 2020 , 28, 16163-16174	2
402	Theoretical analysis of optically selective imaging in photoinduced force microscopy. 2020 , 28, 34787-34803	8
401	AgNPs decorated volcano-like Ag arrays for ultra-sensitive Raman detection. 2020 , 10, 3393	4
400	Thin silica shell coated Ag assembled nanostructures for expanding generality of SERS analytes. 2017 , 12, e0178651	13
399	Graphene and Graphene Oxide Applications for SERS Sensing and Imaging. 2019 , 26, 6878-6895	17
398	Optical nanoantennas. 2013 , 183, 561-589	17
397	Applications of Analytical Instruments in Biotechnology: A Comparative Review. 2013 , 4, 1-7	1
396	Controlled Clustering of Gold Nanoparticles using Solid-support for Surface-enhanced Raman Spectroscopic Probes. 2014 , 35, 941-944	1
395	Fabrication of Large-area 3-D Ordered Silver-coated Colloidal Crystals and Macroporous Silver Films Using Polystyrene Templates. 2013 , 5, 182	1
394	Interfacial water and catalysis. 2019 , 68, 016803	1
393	Surface-enhanced Raman scattering of subwavelength metallic structures. 2019 , 68, 147401	2
392	Research progress of coupling theory of metal surface plasmon. 2019 , 68, 247301	6
391	A Colloidal Route to Detection of Organic Molecules Based on Surface-Enhanced Raman Spectroscopy Using Nanostructured Substrate Derived from Aerosols. 2011 , 50, 06GG10	3
390	Linear chains of Ag nanoparticles embedded in dielectric films for SERS applications in analytical chemistry.	1
389	Rapid field trace detection of pesticide residue in food based on surface-enhanced Raman spectroscopy. 2021 , 188, 370	5
388	Enhanced Surface-Enhanced Raman Scattering Activity of MoS ₂ /Ag-Reduced Graphene Oxide: Structure-Mediated Excitonic Transition. 2021 , 125, 23259-23266	1
387	Recent advancements and future submissions of silica core-shell nanoparticles. 2021 , 609, 121173	8
386	Controllable synthesis of the homogeneous 3D Ag nanoflowers on FTO substrate for ultra-sensitive SERS detection. 2021 , 139165	1

- 385 Heterostructures Built through Site-Selective Deposition on Anisotropic Plasmonic Metal Nanocrystals and Their Applications. 2100101 5
- 384 Highly Sensitive and Stable Copper-Based SERS Chips Prepared by a Chemical Reduction Method. **2021**, 11, 4
- 383 Plasmonic core-shell nanostructures enhanced spectroscopies. 0
- 382 Plasmonic Properties of Al₂O₃ Nanoshell with a Metallic Core. **2021**, 13, 3
- 381 Hollow Multi-Shelled V₂O₅ Microstructures Integrating Multiple Synergistic Resonances for Enhanced Semiconductor SERS. 2101866 3
- 380 Kinetic Study on the Adsorption of 2,3,5,6-Tetrafluoro-7,7,8,8-tetracyanoquinodimethane on Ag Nanoparticles in Chloroform: Implications for the Charge Transfer Complex of Ag@TCNQ. 0
- 379 Label-free identification of lung cancer cells from blood cells based on surface-enhanced Raman scattering and support vector machine. **2021**, 248, 168157 0
- 378 Analytical chemistry: Smart dust. **2010**, 0
- 377 Optics: Smart dust. **2010**, 2, 91-91 0
- 376 Molecular alignment of nano-thin film using Raman spectroscopy. **2011**, 60, 098109 0
- 375 Plasmon-Assisted Spectroscopy and Photochemistry at Well-Defined Metal-molecular Interfaces. **2011**, 5, A0040 0
- 374 Broad-bandwidth and ultrafast electromagnetic response of coupled bimetal nanoantennas in few-cycle laser applications. **2012**, 61, 014207 0
- 373 Immunoassays and Imaging Based on Surface-Enhanced Raman Spectroscopy. **2012**, 261-289 0
- 372 Properties of DNA-Capped Nanoparticles. **2014**, 1227-1262 0
- 371 4.?????????????????????????????????????. **2015**, 83, 112-115 0
- 370 Chemical Analysis of Buried Interface Using SERS Sensors. **2016**, 37, 435-440 0
- 369 Chapter 5 Plasmonic Enhancement. **2016**, 225-286 0
- 368 Terahertz surface polaritons. **2017**, 66, 148705 0

- 367 Chapter 1. Raman Spectroscopic Sensing in Food Safety and Quality Analysis. **2017**, 1-16 1
- 366 Superhydrophobic SERS Substrates based on Plasmonic Hierarchical Micro-nanostructures. **2018**, 1-10 0
- 365 Gap-Mode Raman Spectroscopy. **2018**, 205-209
- 364 Plasmonics Yields Surprisingly Efficient Electron Transport Via Assembly of Shell-Insulated Au Nanoparticles. 1
- 363 Quantifying the concentration of glucose, urea, and lactic acid in mixture by confocal Raman microscopy. **2018**, 1-10 0
- 362 Advances in dynamically tunable plasmonic materials and devices. **2019**, 68, 147303 0
- 361 Surface plasmon resonance hot spots and near-field enhanced spectroscopy at interfaces. **2019**, 68, 147801 1
- 360 Surface plasmon mediated chemical reaction. **2019**, 68, 147102 1
- 359 Molecular Level Understanding of Reaction Mechanisms in the Electrodeposition and Electroless Deposition by Theoretical Analyses. **2019**, 70, 82-87 1
- 358 A Review of SERS for Biomaterials Analysis Using Metal Nanoparticles. **2019**, 22, 281-300
- 357 Nanostructures for enhancing the SERS signal of a graphene monolayer in water and visible light absorption in a graphene monolayer. **2019**, 1-10 0
- 356 The application of Ag⁺ detection based on porous silicon SERS substrates. **2019**, 1-10 0
- 355 Raman Spectroscopic Characterizations of Self-Catalyzed InP/InAs/InP One-Dimensional Nanostructures on InP(111)B Substrate using a Simple Substrate-Tilting Method. **2019**, 14, 355 1
- 354 Surface-Enhanced Raman Scattering Substrates: Fabrication, Properties, and Applications. **2020**, 83-118 1
- 353 Electrochemical Behavior of Single Crystal Electrodes on Model Processes. **2020**, 1117-1158
- 352 Preparation of 3D ZnTiO₃/Ag NPs composite as the photocatalytic SERS-active substrate with well reusability. **2020**, 59, 5589 0
- 351 Analytical techniques for electrochemical deposition processes using theoretical and spectroscopic approaches. **2020**, 88, 151-161
- 350 Surface enhanced Raman scattering on ion-beam-deposited TiN_x/Si substrates. **2020**, 472, 24-31 3

- 349 Strong histamine torsion Raman spectrum enables direct, rapid, and ultrasensitive detection of allergic diseases. **2021**, 24, 103384 1
- 348 Three-dimensional surface-enhanced Raman scattering substrates constructed by integrating template-assisted electrodeposition and post-growth of silver nanoparticles. **2021**, 608, 2111-2119 5
- 347 Plasmonic band structures and its applications. **2020**, 69, 157301 2
- 346 Plasmon-Boosted Cu-Doped TiO Oxygen Vacancy-Rich Luminol Electrochemiluminescence for Highly Sensitive Detection of Alkaline Phosphatase. **2021**, 93, 15183-15191 3
- 345 Metal-organic framework engineered corn-like SERS active Ag@Carbon with controllable spacing distance for tracking trace amount of organic compounds. **2021**, 424, 127686 3
- 344 Self-generating nanogaps for highly effective surface-enhanced Raman spectroscopy. 1 0
- 343 Surface Hydride Formation on Cu(111) and Its Decomposition to Form H in Acid Electrolytes. **2021**, 12, 10936-10941 1
- 342 Ultra-Fine Control of Silica Shell Thickness on Silver Nanoparticle-Assembled Structures. **2021**, 22, 0
- 341 Surface-enhanced Raman scattering with gold-coated silicon nanopillars arrays: The influence of size and spatial order. **2021**, 120582
- 340 Electrochemical and Plasmonic Photochemical Oxidation Processes of para-Aminothiophenol on a Nanostructured Gold Electrode. 1
- 339 Construction of Optimal SERS Hotspots Based on Capturing the Spike Receptor-Binding Domain (RBD) of SARS-CoV-2 for Highly Sensitive and Specific Detection by a Fish Model. **2021**, 93, 16086-16095 6
- 338 Electrochemical Reactions on Single Crystal Electrodes of Noble Metals. **2020**, 59, 379-386
- 337 Plasmonic Smart Nanosensors for the Determination of Environmental Pollutants. **2020**, 237-279 1
- 336 Food safety and security: what were favourite topics for research in the last decade?. **2011**, 1, 72-8 12
- 335 Improving the stability of plasmonic magnesium nanoparticles in aqueous media. **2021**, 1
- 334 Fabrication of sea urchin-like Au@SiO₂ nanoparticles SERS substrate for the determination of malachite green in tilapia. **2022**, 118, 103319 1
- 333 In situ studies of energy-related electrochemical reactions using Raman and X-ray absorption spectroscopy. **2022**, 43, 33-46 2
- 332 Boron nitride nanosheets for surface-enhanced Raman spectroscopy. **2022**, 22, 100575 0

- 331 The Inadvertent Activation of Silicate Minerals Flotation and Their Depression in Molybdenite Beneficiation. **2021**, 11, 1296
- 330 Highly ordered arrays of hat-shaped hierarchical nanostructures with different curvatures for sensitive SERS and plasmon-driven catalysis. **2021**, 15
- 329 Watching Reactions at Solid-Liquid Interfaces with in Situ Raman Spectroscopy. 1
- 328 Raman Scattering Enhancement Based on High-Pressure High-Temperature Diamonds **2021**, 42, 671
- 327 Single-Atom Engineering to Ignite 2D Transition Metal Dichalcogenide Based Catalysis: Fundamentals, Progress, and Beyond. **2021**, 20
- 326 Raman Fiber Photometry for Understanding Mitochondrial Superoxide Burst and Extracellular Calcium Ion Influx upon Acute Hypoxia in the Brain of Freely Moving Animals.. **2022**, 61, e202111630 3
- 325 Smartphone-Based Colorimetric Detection of Chromium (VI) by Maleic Acid-Functionalized Gold Nanoparticles. **2021**, 11, 10894 1
- 324 Real-Time Monitoring of Surface Effects on the Oxygen Reduction Reaction Mechanism for Aprotic Na-O Batteries. **2021**, 143, 20049-20054 2
- 323 Structural engineering of transition-metal nitrides for surface-enhanced Raman scattering chips. 1 1
- 322 Review on combining surface-enhanced Raman spectroscopy and electrochemistry for analytical applications.. **2022**, 1209, 339250 4
- 321 Flexible Plasmonic Biosensors for Healthcare Monitoring: Progress and Prospects. **2021**, 13
- 320 Multifunctional Ag-coated CuO microbowl arrays for highly efficient, ultrasensitive, and recyclable surface-enhanced Raman scattering. **2021**, 354, 131097 1
- 319 Spontaneous emission mediated by graphene/hexagonal boron nitride/graphene sandwich structure. 0
- 318 Raman Fiber Photometry for Understanding Mitochondrial Superoxide Burst and Extracellular Calcium Ion Influx upon Acute Hypoxia in the Brain of Freely Moving Animals. 0
- 317 Ultra-rapid and highly efficient enrichment of organic pollutants via magnetic mesoporous nanosponge for ultrasensitive nanosensors. **2021**, 12, 6849 5
- 316 Raman Imaging and Fluorescence Lifetime Imaging Microscopy for Diagnosis of Cancer State and Metabolic Monitoring. **2021**, 13, 1
- 315 Two-dimensional materials for electrochemical CO reduction: materials, / characterizations, and perspective. **2021**, 2
- 314 Ultrasensitive detection of vitamin E by signal conversion combined with core-satellite structure-based plasmon coupling effect.. **2022**, 0

313	Optical Spectroscopy of Surfaces, Interfaces, and Thin Films.. 2022 ,	1
312	Dynamic Evolution of Active Sites in Electrocatalytic CO ₂ Reduction Reaction: Fundamental Understanding and Recent Progress. 2111193	6
311	Featuring few essential Raman spectroscopic signatures between heterogeneous cells.. 2022 , e202100338	
310	Exploration of Metal-Molecule interaction of subnanometric heterogeneous catalysts via simulated Raman spectrum. 2022 , 579, 152194	0
309	Highly sensitive and recyclable surface-enhanced Raman scattering (SERS) substrates based on photocatalytic activity of ZnSe nanowires. 2022 , 356, 131360	3
308	Synergistic Contribution for Enhanced Charge Transfer of Ag/4-MBA/PAN System: Thickness-Dependent of PAN.	
307	Unmasking the Critical Role of the Ordering Degree of Bimetallic Nanocatalysts on Oxygen Reduction Reaction by In-situ Raman Spectroscopy.	
306	Sensitive and Homogeneous Surface-Enhanced Raman Scattering Detection Using Heterometallic Interfaces on Metal-Organic Framework-Derived Structure. 2102122	1
305	In situ Raman, FTIR, and XRD spectroscopic studies in fuel cells and rechargeable batteries. 1	3
304	Simulation of Surface Enhanced Raman Scattering from Nanoparticles with Wideband Nested Equivalence Source Approximation. 2022 , 1-1	2
303	Plasmonic Rare-Earth Nanosheets as Surface Enhanced Raman Scattering Substrates with High Sensitivity and Stability for Multicomponent Analysis.. 2022 ,	2
302	The concept of active site in heterogeneous catalysis. 2022 , 6, 89-111	17
301	Plasmonic Core-Shell Materials: Synthesis, Spectroscopic Characterization, and Photocatalytic Applications.	1
300	Plasmonic locator with sub-diffraction-limited resolution for continuously accurate positioning.	1
299	Amorphous Co(OH) ₂ nanocages achieving efficient photo-induced charge transfer for significant SERS activity. 2022 , 10, 1632-1637	1
298	Metal-Organic Frameworks-Based Sensors for Food Safety.. 2022 , 11,	2
297	Microfluidics and surface-enhanced Raman spectroscopy, a win-win combination?. 2022 ,	5
296	Research progress of SERS on uranyl ions and uranyl compounds: a review.	1

295	Visualizing an Electrochemically Induced Radical Cation of Bipyridine at Au(111)/Ionic Liquid Interfaces toward a Single-Molecule Switch.. 2022,	3
294	Nanomaterials of metal and metal oxides for optical biosensing application. 2022, 321-352	
293	Serum Raman spectroscopy combined with Gaussian convolutional neural network models to quickly detect liver cancer patients. 1-12	1
292	Verification and Analysis of Single-Molecule SERS Events via Polarization-Selective Raman Measurement.. 2022,	2
291	Surface-Enhanced Electronic Raman Scattering at Various Metal Surfaces. 2100589	2
290	Unmasking the Critical Role of the Ordering Degree of Bimetallic Nanocatalysts on Oxygen Reduction Reaction by In-situ Raman Spectroscopy.. 2022,	2
289	Structural characterization and plasmonic properties of manganese oxide-coated gold nanorods.. 2022, 272, 120988	1
288	Spectroscopy shines light on an electrode/water interface. 2022, 75, 18-19	
287	Microporous-Ceria-Wrapped Gold Nanoparticles for Conductometric and SERS Dual Monitoring of Hazardous Gases at Room Temperature. 2102107	2
286	Identifying infectiousness of SARS-CoV-2 by ultra-sensitive SnS SERS biosensors with capillary effect.. 2021,	15
285	Fabrication of stable substoichiometric W ₂ O ₃ films with high SERS sensitivity by thermal treatment. 2022, 198, 110884	0
284	A dual-mode strategy combining SERS with MALDI FTICR MS based on core-shell silver nanoparticles for dye identification and semi-quantification in unearthed silks from Tang Dynasty.. 2022, 241, 123277	2
283	UV excited enhanced Raman scattering on carbon-doped SnS ₂ nanoflowers. 2022, 150, 111757	0
282	Localized Plasmonic Sensor for the Direct Identifying Lung and Colon Cancer from the Blood.	
281	Monitoring the rapid nanocrystal transformation via trapped intermediates of silica encapsulation. 1	
280	Unraveling molecular structures and ion effects of electric double layers at metal water interfaces. 2022, 100759	2
279	Pushing the limit of 3d transition metal-based layered oxides that use both cation and anion redox for energy storage.	10
278	Surface enhanced Raman spectroscopy for tumor nucleic acid: Towards cancer diagnosis and precision medicine.. 2022, 204, 114075	3

277	In situ Raman spectroscopy reveals the structure and dissociation of interfacial water. <i>Nature</i> , 2021 , 600, 81-85	50.4	57
276	Tuning the binding configurations of single-molecule junctions by molecular co-assembly.. 2022 ,		1
275	Determination of lentiviral titer by surface enhanced Raman scattering.. 2022 ,		0
274	fluorescence yield soft X-ray absorption spectroscopy of electrochemical nickel deposition processes with and without ethylene glycol.. 2022 , 12, 10425-10430		0
273	Electrochemically activated carbon-halogen bond cleavage and C-C coupling monitored by shell-isolated nanoparticle-enhanced Raman spectroscopy.. 2022 ,		2
272	Shell isolated nanoparticle enhanced Raman spectroscopy for mechanistic investigation of electrochemical reactions.. 2022 , 9, 9		3
271	Periodic Arrays of 3D AuNP-Capped VO ₂ Shells and Their Temperature-Tunable SERS Performance. 2102615		1
270	Shell-Isolated Nanoparticle-Enhanced Raman Spectroscopy for Probing Riboflavin on Graphene.. 2022 , 15,		0
269	Visualized SERS Imaging of Single Molecule by Ag/Black Phosphorus Nanosheets.. 2022 , 14, 75		6
268	Interface Behavior of Electrolyte/Quinone Organic Active Material in Battery Operation by Surface-Enhanced Raman Spectroscopy.. 2022 , 38, 3951-3958		1
267	(Bio)Analytical Nanoscience & Nanotechnology. 1-31		
266	PLGA-Gold Nanocomposite: Preparation and Biomedical Applications.. 2022 , 14,		0
265	Experimental characterization techniques for plasmon-assisted chemistry.		8
264	Spectroscopic investigation of the structure of a pyrrolidinium-based ionic liquid at electrified interfaces.. 2022 , 156, 114701		0
263	Superhydrophobic Ag-Decorated CuO Nanowire Arrays with Analyte-Concentrating and Self-Cleaning Binary Functions for Ultrasensitive and Recyclable Surface-Enhanced Raman Scattering. 2200047		1
262	In Situ Monitoring of Palladium-Catalyzed Chemical Reactions by Nanogap-Enhanced Raman Scattering using Single Pd Cube Dimers.. 2022 ,		5
261	Simultaneous Raman and reflection UV/Vis absorption spectroelectrochemistry. 1		0
260	A stable quasi-solid electrolyte improves the safe operation of highly efficient lithium-metal pouch cells in harsh environments.. 2022 , 13, 1510		7

259	Ultrasensitive and ultrafast nonlinear optical characterization of surface plasmons. 2022 , 10, 030701	1
258	Precise real-time quantification for photocatalytic reaction: integration of the sensitive in-situ SERS sensor and high-efficiency photocatalyst.. 2022 ,	
257	Abnormally Weak Surface-Enhanced Raman Scattering Activity of Tip-Rich Au Nanostars: The Role of Interfacial Defects.. 2022 , 2428-2433	0
256	Single-particle Raman spectroscopy for studying physical and chemical processes of atmospheric particles. 2022 , 22, 3017-3044	1
255	Elucidating the Correlation between ORR Polarization Curves and Kinetics at Metal-Electrolyte Interfaces.. 2022 ,	3
254	High-Throughput Fabrication of Triangular Nanogap Arrays for Surface-Enhanced Raman Spectroscopy.. 2022 ,	1
253	Strong Out-of-Plane Vibrations and Ultrasensitive Detection of Dopamine-like Neurotransmitters.. 2022 , 3325-3331	0
252	Monitoring electrode/electrolyte interfaces of Li-ion batteries under working conditions: A surface-enhanced Raman spectroscopic study on LiCoO ₂ composite cathodes.	
251	Deep Learning-Based Spectral Extraction for Improving the Performance of Surface-Enhanced Raman Spectroscopy Analysis on Multiplexed Identification and Quantitation.. 2022 ,	0
250	Flexible microsphere-coupled surface-enhanced Raman spectroscopy (McSERS) by dielectric microsphere cavity array with random plasmonic nanoparticles.	0
249	An efficient nickel hydrogen oxidation catalyst for hydroxide exchange membrane fuel cells.. 2022 ,	8
248	Synergistic contribution to the enhanced charge transfer of the silver/4-mercaptobenzoic acid/polyaniline (Ag/MBA/PAN) system: thickness-dependent of PAN. 2022 , 586, 152863	
247	Biosensors for detection of organophosphate pesticides: Current technologies and future directives. 2022 , 178, 107420	2
246	Rapid and Simple Analysis of the Human Pepsin Secondary Structure Using a Portable Raman Spectrometer.. 2021 ,	0
245	Surface Enhanced Raman Spectroscopy: Applications in Agriculture and Food Safety. 2021 , 8, 568	3
244	Direct Spectroscopic Evidence for Solution-Mediated Oxygen Reduction Reaction Intermediates in Aprotic Lithium-Oxygen Batteries.. 2021 ,	2
243	Enhanced photoluminescence and shortened lifetime of DCJTB by photoinduced metal deposition on a ferroelectric lithography substrate.. 2022 , 12, 6173	0
242	Tailoring the solvation sheath of cations by constructing electrode front-faces for rechargeable batteries.. 2022 , e2201339	9

- 241 Nonlinear Electrochemical Analysis: Worth the Effort to Reveal New Insights into Energy Materials. 2200708 1
- 240 Surface-enhanced Raman scattering biosensor-based sandwich-type for facile and sensitive detection of *Staphylococcus aureus*. **2022**, 131929 0
- 239 Hyperbranched phthalocyanine enabling black-phase formamidinium perovskite solar cells processing and operating in humidity open air. **2022**, 0
- 238 Formic acid electro-oxidation: Mechanism and electrocatalysts design. 1
- 237 Probing the role of surface speciation of tin oxide and tin catalysts on CO₂ electroreduction combining in situ Raman spectroscopy and reactivity investigations. **2022**, 43, 1473-1477 0
- 236 Label-free SERS strategy for rapid detection of capsaicin for identification of waste oils.. **2022**, 245, 123488 0
- 235 Magnetic iron oxide cores with attached gold nanostructures coated with a layer of silica: An easily, homogeneously deposited new nanomaterial for surface-enhanced Raman scattering measurements.. **2022**, 277, 121266 3
- 234 Facile synthesis of Au@palladium oxide nano-sunflowers for ultrasensitive surface-enhanced Raman scattering analysis.
- 233 Single-atom vanadium-doped 2D semiconductor platform for attomolar-level molecular sensing. 2
- 232 Bioinspired hollow g-C₃N₄-CuPc heterostructure with remarkable SERS enhancement and photosynthesis-mimicking property for theranostic applications. 0
- 231 Enhanced electroreduction of CO₂ to C₂⁺ products on heterostructured Cu/oxide electrodes. **2022**, 2
- 230 PDMS based SERS substrate of high sensitivity and uniformity and its application in in-situ detection of tricyclazole.
- 229 Statistical Strategy for Quantitative Evaluation of Plasmon-Enhanced Spectroscopy.
- 228 Microspheres on a Silver Film over Nanoparticle Arrays as Optoplasmonic Hybrid Materials for Surface-Enhanced Raman Spectroscopy. **2022**, 126, 7542-7547 1
- 227 Highly Stable, Graphene-Wrapped, Petal-like, Gap-Enhanced Raman Tags. **2022**, 12, 1626
- 226 A review of applications of surface-enhanced raman spectroscopy laser for detection of biomaterials and a quick glance into its advances for COVID-19 investigations.. **2022**, 1-20 1
- 225 Dimensional Design for Surface-Enhanced Raman Spectroscopy. 1
- 224 Fabrication of magnetic Au/Fe₃O₄/MIL-101(Cr) (AF-MIL) as sensitive surface-enhanced Raman spectroscopy (SERS) platform for trace detection of antibiotics residue. **2022**, 153550 2

223	In Situ Raman Monitoring of Potential-Dependent Adlayer Structures on the Au(111)/Ionic Liquid Interface.. 2022 ,	1
222	The First Silver-Based Plasmonic Nanomaterial for Shell-Isolated Nanoparticle-Enhanced Raman Spectroscopy with Magnetic Properties. 2022 , 27, 3081	2
221	Real-Time Plasmonic Imaging of the Compositional Evolution of Single Nanoparticles in Electrochemical Reactions.. 2022 ,	1
220	Au@ZrO ₂ Core-Shell Nanoparticles as a SERS Substrate for OPs Compounds Detection.	0
219	Selective Enhancement of Methane Formation in Electrochemical CO ₂ Reduction Enabled by a Raman-Inactive Oxygen-Containing Species on Cu. 6036-6046	2
218	Graphene-Covered Silver Nanoisland Array Coupling with Hyperbolic Metamaterials for SERS Sensing.	1
217	Multiple Valence States of Fe Boosting SERS Activity of Fe ₃ O ₄ Nanoparticles and Enabling Effective SERS-MRI Bimodal Cancer Imaging. 2022 ,	
216	Understanding the complementarities of surface-enhanced infrared and Raman spectroscopies in CO adsorption and electrochemical reduction.. 2022 , 13, 2656	5
215	Investigating the presence of adsorbed species on Pt steps at low potentials.. 2022 , 13, 2550	2
214	Localized plasmonic sensor for direct identifying lung and colon cancer from the blood. 2022 , 114372	2
213	Metal Graphitic Nanocapsules for Theranostics in Harsh Conditions. 2022 , 10,	
212	Ultrafast Detection of SARS-CoV-2 Spike Protein (S) and Receptor-Binding Domain (RBD) in Saliva Using Surface-Enhanced Raman Spectroscopy. 2022 , 12, 5039	0
211	Highly Sensitive and Reproducible SERS Substrates with Binary Colloidal Crystals (bCCs) based on MIM Structures. 2022 , 153654	0
210	Selected applications of operando Raman spectroscopy in electrocatalysis research. 2022 , 101042	1
209	Moving MoO ₃ /C Nanospheres with the Functions of Enrichment and Sensing for Online-High-Throughput SERS Detection.. 2022 ,	0
208	Colloidal Multiscale Assembly via Photothermally Driven Convective Flow for Sensitive In-Solution Plasmonic Detections.. 2022 , e2201075	1
207	Surface-Enhanced Luminescence of Cr ³⁺ -doped ZnAl ₂ O ₄ and MgAl ₂ O ₄ using Ag@SiO ₂ and Au@SiO ₂ core-shell nanoparticles.	
206	High Performance Carbon Dioxide Electroreduction in Ionic Liquids with in Situ Shell-Isolated Nanoparticle-Enhanced Raman Spectroscopy.	

205 Semiconductor catalysts based on surface-modified nanomaterials (SMNs) for sensors. **2022**, 197-222

204 MnO₂ coated Au nanoparticles advance SERS detection of cellular glutathione. **2022**, 114388 1

203 Broadband Nanoscale Surface-Enhanced Raman Spectroscopy by Multiresonant Nanolaminate Plasmonic Nanocavities on Vertical Nanopillars. 2202231 0

202 Plasmonic rhenium trioxide self-assembled microtubes for highly sensitive, stable and reproducible surface-enhanced raman spectroscopy detection. **2022**, 1

201 A biochip based on shell-isolated Au@MnO₂ nanoparticle array-enhanced fluorescence effect for simple and sensitive exosome assay. **2022**, 114373 0

200 Monitoring the infection of powdery mildew pathogen on strawberry leaves by ATR-IR technique. 0

199 Effects of Near- and Far-Field Coupling on the Enhancement Factor of the Radiative Decay Rate of Multiple Emitters Near a Silver Nanoparticle Sphere. 2

198 Ag Nanoparticles with Ultrathin Au Shell-Based Lateral Flow Immunoassay for Colorimetric and SERS Dual-Mode Detection of SARS-CoV-2 IgG. 2

197 Application of Dual-Enhanced Surface-Enhanced Raman Scattering Probe Technology in the Diagnosis of Tumor Cells In Vitro. **2022**, 27, 3582

196 Enclosed Cells for Extending Soft X-ray Spectroscopies to Atmospheric Pressures and Above. 175-218 1

195 Charge Transfer in Patterned Bilayer Film of Ag/ZnS Composite by Magnetron Control Sputtering. **2022**, 27, 3805

194 Nanoparticle core size and spacer coating thickness dependence on metal-enhanced luminescence in optical oxygen sensors. **2022**, 123690

193 Femtomolar-Level Molecular Sensing of Monolayer Tungsten Diselenide Induced by Heteroatom Doping with Long-Term Stability. 2200273 0

192 Large-Area Hexagonal Boron Nitride Layers by Chemical Vapor Deposition: Growth and Applications for Substrates, Encapsulation, and Membranes. 2

191 Constructing a Highly Sensitivity SERS Sensor Based on a Magnetic Metal-Organic Framework (MOF) to Detect the Trace of Thiabendazole in Fruit Juice. 1

190 Graphene Oxide-Based Three-Dimensional Au Nanofilm with High-density and Controllable Hotspots: A Powerful Film-Type SERS Tag for Immunochromatographic Analysis of Multiple Mycotoxins in Complex Samples. **2022**, 137760 4

189 Future prospects of carbon dots application in agriculture. **2022**, 263-285

188 Single-Molecule Surface-Enhanced Raman Spectroscopy. **2022**, 22, 4889 3

187	Kinetic Regulation Engineering and In-Situ Spectroscopy Studies on Transition-Metal-Based Electrocatalysts for Water Splitting.	0
186	Long-Life and pH-Stable SnO ₂ -Coated Au Nanoparticles for SHINERS.	1
185	Recent advances in the application of Raman spectroscopy for fish quality and safety analysis.	0
184	Polyaniline-Based Rose-like Chiral Nanostructures for Raman Enhancement.	0
183	Evaluation of classification ability of Logistic Regression model on SERS data of miRNAs.	1
182	Nonstoichiometric tungsten oxide nanosheets with abundant oxygen vacancies for defects-driven SERS sensing.	0
181	Mapping Surface Chemistry During Superfilling with Shell-Isolated Nanoparticle Enhanced Raman Spectroscopy and X-Ray Photoelectron Spectroscopy.	1
180	Inhomogeneity of fluorescence lifetime and intensity in a plasmonic nanocavity. 2022 , 45, 101548	0
179	Effect of surface hydroxyls and porous nanostructured sensors integrated for SERS monitoring and efficient removal of organic pollutants. 2022 , 601, 154123	0
178	Molybdenum Nitride Porous Prisms with a Strong Plasmon Resonance Effect in the Visible Region for Surface-Enhanced Raman Spectroscopy. 2022 , 13, 6777-6782	1
177	Large-Area Metal-Dielectric Heterostructures for Surface-Enhanced Raman Scattering.	
176	Electrochemical behavior of chalcocite exposed to 2-mercaptobenzothiazole aqueous solution. 2022 , 602, 154306	
175	Detection of mercury ions using graphene oxide sensors assisted by Ag@SiO ₂ .	
174	Manipulating the light-matter interactions in plasmonic nanocavities at 1 nm spatial resolution. 2022 , 11,	3
173	Phononic Cavity Optomechanics of Atomically Thin Crystal in Plasmonic Nanocavity. 2022 , 16, 12711-12719	0
172	Anion Effects on the Interfacial Structure and Bulk Physical Properties in Choline-Based Hydrogen-Bonded Electrolytes.	
171	Enhancing Hydrogen Oxidation and Evolution Kinetics by Tuning the Interfacial Hydrogen-Bonding Environment on Functionalized Platinum Surfaces.	
170	Enhancing Hydrogen Oxidation and Evolution Kinetics by Tuning the Interfacial Hydrogen-Bonding Environment on Functionalized Platinum Surfaces.	2

- 169 In Situ Surface Restraint-Induced Synthesis of Transition-Metal Nitride Ultrathin Nanocrystals as Ultrasensitive SERS Substrate with Ultrahigh Durability. **2022**, 16, 13123-13133 1
- 168 A Dual-Mode NADH Biosensor Based on Gold Nanostars Decorated CoFe₂ Metal-Organic Frameworks to Reveal Dynamics of Cell Metabolism. 1
- 167 Shell-Isolated Nanoparticle-Enhanced Electrochemiluminescence. 2203513 0
- 166 Silica Shell Thickness-Dependent Fluorescence Properties of SiO₂@Ag@SiO₂@QDs Nanocomposites. **2022**, 23, 10041 1
- 165 Au ETHH@ZIF-8 based "three-in-one" multifunctional substrate with analyte enrichment, filtration and enhanced SERS performance. **2022**, 606, 154914 0
- 164 High performance carbon dioxide electroreduction in ionic liquids with in situ shell-isolated nanoparticle-enhanced Raman spectroscopy. **2023**, 451, 138975 2
- 163 SERS-active substrates based on Ag-coated TiO₂ nanotubes and nanograss. **2023**, 145, 115499 1
- 162 Elucidating electrochemical CO₂ reduction reaction processes on Cu(hkl) single-crystal surfaces by in situ Raman spectroscopy. **2022**, 15, 3968-3977 5
- 161 Construction of a HPLC-SERS hyphenated system for continuous separation and detection based on paper substrates. **2022**, 147, 4073-4081 0
- 160 Facile fabrication of Ag@C@C₈ nanoparticles as a SERS substrate and their environmental applications. **2022**, 147, 4026-4039 0
- 159 Single-molecule detection with enhanced Raman scattering of tungsten oxide nanostructure. 0
- 158 Plasmonic nanosensors and their spectroscopic applications—current trends and future perspectives. **2022**, 337-372 0
- 157 Understanding hydrogen oxidation/evolution electrochemical interfaces through in situ Raman scattering and infrared absorption spectroscopies. **2023**, 0
- 156 Revealing *OOH key intermediates and regulating H₂O₂ photoactivation by surface relaxation of Fenton-like catalysts. **2022**, 119, 2
- 155 Creating and moving nanoantenna cold spots anywhere. **2022**, 11, 0
- 154 Molecular Degradation of Iron Phthalocyanine during the Oxygen Reduction Reaction in Acidic Media. **2022**, 12, 11097-11107 2
- 153 Metal-organic frameworks based surface-enhanced Raman spectroscopy technique for ultra-sensitive biomedical trace detection. 2
- 152 Plasmonics in Bioanalysis: SPR, SERS, and Nanozymes. **2023**, 37-83 0

151	Recent Progress in Developing a LiOH-based Reversible Nonaqueous Lithium-Air Battery. 2201384	1
150	High-Quality Cs ₃ Cu ₂ I ₅ Single-Crystal is a Fast-Decaying Scintillator. 2201161	1
149	Design Strategies and in situ Infrared, Raman, and X-ray Absorption Spectroscopy Techniques Insight into the Electrocatalysts of Hydrogen Energy System. 2200201	0
148	Interfacial Structure of Pt(110) Electrode during Hydrogen Evolution Reaction in Alkaline Solutions. 2022, 13, 8403-8408	0
147	Molecularly imprinted core-shell Au nanoparticles for 2,4-dichlorophenoxyacetic acid detection in milk using surface-enhanced Raman spectroscopy. 2022, 1227, 340333	0
146	Serrated Au Nanoplates via the Sharpening Etching Mode. 2022, 34, 8213-8218	0
145	Directly Convert Carbonaceous Microspheres to Three-Dimensional Porous Carbon Microspheres with a Robust Self-Supporting Structure as a Metal-Free SERS Substrate for Online High-Throughput Analysis.	0
144	SERS enhancement induced by the Se vacancy defects in ultra-thin hybrid phase SnSex nanosheets. 2022, 30, 37795	0
143	From Atomic Physics to Superatomic Physics.	0
142	Unconventional interfacial water structure of highly concentrated aqueous electrolytes at negative electrode polarizations. 2022, 13,	2
141	Facile Regulation of Shell Thickness of the Au@MOF Core-Shell Composites for Highly Sensitive Surface-Enhanced Raman Scattering Sensing. 2022, 22, 7039	0
140	Molecularly Imprinted and Cladded Nanotags Enable Specific SERS Bioimaging of Tyrosine Phosphorylation.	0
139	A novel cellulosic non-enzymatic nanosensor based on carbon shell silver (Ag@C) nanoparticles for colorimetric detection of Chlorpyrifos in agricultural products.	0
138	Photoinduced Enhanced Raman Spectroscopy for the Ultrasensitive Detection of a Low-Cross-Section Chemical, Urea, Using Silver-Titanium Dioxide Nanostructures.	0
137	Rational Design of Surface-Enhanced Raman Scattering Substrate for Highly Reproducible Analysis.	1
136	Molecular Plasmonics with Metamaterials.	3
135	Rapid Immobilization of Silver Nanoparticles via Amino-quinone Coatings Enables Surface-Enhanced Raman Scattering Detection.	0
134	Floating Ag-NPs@Cu-NWs bundles fabricated on cooper mesh for highly sensitive SERS detection of uric acid in pretreatment-free urine.	0

- 133 Measurement and Analysis of Plasmon-Driven Photocatalysis. **2022**, 47-61 0
- 132 Reconciling the experimental and computational methanol electro-oxidation activity via potential-dependent kinetic mechanism analysis. 0
- 131 Effect of the Combination of Gold Nanoparticles and Polyelectrolyte Layers on SERS Measurements. **2022**, 12, 895 1
- 130 Beginner's Guide to Raman Spectroelectrochemistry for Electrocatalysis Study. 0
- 129 Electrochemical Shell-Isolated Nanoparticle-Enhanced Raman Spectroscopy of Imidazole Ring Functionalized Monolayer on Smooth Gold Electrode. **2022**, 27, 6531 0
- 128 Electrochemical In Situ/operando Spectroscopy and Microscopy Part 2: Battery Applications. **2022**, 90, 102010-102010 0
- 127 A Metallic Niobium Nitride with Open Nanocavities for Surface-Enhanced Raman Spectroscopy. **2022**, 94, 14635-14641 0
- 126 Why Does Pt Shell Bearing Tensile Strain Still Have Superior Activity for the Oxygen Reduction Reaction?. **2022**, 126, 17913-17922 0
- 125 Large Area Patterning of Highly Reproducible and Sensitive SERS Sensors Based on 10-nm Annular Gap Arrays. **2022**, 12, 3842 0
- 124 Single-model multi-tasks deep learning network for recognition and quantitation of surface-enhanced Raman spectroscopy. **2022**, 30, 41580 1
- 123 Electrochemical In Situ/operando Spectroscopy and Microscopy Part 1: Fundamentals. **2022**, 90, 102009-102009 0
- 122 Multi-Effect Enhanced Raman Scattering Based on Au/ZnO Nanorods Structures. **2022**, 12, 3785 1
- 121 Optical Detection and Imaging of Nonfluorescent Matter at the Single-Molecule/Particle Level. **2022**, 13, 9618-9631 0
- 120 Recent Development of Multifunctional Nanocomposites Based on Bacterial Nanocellulose. **2023**, 75-105 0
- 119 Surface-enhanced vibrational spectroscopies in electrocatalysis: Fundamentals, challenges, and perspectives. **2022**, 43, 2757-2771 0
- 118 Fabrication of Gyroid-Structured Metal/Semiconductor Nanoscaffolds with Ultrasensitive SERS Detection via Block Copolymer Templating. **2022**, 2202280 1
- 117 Ultra-thin silica shell-guarded nanoflares for high-fidelity live cell miRNA-21 imaging by fully avoiding the interference of biothiols. 0
- 116 Surface-enhanced Raman spectroscopy for food quality and safety monitoring. **2023**, 31-54 0

- 115 Efficient manipulation of plasmonic modes in single symmetry-breaking Ag nanocube. **2023**, 611, 155650 o
- 114 Centrifugation assembly proceeded tube-based SERS sensor for field-deployable solution detection. **2023**, 376, 132982 o
- 113 Surface Water as an Initial Proton Source for the Electrochemical CO Reduction Reaction on Copper Surfaces. o
- 112 Metal-Organic-Frameworks-Isolated Au Nanobipyramids as Synergetic Surface-Enhanced-Raman-Scattering Substrates. 2506-2514 1
- 111 Silica Nanospheres Coated Silver Islands as an Effective Opto-Plasmonic SERS Active Platform for Rapid and Sensitive Detection of Prostate Cancer Biomarkers. **2022**, 27, 7821 1
- 110 Surface Water as an Initial Proton Source for the Electrochemical CO Reduction Reaction on Copper Surfaces. 1
- 109 Pd^{II} Species on Electrode Stabilized by Solvent Co-Adsorption: Observation by Operando IR Spectroscopy. **2022**, 126, 19376-19385 1
- 108 An improved 9 micron thick separator for a 350 Wh/kg lithium metal rechargeable pouch cell. **2022**, 13, 1
- 107 Surface-enhanced Raman scattering integrated with microfluidic device fabricated using atomic force microscopy tip-based nanomachining approach. 095440542211365 o
- 106 Tunable surface plasmon resonance wavelengths response from Au/Ag nanocomposite system. **2022**, 139602 o
- 105 Surface-enhanced Raman spectroscopy with nanomaterials. **2022**, o
- 104 In situ probing of liquid-solid interfaces using core-shell nanoparticles-enhanced Raman spectroscopy. **2023**, o
- 103 Spotting the Driving Forces for SERS of Two-Dimensional Nanomaterials. o
- 102 Capillary-force-assisted self-assembly of gold nanoparticles into highly ordered plasmonic thin films for ultrasensitive SERS. o
- 101 Cathodic corrosion to fabricate Au electrodes with unique properties for single-crystal electrochemistry, electrocatalysis, and SER spectroscopy. **2023**, o
- 100 Au@Ag-Au core@double shell SERS bioprobes for high-resolution tumor cells imaging. **2023**, 51, 100204 o
- 99 Facile fabrication of field deployable surface enhanced Raman scattering smart sand from sea sand. **2023**, 333, 133655 o
- 98 Microwave-ultra-fast recovery of valuable metals from spent lithium-ion batteries by deep eutectic solvents. **2023**, 156, 139-147 o

- 97 A general approach to hybrid platform of Au nanoparticles on monolayer semiconductor for ultrasensitive Raman enhancement of 2D materials and molecule detection. **2023**, 938, 168468 ○
- 96 Thermal treatment induced the surface enhanced Raman scattering of WO₃-TiO₂ heterogeneous composite films. **2023**, 613, 155975 ○
- 95 Studies of Bis-(Sodium-Sulfopropyl)-Disulfide and 3-Mercapto-1-Propanesulfonate on/into the Copper Electrodeposited Layer by Time-of-Flight Secondary-Ion Mass Spectrometry. **2022**, 27, 8116 ○
- 94 Ultrafast Ion Sputtering Modulation of Two-Dimensional Substrate for Highly Sensitive Raman Detection. **2022**, 4, 2622-2630 ○
- 93 Engineered Au@CuO Nanoparticles for Wide-Range Quantitation of Sulfur Ions by Surface-Enhanced Raman Spectroscopy. **2022**, 94, 17169-17176 ○
- 92 Dual Biomimetic Recognition-Driven Plasmonic Nanogap-Enhanced Raman Scattering for Ultrasensitive Protein Fingerprinting and Quantitation. **2022**, 22, 9664-9671 ○
- 91 Plasmonic Ag/ZnO Nanoscale Villi in Microstructure Fibers for Sensitive and Reusable Surface-Enhanced Raman Scattering Sensing. ○
- 90 An isolated single-particle-based SECM tip interface for single-cell NO sensing. **2022**, 115048 ○
- 89 Rapid Point-of-Care Assay by SERS Detection of SARS-CoV-2 Virus and Its Variants. **2022**, 94, 17795-17802 2
- 88 Surface Plasmon Resonance-Triggered Local Electromagnetic Field Advances Photocatalytic and Photoelectrochemical Performance of Plasmonic Metal/Semiconductor Composite. ○
- 87 Quantitatively Revealing the Anomalous Enhancement in Shell-Isolated Nanoparticle-Enhanced Raman Spectroscopy Using Single-Nanoparticle Spectroscopy. ○
- 86 Inducing SERS Activity at Graphitic Carbon Using Graphene-Covered Ag Nanoparticle Substrates: Spectroelectrochemical Analysis of a Redox-Active Adsorbed Anthraquinone . ○
- 85 Lossless enrichment of trace analytes in levitating droplets for multiphase and multiplex detection. **2022**, 13, 1
- 84 The evolution and recent research trends of Surface Enhanced Raman Scattering sensors using plasmonics: Citation network analysis. **2022**, 127255 ○
- 83 Ag@ZIF-67 nanocomposites for ultra-sensitive SERS detection to thiram molecules. ○
- 82 In situ electrochemical Raman spectroscopy and ab initio molecular dynamics study of interfacial water on a single-crystal surface. ○
- 81 SERS Labels for Optical Anticounterfeiting: Structure, Fabrication, and Performance. 2201549 ○
- 80 Probing solid/liquid interfaces at a single-molecule level by in-situ break junction techniques. **2023**, ○

- 79 An experimental guide to in operando electrochemical Raman spectroscopy. ○
- 78 Numerical investigation of gold nano-polygonal structures as SERS-active substrates using near and far-sided excitation. **2023**, 103497 ○
- 77 Interaction of Bis-(sodium-sulfopropyl)-Disulfide and Polyethylene Glycol on the Copper Electrodeposited Layer by Time-of-Flight Secondary-Ion Mass Spectrometry. **2023**, 28, 433 ○
- 76 Creation and Application of Nano/microsystems That Control Ideal Experimental Conditions. **2023**, 26, 57-64 ○
- 75 Electrocatalysis Mechanism and Structure-Activity Relationship of Atomically Dispersed Metal-Nitrogen-Carbon Catalysts for Electrocatalytic Reactions. 2201524 ○
- 74 Applications of In Situ Raman Spectroscopy on Rechargeable Batteries and Hydrogen Energy Systems. ○
- 73 Sensitive Detection of p-Chlorobenzaldehyde in Environmental Water Based on Au@Ag-MOFs Nanoparticle by Surface-Enhanced Raman Scattering. ○
- 72 Ag@C Decorated GaN Nanoflower enabled Super-stable, Single molecule level SERS substrate Integrated with Machine Learning for Multiple Analytes Identification. **2023**, 100305 ○
- 71 Noise Learning of Instruments for High-contrast, High-resolution and Fast Hyperspectral Microscopy and Nanoscopy. ○
- 70 Electric, magnetic, and shear field-directed assembly of inorganic nanoparticles. ○
- 69 Monitoring hydrogen transport through graphene by in situ surface-enhanced Raman spectroscopy. ○
- 68 Silver Nanostructure Modified Graphite Electrode for In-operando SERRS Investigation of Iron Porphyrins during High Potential Electrocatalysis. ○
- 67 Quantitative determination of carbosulfan residues by surface-enhanced Raman spectroscopy. **2023**, 290, 122315 ○
- 66 Plasma synthesized molybdenum derived nano-fiber films: The influence of surface composition on their SERS effect. **2023**, 175, 111207 ○
- 65 Graphene-Isolated Satellite Nanostructure Enhanced Raman Spectroscopy Reveals the Critical Role of Different Intermediates on the Oxygen Reduction Reaction. **2023**, 13, 849-855 ○
- 64 Enhanced Sum Frequency Generation for Monolayers on Au Relative to Silica: Local Field Factors and SPR Effect. **2023**, 39, 659-667 ○
- 63 Interfacial Evolution on Co-based Oxygen Evolution Reaction Electrocatalysts Probed by Using In Situ Surface-Enhanced Raman Spectroscopy. ○
- 62 Nanostructures for In Situ SERS Analysis of High-Temperature Processes. **2023**, 11, 21 ○

- 61 Rapid Detection of SARS-CoV-2 Spike RBD Protein in Body Fluid: Based on Special Calcium Ion-Mediated Gold Nanoparticles Modified by Bromide Ions. **2023**, 14, 88-94 ○
- 60 Ionic-Wind-Enhanced Raman Spectroscopy without Enhancement Substrates. ○
- 59 Surface-Enhanced Raman Spectroscopic Probing in Digital Microfluidics through a Microspray Hole. ○
- 58 Plasmonic Gradient and Plexcitonic Effects in Single-Molecule Tip-Enhanced (Resonance) Raman Spectroscopy. **2023**, 127, 476-489 ○
- 57 Capillary Tube Surface-Enhanced Raman Scattering Substrate and High-Sensitivity Molecule Detection. **2023**, 127, 378-383 ○
- 56 Band Alignment Enabling Effective Charge Transfer for the Highly Enhanced Raman Scattering and Fluorescence of Metal-Nanoparticle-Decorated Conjugated Polymer Nanowires. **2023**, 14, 750-762 ○
- 55 Surface pH Effects on Catalytic Behavior of Pyridinic Nitrogen on Nitrogen-doped Carbon Nanotube in CO₂; Electrochemical Reduction. **2023**, ○
- 54 Charge transfer in the Ag/polymer/fullerene system of organic solar cells (OSCs) observed by surface-enhanced Raman spectroscopy: donor/acceptor concentration-dependent. ○
- 53 Tunable orientation of two-dimensional assembled Au octahedron superlattices in polymer films as flexible SERS substrates. ○
- 52 Large-Area, Ultrahigh-Enhancement, and Array-Type Hot Spots in Plasmonic Nanocube Dimer-on-Film Nanocavity. ○
- 51 Pd-based Nanocatalysts for Oxygen Reduction Reaction: Preparation, Performance, and in-Situ Characterization. **2023**, 100021 ○
- 50 Quantum coherent manipulation of magnetic molecules. **2023**, ○
- 49 Ultrahigh Raman-Fluorescence Dual-Enhancement in Nanogaps of Silver-Coated Gold Nanopetals. ○
- 48 Recent advances in plasmon-enhanced luminescence for biosensing and bioimaging. **2023**, 1254, 341086 ○
- 47 Gold-silver alloy hollow nanoshells-based lateral flow immunoassay for colorimetric, photothermal, and SERS tri-mode detection of SARS-CoV-2 neutralizing antibody. **2023**, 1255, 341102 ○
- 46 Au@SiO₂ SERS nanotags based lateral flow immunoassay for simultaneous detection of aflatoxin B1 and ochratoxin A. **2023**, 258, 124401 ○
- 45 Process and mechanism of enhanced HCl leaching of platinum group metals from waste three-way catalysts by Li₂CO₃ calcination pretreatment. **2023**, 452, 131348 ○
- 44 Instant micro-arc oxidation constructing the ultrafine nanoparticles as high-performance catalyst and mechanism study. **2023**, 301, 127654 ○

43	Doubly-resonant enhanced second-harmonic generation and its wide-band tunability. 2023 , 539, 129493	o
42	Localized surface plasmon controlled chemistry at and beyond the nanoscale. 2023 , 4, 021301	o
41	Introduction of multilayered magnetic core-shell SERS tags into lateral flow immunoassay: A highly stable and sensitive method for the simultaneous detection of multiple veterinary drugs in complex samples. 2023 , 448, 130912	1
40	Amorphous Nitrogen-Doped Carbon Nanocages with Excellent SERS Sensitivity and Stability for Accurate Identification of Tumor Cells. 2023 , 95, 4671-4681	o
39	Core-shell nanoparticle enhanced Raman spectroscopy in situ probing the composition and evolution of interfacial species on PtCo surfaces.	o
38	Toward a New Era of SERS and TERS at the Nanometer Scale: From Fundamentals to Innovative Applications. 2023 , 123, 1552-1634	3
37	Ag/ZIF-8 Substrate with Enhanced SERS via the Plasmonic Nanogap and MOF-Enabled Molecular Preconcentration Effect. 2023 , 127, 3542-3550	o
36	Near-field optical microscopy toward its applications for biological studies. 2023 , 20, n/a	o
35	Electrolyte effect for carbon dioxide reduction reaction on copper electrode interface: A DFT prediction. 2023 , 158, 094704	o
34	Raman Spectroscopy for Hydrogen Production. 121-146	o
33	Electrostatic Adsorption of Dense AuNPs onto Silica Core as High-Performance SERS Tag for Sensitive Immunochromatographic Detection of Streptococcus pneumoniae. 2023 , 12, 327	o
32	In-situ/operando Raman techniques for in-depth understanding on electrocatalysis. 2023 , 461, 141939	o
31	Electrochemical Dealloying Preparation and Morphology Evolution of Nanoporous Au with Enhanced SERS Activity. 2023 , 13, 489	o
30	Development of Line-Detected UV-Vis Absorption Microscope and Its Application to Quantitative Evaluation of Lithium Surface Reactivity. 2023 , 95, 4550-4555	o
29	Efficient Manipulation of Strong Coupling Towards the Deep Ultraviolet Region. 2023 , 18, 793-801	o
28	Plasmonic Au@Cu nanostructures: Synthesis and applications. 11,	o
27	High-throughput surface-enhanced Raman scattering sensors for near-infrared detection of biochemical molecules. 2023 , 11, 4486-4491	o
26	Chemical Sensors Based on Graphene and 2D Graphene Analogs. 2200057	o

- 25 Surface-Enhanced Raman Spectroscopic Analysis of Flavoenzyme Cofactors: Guidance for Flavin-Related Bio- and Chemo- Sensors. **2023**, 11, 190 ○
- 24 Wavelength-Dependent Metal-Enhanced Fluorescence Biosensors via Resonance Energy Transfer Modulation. **2023**, 13, 376 ○
- 23 Plastic spectral interference in the biological characterization by Raman or SERS spectroscopy. ○
- 22 A robust SERS calibration using a pseudo-internal intensity reference. ○
- 21 Oxygen Evolution/Reduction Reaction Catalysts: From In Situ Monitoring and Reaction Mechanisms to Rational Design. ○
- 20 Recent advances of bismuth-based electrocatalysts for CO₂ reduction: Strategies, mechanism and applications. **2023**, 100191 ○
- 19 Ultrathin Graphdiyne Nanowires with Diameters below 3 nm: Synthesis, Photoelectric Effect, and Enhanced Raman Sensing. ○
- 18 Plasmonic Molybdenum Dioxide Ultrathin Nanowire Bundles for Highly Sensitive, Stable, and Reproducible Surface-Enhanced Raman Spectroscopy. **2023**, 127, 6439-6445 ○
- 17 High-Density Optophysiology for Recording Intracellular and Extracellular Signals across the Brain of Free-Moving Animals. ○
- 16 High-Density Optophysiology for Recording Intracellular and Extracellular Signals across the Brain of Free-Moving Animals. ○
- 15 Wearable Plasmonic Sweat Biosensor for Acetaminophen Drug Monitoring. ○
- 14 Insights into Chemical Changes Causing Transient Potential Patterns during Cobalt Electrodeposition: An Operando SHINERS Investigation. **2023**, 14, 3376-3383 ○
- 13 Direct characterization of shear phonons in layered materials by mechano-Raman spectroscopy. ○
- 12 Nanozymes towards Personalized Diagnostics: A Recent Progress in Biosensing. **2023**, 13, 461 ○
- 11 Fabry-Pérot Cavity Control for Tunable Raman Scattering. ○
- 10 Recognition of dipole-induced electric field in 2D materials for surface-enhanced Raman scattering. 11, ○
- 9 Transitioning surface-enhanced Raman spectroscopy (SERS) into the forensic drug chemistry and toxicology laboratory: Current and future perspectives. ○
- 8 Silver nanostructure-decorated hierarchical titanium dioxide nanoflowers for SERS and photocatalytic applications. **2023**, 178, 106672 ○

- 7 Application of SERS-based nanobiosensors to metabolite biomarkers of CKD. **2023**, 232, 115311 o
- 6 Light-Triggered Reversible Tuning of Second-Harmonic Generation in a Photoactive Plasmonic Molecular Nanocavity. o
- 5 Superconformal Film Growth: From Smoothing Surfaces to Interconnect Technology. o
- 4 Metal/Silicon-based sensing (molecular, photon). **2023**, 295-315 o
- 3 Recent Progresses in Machine Learning Assisted Raman Spectroscopy. o
- 2 Recent development of surface-enhanced Raman scattering for biosensing. **2023**, 21, o
- 1 Recent advances in Raman and surface enhanced Raman spectroelectrochemistry. 4, o